

Advances in Patterning Materials for 193 nm Immersion Lithography

Daniel P. Sanders*

IBM Almaden Research Center, 650 Harry Road, San Jose, California 95136

Received July 6, 2009

Contents

1. Overview	321	4.3.2. Silicon-Based High Refractive Index Photoresists	348
2. Background	322	4.3.3. Nanocomposite-Based High Refractive Index Photoresists	349
2.1. Optical Lithography	322	4.4. Status of High-Index Immersion Lithography	350
2.2. Immersion Lithography at 193 nm	323	5. Summary	350
2.3. Photoresists for Optical Lithography	324	6. Acknowledgments	350
3. Materials for 193 nm Water Immersion Lithography	325	7. References	350
3.1. Properties of Water Relevant to 193 nm Immersion Lithography	325		
3.1.1. Photochemistry of Water at 193 nm	326		
3.1.2. Scattering and Bubble Formation	326		
3.2. Interaction of Water with 193 nm Photoresist Materials	326		
3.2.1. Diffusion of Water into Photoresists	327		
3.2.2. Extraction of Photoresist Components into Water	328		
3.2.3. Water Contact Angles, Film Pulling, And Fluid Handling	330		
3.2.4. Defectivity Issues in Water Immersion Lithography	331		
3.3. Topcoat Materials for Water Immersion Lithography	332		
3.3.1. Organic-Developable Topcoat Materials	333		
3.3.2. Water-Castable Topcoat Materials	333		
3.3.3. Alkali-Soluble Topcoat Materials	334		
3.3.4. Performance of Immersion Topcoat Materials	336		
3.4. Topcoat-Free Photoresists for Water Immersion Lithography	337		
3.4.1. Hydrophobic Resists with Low Leaching PAGs	337		
3.4.2. Surface-Segregating Additives Containing Silicon or Fluorine	337		
3.4.3. Performance of Topcoat-Free Photoresists	341		
4. Materials for 193 nm High-Index Immersion Lithography	341		
4.1. High Refractive Index Lens Materials	342		
4.2. High Refractive Index Immersion Fluids	342		
4.2.1. Second-Generation Organic Immersion Fluids	343		
4.2.2. Second-Generation Aqueous and Other Immersion Fluids	345		
4.2.3. Third-Generation Fluids Based on Boron, Silicon, And Germanium	347		
4.2.4. Third-Generation Nanoparticle-Based Immersion Fluids	347		
4.3. High Refractive Index Photoresists	347		
4.3.1. Organic High Refractive Index Photoresists	348		

1. Overview

Advancements in optical lithography tools, processes, and patterning materials have been critical to the continued performance increases of semiconductor devices as well as to the overall economics of the semiconductor industry.¹ Reducing the wavelength of the source radiation has been a traditional pathway to increase resolution in optical lithography.^{1–3} In recent years, the technological challenges and the soaring costs associated with developing new exposure tools and new imaging materials have slowed the progress of wavelength scaling, evidenced by the decision not to commercialize 157 nm (F₂ excimer) lithography in 2004.⁴ Rather than reducing the vacuum wavelength of the illumination, the semiconductor industry instead turned to scaling the effective wavelength via immersion lithography to extend the resolution capabilities of 193 nm lithography. Immersion lithography, which utilizes a coupling medium with a refractive index greater than that of air between the last lens element (LLE) and the photoresist, provides an increased depth-of-focus (DOF) and enables imaging systems with numerical apertures greater than one.^{5–13} This approach is economically attractive since it continues to use large amounts of the existing lithographic tooling infrastructure and patterning materials. In particular, the rapid development and commercialization of 193 nm water immersion lithography helped seal the fate of 157 nm lithography.

This article reviews the current understanding of the interactions of water with photoresist materials as well as the chemistry and lithographic performance of patterning materials (e.g., immersion topcoats and topcoat-free photoresists) developed to control these interactions in 193 nm water immersion lithography. In order to extend the patterning capabilities of 193 nm immersion lithography, further reduction of the effective wavelength through the use of immersion fluids with higher refractive indices than that of water has been explored. This article also reviews the development of high index immersion lithography, including progress in high refractive index lens materials, high refractive index immersion fluids, and high refractive index photoresists.

* Corresponding author: dsand@us.ibm.com.



Dan Sanders received a B.S.E. in Polymer Science and Engineering and M.S.E. in Macromolecular Science from Case Western Reserve University. Later, he received a Ph.D. in Chemistry from the California Institute of Technology for his work in the research lab of Prof. Robert H. Grubbs on the transition metal-catalyzed synthesis of fluoropolymers for use as 157 nm photoresists. Subsequently, he joined the lithography group at the IBM Almaden Research Center in December 2004, where his research has focused on materials for 193 nm immersion lithography, 193 nm high index immersion lithography, and lithographically directed self-assembly of polymeric systems.

2. Background

2.1. Optical Lithography

The photolithographic process used to fabricate semiconductor devices is outlined in Figure 1. In photolithography, a photosensitive material (i.e., a photoresist or resist) on a substrate is exposed patternwise through a mask.^{1–3} The incident radiation induces a change in the material (typically in its solubility) in the exposed regions. For the positive-tone photoresist material shown in Figure 1, the solubility of the photoresist in the exposed regions is altered such that it can be selectively removed by a developing solvent, typically 0.26 N aqueous tetramethylammonium hydroxide (TMAH). The resultant photoresist pattern is then used as an etch mask during subsequent pattern transfer steps in order to define features on the wafer.

The minimum resolution (i.e., critical dimension or minimum half-pitch) that can be achieved by a lithographic process is described by the Rayleigh equation,

$$R = k_1 \frac{\lambda_0}{n \cdot \sin \theta} \quad (1)$$

wherein R is the resolution or critical dimension, k_1 is the Rayleigh coefficient of resolution, λ_0 is the vacuum wavelength,

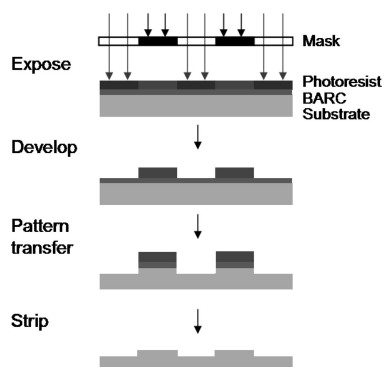


Figure 1. Lithographic process using a positive-tone photoresist.

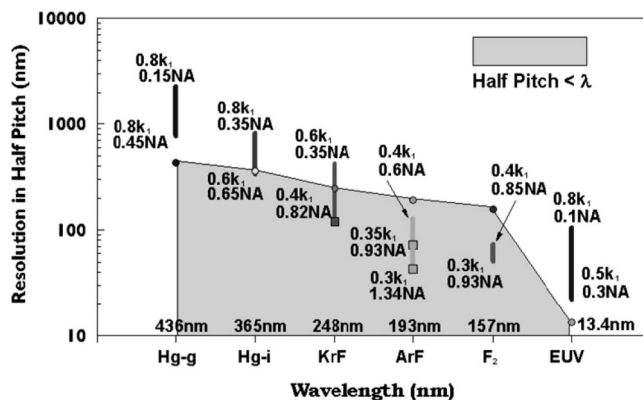


Figure 2. Capabilities of various lithographic technologies. For each lithography technology, the resolution in half-pitch for various combinations of NA and k_1 are indicated by a vertical bar. The transition to subwavelength imaging (as indicated by the shaded region) occurred with 248 nm lithography. Reprinted with permission from “The ending of optical lithography and the prospects of its successors”; *Microelectronic Engineering*; Lin, B. J., Ed.; Vol. 83, pp 604–613. Copyright 2006 Elsevier.

n is the refractive index of the incident medium, and θ is the angular aperture of the lens.^{1,2,5} The product $n \cdot \sin \theta$ is also referred to as the numerical aperture (NA) of the imaging system. The k_1 term is a process-dependent factor that is determined by illumination conditions, mask technology, and photoresist capabilities. The lower limit of k_1 is 0.25 for single-exposure optical lithography.² Resolution has been traditionally improved by reducing the exposure wavelength, improving the photoresist materials, and using increasingly refined optical illumination techniques. Past examples of wavelength scaling include transitions from early 436 nm (g-line) and 365 nm (i-line) lithography to 248 nm (KrF) and then 193 nm (ArF) lithography.^{1–3} The capabilities of these various optical lithographic technologies are shown in Figure 2.

With each exposure technology, lithographers have employed a variety of optical techniques to improve process windows at lower k_1 values in order to incrementally increase the practical resolution limit. These resolution enhancement techniques (RETs) include optimization of the illumination conditions (e.g., off-axis illumination (OAI), polarized illumination, and source mask optimization (SMO)) and photomask improvements (e.g., phase-shifting masks (PSMs), optical proximity correction (OPC), and subresolution assist features (SRAFs)) as shown in Figure 3.^{2,14,15} The development of higher NA imaging systems and the aggressive use of RETs has prolonged the lifetime of 248 and 193 nm lithography several lithographic nodes beyond initial projections. The progression of NA and k_1 in optical lithography is outlined in Figure 4.

In order to view the development of immersion lithography in the appropriate historical context, one can consult the roadmap for potential lithography solutions outlined in the 2001 International Technology Roadmap for Semiconductors.¹⁷ At that time, 157 nm lithography was positioned as the leading candidate to succeed 193 nm dry lithography for the expected production of semiconductor devices at the 65 nm node beginning in 2007. However, 157 nm lithography struggled to overcome a number of difficult materials challenges (including new resists, pellicles, and lens materials),⁴ and alternative next-generation lithography (NGL) systems such as extreme ultraviolet lithography (EUV, 13.5 nm),¹⁸ electron projection lithography, nanoimprint lithography, and maskless multibeam e-beam direct write lithog-

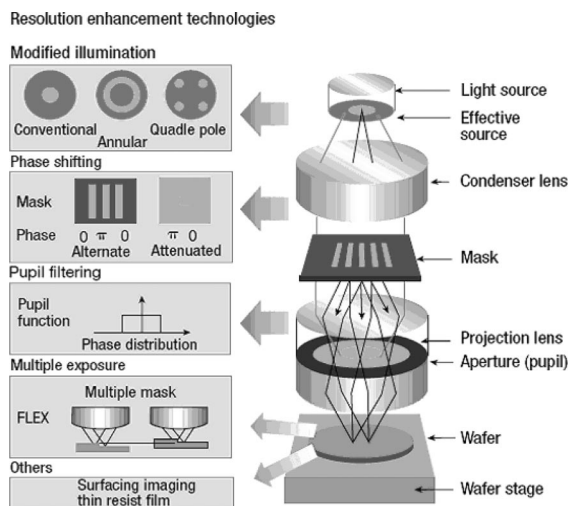


Figure 3. Resolution enhancement techniques for improving the resolution of optical lithography. Reprinted with permission from ref 15. Copyright 2000 Macmillan Publishers Ltd.

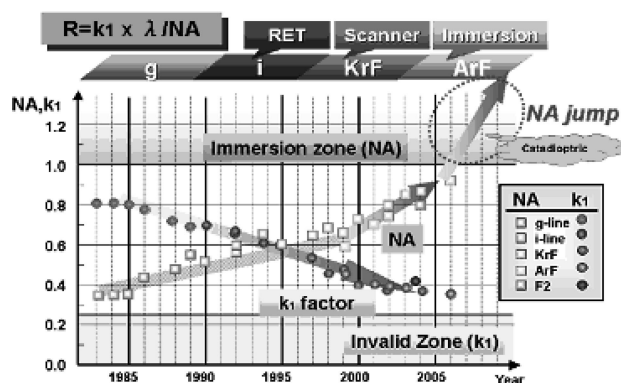


Figure 4. Progression of NA and k_1 in semiconductor lithography. Reprinted with permission from ref 16. Copyright 2008 SPIE.

raphy remained far from ready. As a result, the stage was set for immersion lithography to disrupt the planned transition to 157 nm lithography and extend the patterning capabilities of 193 nm optical lithography.⁶

2.2. Immersion Lithography at 193 nm

A number of detailed descriptions of the benefits^{5–13} of immersion lithography and its historical development^{19–21} with respect to semiconductor technology have been published. In short, after being explored both theoretically and experimentally in a sporadic manner over many years,^{22–28} interest in immersion lithography intensified when research into potential successors to 193 nm dry lithography began.

According to eq 1, the use of a coupling medium with a higher refractive index than air makes possible imaging systems with numerical apertures greater than one (so-called hyper-NA systems) and increased resolution. These same concepts, dating back to the late 1800s, have been widely employed in optical microscopy.²⁹ By employing a coupling medium with a higher refractive index than air (i.e., $n_{\text{medium}} > 1$), the effective wavelength ($\lambda_{\text{eff}} = \lambda_0/n_{\text{medium}}$) can be scaled without changing the vacuum wavelength (λ_0) of the illumination source. For example, using water as an immersion fluid enables a reduction in the effective wavelength of 193 nm radiation by ~30%, which is more than would be achieved by moving to 157 nm lithography (see Table 1). Changing the vacuum wavelength of the incident radiation changes its frequency

Table 1. Effective Wavelength for a Variety of Lithographic Technologies (Adapted with permission from ref 10a; Copyright 2004 SPIE)

light source	λ_0	coupling medium	n_{medium}	$\lambda_0/n_{\text{medium}}$
ArF	193 nm	air	1.0	193 nm
F ₂	157 nm	N ₂	1.0	157 nm
ArF	193 nm	water	1.44	134 nm
ArF	193 nm	high-index fluid	1.64	118 nm
F ₂	157 nm	perfluoropolyether	1.37	115 nm

and its photon energy, typically requiring the development of new optical lens materials and new imaging materials.^{7,8} Since scaling the effective wavelength does not change the frequency of the incident radiation, immersion lithography at 193 nm can continue to utilize much of the existing mask, lens, photoresist, and antireflective coating materials technology used in 193 nm dry lithography.

The benefits of immersion lithography can be broken into two regimes: increased depth-of-focus (DOF) for lower NA imaging and improved resolution via hyper-NA (i.e., NA > 1) imaging as shown in Figure 5.^{11,12} In the case of imaging at numerical apertures less than one, immersion lithography provides an increased DOF relative to dry lithography performed at the same numerical aperture.¹² This advantage can be illustrated qualitatively by considering the approximate DOF scaling equation

$$\text{DOF} = k_2 \frac{\lambda_0}{n \sin^2 \theta} = nk_2 \frac{\lambda_0}{(\text{NA})^2} \quad (2)$$

wherein k_2 is the Rayleigh coefficient of DOF.^{7–10,30,31} From eq 2, the DOF in immersion lithography is increased by a factor of n relative to dry lithography at the same NA.¹² In practice, even larger gains in DOF are realized due to the use of very large incident illumination angles in immersion lithography. More general treatments of DOF that are valid at high NAs have been published elsewhere^{5,7,12,30,32} and are beyond the scope of this review.

The increased DOF of immersion lithography relaxes process control requirements by improving the focus latitude. Conceptually, while the angle of light in the resist does not change for a given NA, the angle in the immersion fluid becomes smaller than that in air, which makes the focus less sensitive to minor variations in the vertical position of the wafer (Figure 5b).^{7,12,31} Additionally, the increased DOF may also reduce design restrictions, change the RET choices, and simplify the mask design.¹¹ The benefits of immersion lithography on DOF in this regime are shown for the case of dense line-space (L/S) patterns in Figure 6.

Immersion lithography can also increase resolution by allowing a larger angle in the coupling medium and thereby enabling hyper-NA imaging (Figure 5b).¹² Whereas light at larger incident angles will be lost to total internal reflection

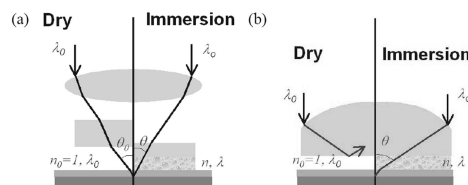


Figure 5. Benefits of immersion lithography. (a) Increased depth-of-focus due to a smaller angle θ in the coupling medium. (b) Increased resolution with higher numerical aperture optics by coupling light at larger incident angles. Reprinted with permission from ref 12. Copyright 2005 SPIE.

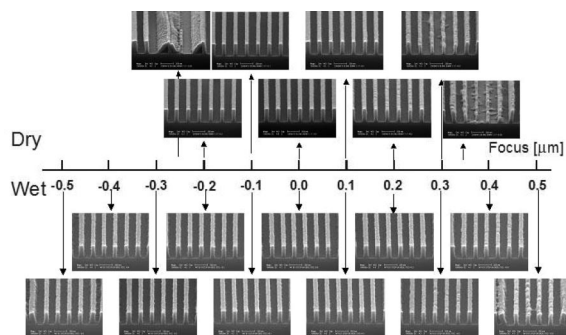


Figure 6. Cross-sectional scanning electron micrographs of 90 nm 1:1 L/S patterns showing the increased DOF enabled by water immersion lithography at 0.75 NA. Reprinted with permission from ref 9. Copyright 2004 SPIE.

within the lens in dry lithography, light at these large angles can be coupled into the higher index immersion fluid. Thus, the immersion fluid enables light containing the higher spatial frequency information (which propagates at larger values of θ) to be coupled into the resist.⁷ However, building a lens system capable of hyper-NA imaging with a practical field and lens size has required shifting from all refractive dioptric lens designs to mirror-containing catadioptric designs.^{8,10,33–35} The numerical apertures of state-of-the-art 193 nm water immersion lithography scanners are 1.3–1.35 NA.⁷

Immersion lithography has been considered at wavelengths other than 193 nm. Unfortunately, any increase in numerical aperture using immersion at 248 nm is offset by using the longer wavelength. For example, a fluid with a refractive index of 1.84 at 248 nm would be required to simply match the effective wavelength in 193 nm water immersion lithography. Immersion lithography at 157 nm would provide a benefit with a much lower refractive index immersion fluid (see Table 1);³⁶ however, finding materials with a high refractive index and high transparency at 157 nm is even more challenging than at 193 nm. Although some laboratory demonstrations^{36–39} of 157 nm immersion lithography have been able to pattern 32 nm half-pitch features and below using perfluoropolyether ($n \approx 1.37$) and siloxane immersion fluids ($n \approx 1.5$), no fluid with both satisfactory refractive index and transparency has yet been identified.^{37,40–42}

Meanwhile, the high refractive index ($n = 1.437$)^{37,40,43} and high transparency ($\alpha_{10} < 0.036 \text{ cm}^{-1}$)^{19,44a} of water at 193 nm and its ready availability within fabs with high purity at low cost made 193 nm water immersion lithography a potentially attractive option. Initial demonstrations of immersion lithography using water as an immersion fluid were made using 442,⁴⁵ 213,^{46,47} and 193 nm radiation.⁴⁸ Development of 193 nm immersion lithography proceeded very rapidly, moving from the first serious consideration by industry in mid-to-late 2002 to the development of alpha immersion exposure tools in late 2003 to the first imaging on a full-field scanner in early 2004.²¹ By late 2004, the fabrication of the first electrically yielding chips using immersion lithography was demonstrated.^{12,49} Immersion lithography was initially implemented into high volume manufacturing at the 55 nm node by several flash memory manufacturers.⁵⁰

The rapid progress of 193 nm immersion lithography would not have been possible without a considerable number of advances in patterning materials. In particular, the imposition of an immersion fluid in direct contact with the imaging layer places new demands upon the photoresist. However, before discussing specific immersion fluid-resist interactions and the development of immersion-compatible patterning materials, it

is instructive to briefly review the historical development of photoresist materials leading up to this point.

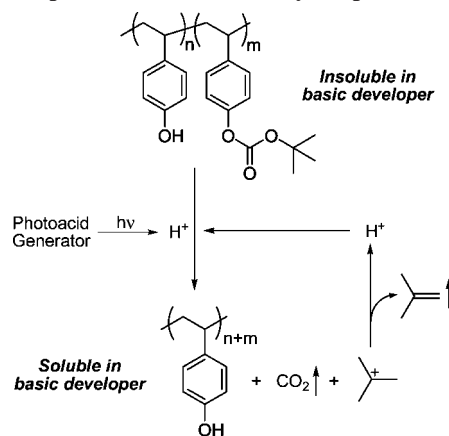
2.3. Photoresists for Optical Lithography

A number of excellent reviews have been published on nonchemically amplified g-/i-line photoresists⁵¹ and chemically amplified deep-ultraviolet (DUV) (e.g., 248, 193, and 157 nm) photoresists.^{52,53} Previous wavelength reductions have required significant changes in photoresist technology to accommodate the transparency and sensitivity requirements imposed by the new illumination wavelength and source power, respectively.¹ For example, the diazonaphthoquinone (DNQ)/novolac resists⁵¹ used in g-/i-line lithography were replaced by resists based on poly(hydroxystyrene), which are more transparent at 248 nm.^{52,53} In addition, photoresists such as g-/i-line resists that operate via a dissolution inhibition mechanism lacked sufficient photo-speed to maintain high wafer throughput given the lower power output of mercury lamp sources in the deep UV. Although high-intensity excimer laser sources were developed for 248 nm lithography, extensive line narrowing reduces the available power significantly and, therefore, these new sources did not dispense with the need for higher sensitivity resists.¹ New photoresists were developed that employed a chemically amplified solubility change mechanism (Scheme 1).^{52–54} Chemically amplified (CA) resists typically employ a photoacid generator (PAG), which produces a strong acid upon exposure with DUV radiation. This strong acid catalyzes a chemical reaction (such as the cleavage of the *t*-butoxycarbonyl (tBOC) group in Scheme 1) that changes the solubility of the photoresist in alkaline developer. Since a single photogenerated acid can catalyze many deprotection reactions, this catalytic cycle “chemically amplifies” the quantum yield of the overall process.^{52–54}

The high absorbance of the aromatic poly(hydroxystyrene) (PHS) resists at 193 nm necessitated the switch to more transparent polymer backbones (see Figure 7). Unfortunately, many polymers that are suitably transparent at 193 nm (such as acrylic polymers) lack the etch resistance of aromatic polymers.⁵⁵ To increase etch resistance, carbon-rich alicyclic groups were incorporated as side groups in acrylic resists or as main chain structures in cyclic olefin (e.g., norbornene-type) resists.^{52,53,56}

The planned transition from 193 to 157 nm lithography placed extreme demands upon the resist materials due to the high photon energy at 157 nm and the fact that many organic functional groups absorb at that wavelength.⁵⁷ The only two

Scheme 1. Operation of a Chemically Amplified Photoresist



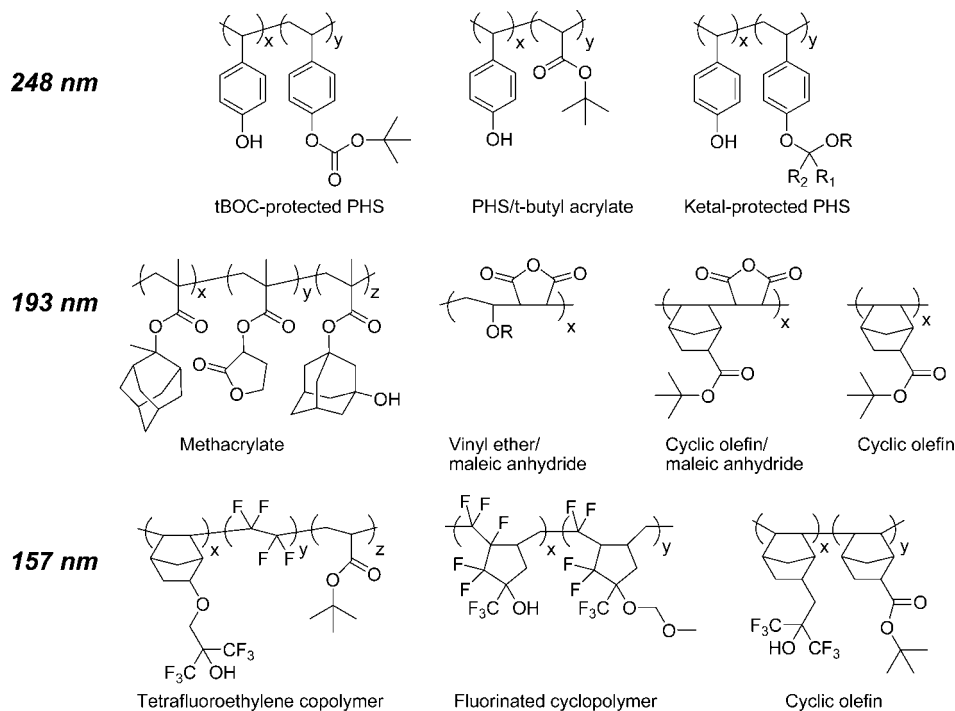


Figure 7. Typical chemically amplified positive-tone photoresist platforms for 248, 193, and 157 nm lithography.

classes of materials found to have high transparency at 157 nm were siloxanes and fluoropolymers. Unfortunately, the phenolic and carboxylic acid groups used as base-solubilizing groups in 248 and 193 nm resists were also too absorbing for use at 157 nm. Fluoroalcohols, such as the 1,1,1,3,3,3-hexafluoroisopropanol group (so-called hexafluoroalcohol (HFA)), can have pK_a 's similar to phenol due to the inductive stabilization of their conjugate bases.⁵⁸ The high transparency and good aqueous base dissolution properties of fluoroalcohol groups resulted in them being introduced as a base-solubilizing moieties in 157 nm resist designs (see Figure 7).⁵² While 157 nm lithography never reached high-volume manufacturing, some HFA-containing materials did find eventual use in 193 nm photoresists.^{52,59}

3. Materials for 193 nm Water Immersion Lithography

Since the imaging layer (i.e., the photoresist or a topcoat and photoresist stack) is in intimate contact with the immersion fluid during exposure, the roles of the tool, optics (including the immersion fluid), and the imaging layer become tightly coupled in immersion lithography. Any discussion of the properties and chemistry of photoresist materials for immersion lithography must also include an analysis of the properties and chemistry of ancillary materials such as topcoats and the immersion fluid itself. Additionally, the interactions of the immersion fluid with the last lens element (LLE), the interactions of the immersion fluid with the imaging layer, and the dynamics of these interactions during the course of wafer scanning must be understood and engineered. This review focuses primarily on the immersion-related developments in patterning materials with respect to 193 nm lithography, with particular emphasis on new immersion topcoats and photoresist materials, immersion fluids, and basic resist/fluid interactions. Readers interested in more detailed coverage of process-related developments in immersion lithography, antireflective coatings for hyper-

NA lithography, and resist shrink and trim processes/materials are referred to a recent text by Wei and Brainard.⁶⁰

3.1. Properties of Water Relevant to 193 nm Immersion Lithography

An ideal immersion fluid should have as large a refractive index as possible to provide the largest possible reduction in the effective wavelength; however, an immersion fluid must be highly transparent as well. Absorption by the immersion fluid leads to image apodization by creating a relative intensity difference between an incident ray that travels the shortest distance from the lens to the photoresist and that of the most oblique ray that travels the longest distance.^{41b} Absorption by the fluid also increases the propensity for radiation damage and heating of the fluid. Therefore, an ideal fluid should possess a low absorption coefficient, a low thermo-optic coefficient (dn/dT), high specific heat capacity, high thermal conductivity, and low viscosity in order to maintain stable optical properties and prevent focus errors and spherical aberrations.^{8,9,41,61–63} For example, the optical path difference between two rays should not exceed a quarter wavelength, requiring

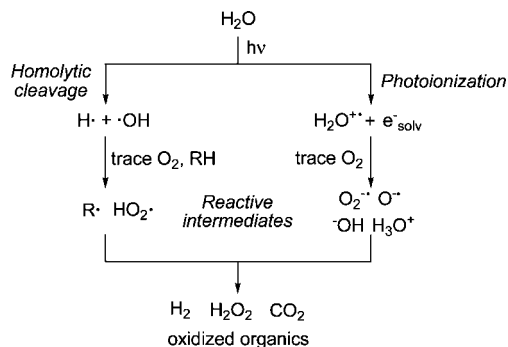
$$\delta n \leq \frac{\lambda \cos \theta}{4t} \quad (3)$$

wherein δn is the change in the refractive index and t is the thickness of the fluid layer.¹³ This relationship is used to define the requirements for local^{10,64} and bulk temperature stability of the immersion fluid, pressure stability, and fluid thickness (i.e., the gap height between the last lens element and the imaging layer).⁸

The values for several properties of water relevant to immersion lithography are listed in Table 2. Most significantly, the refractive index of water is 1.437 at 193.4 nm and its absorption coefficient is 0.036 cm^{-1} ,^{43,44b} however, the measured absorbance of water at 193 nm is very sensitive to trace amounts of extrinsic contaminants. To meet the

Table 2. Properties of Water Relevant to Immersion Lithography

property	value	ref.
n (193.39 nm, 21.50 °C)	1.43662(2)	43
dn/dT (194.5 nm, 21.50 °C)	$-1.00(4) \times 10^{-4} \text{ °C}^{-1}$	43
$dn/d\lambda$ (193.39 nm, 21.50 °C)	$-2.109(17) \times 10^{-3} \text{ nm}^{-1}$	43
absorbance (α_{10})	0.036 cm^{-1}	44b
surface tension	72.76 mN/m	141
viscosity	0.001006 Pa s	141

Scheme 2. Photochemistry of Water under 193 nm Immersion Conditions

stringent property and stability requirements required for immersion lithography, water polishing systems are commonly installed to improve the fab deionized (DI) water stream before it enters the water conditioning systems of the scanner.^{49,65} Water treatment systems remove dissolved gases, particles, soluble organic and inorganic compounds, bacteria, and other contaminants from water and provide the immersion tool with a high flow rate (up to 3 L/min) of water at a stable temperature (within a few mK).^{66,67}

3.1.1. Photochemistry of Water at 193 nm

The photochemical reactions of water during 193 nm immersion exposure have been studied along with their potential impact upon the resist film.⁶⁹ When irradiated by 193 nm light, water undergoes homolytic cleavage to produce hydrogen atoms and hydroxyl radicals and photoionization to produce water radical cations and solvated electrons (Scheme 2).⁷⁰ The short-lived species resulting from irradiation react to

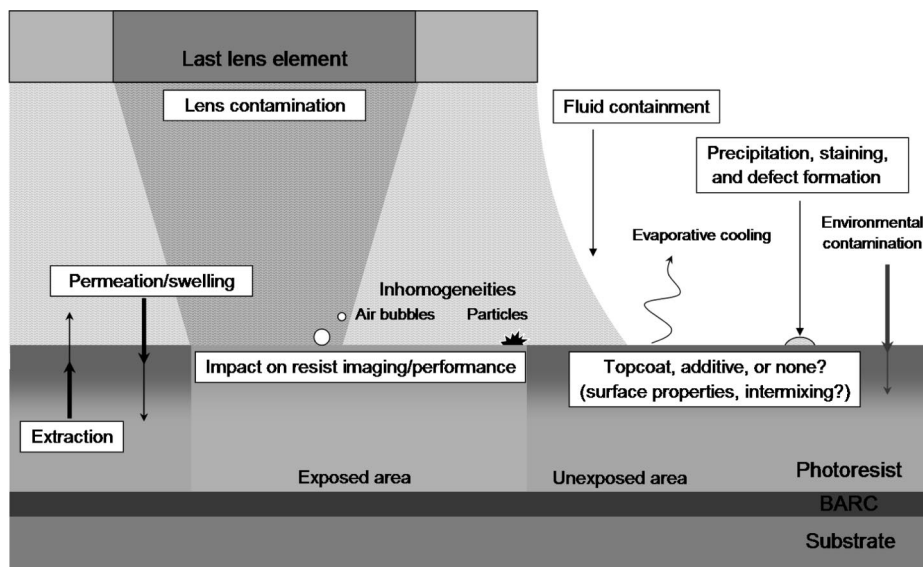
form more stable products such as hydrogen peroxide and molecular oxygen. The ionic photoproducts neutralize each other and have a minimal net impact on the overall pH.⁶⁹ The potent oxidizing agents (particularly hydroxyl radicals) react with dissolved organic compounds in the water to form oxidized species including CO_2 .⁶⁹ In particular, reaction of these oxidizing photoproducts with the resist surface under model immersion exposure conditions was estimated to be confined to the top 10 nm of the resist film and, therefore, was not expected to impact lithographic performance.⁶⁹

3.1.2. Scattering and Bubble Formation

The replacement of a nitrogen atmosphere with an aqueous immersion fluid introduces concerns about the scattering of light by the immersion fluid or inhomogeneities such as air bubbles or particles therein. The integrated total scattering intensity (Rayleigh + Raman scattering) was calculated to produce flare of less than 10^{-6} that of the incident intensity.⁷¹ However, another source of scattering, air bubbles, can arise from air entrainment during fluid filling, fluid flow, or wafer scanning, evolution of dissolved gases, and resist outgassing.⁷ Macroscale air entrainment in the advancing meniscus is calculated to occur only when the substrate velocity is greater than 17 m/s, which is more than 30 times larger than relevant wafer scan rates.⁷² Similarly, air entrainment due to meniscus flow over microscale topographical features during filling or wafer scanning was not found to pose a problem for immersion lithography.^{72,73} Other possible sources of surface-bound air bubbles include the spontaneous formation of nanobubbles on water-immersed hydrophobic surfaces^{71,74,75} and outgassing⁷¹ of volatile resist components. While transient bubbles were formed during exposure of a 248 nm photoresist (APEX-E, which employs a *t*-butoxycarbonyl protecting group) under immersion conditions, no such bubble formation was observed with typical 193 nm resists.^{71,76}

3.2. Interaction of Water with 193 nm Photoresist Materials

A number of important interactions between the immersion fluid and the imaging layer in immersion lithography are illustrated in Figure 8. Among the important interactions to

**Figure 8.** Important fluid/photoresist interactions in immersion lithography.

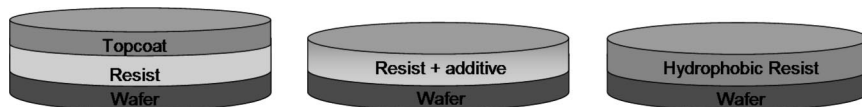


Figure 9. Approaches to immersion-compatible patterning materials.

be understood are the kinetics of water penetration into the photoresist film, the kinetics of photoresist component extraction into the immersion fluid, the influence of resist surface properties on water containment during scanning, the interaction of residual water droplets with the photoresist, the formation of bubbles and particles at the resist surface, and the combined impact of these interfacial phenomena on lithographic profiles (e.g., t-topping, footing, undercutting, etc.), performance (process window, photospeed), and defect formation (i.e., defectivity).^{20,77b,78}

Conventional 193 nm photoresists predate the advent of mainstream immersion lithography and, therefore, tend to not perform well under immersion conditions. Several materials strategies (shown in Figure 9) have been employed to improve the immersion compatibility of conventional imaging materials. The first and most widely explored strategy involves the application of a protective topcoat material on top of the photoresist. Protective topcoat layers enable the continued use of resists designed for dry lithography while protecting the immersion scanner from contamination by resist components (especially PAG) leached into the immersion fluid. Protective polymeric topcoats had been previously used in 193 nm dry imaging to provide reflectivity control⁷⁹ as well as to protect the resist against environmental contamination.^{80–82}

Immersion topcoat materials fall into one of two general categories: solvent-developable and alkali-developable. Solvent-developable topcoats typically consist of extremely hydrophobic fluoropolymers that are alkali-insoluble and, therefore, must be removed with a special solvent prior to development of the photoresist pattern. While these solvent-developable topcoats were the first topcoats demonstrated in immersion lithography,⁴⁷ the extra topcoat-removal steps as well as the cost of the special topcoat-removal solvent increases the costs associated with their use. Recycling systems for the topcoat remover have since been introduced to reduce the added process cost.⁸³ More attractive alkali-soluble topcoats can be stripped during the course of photoresist development using standard 0.26 N tetramethylammonium hydroxide (TMAH) photoresist developer.^{82,84–86} In order to further reduce the added process and materials costs associated with the use of topcoats, a number of topcoat-free immersion-compatible resists have recently been developed based on resists incorporating surface-segregating additives or hydrophobic resist materials with nonleaching PAGs.

Regardless of the strategy employed to improve immersion compatibility, a host of materials properties and interactions must be understood. In the case of the addition of a topcoat layer into the imaging stack, these new interactions include the impact of a topcoat on water uptake and resist component leaching, the ability of a topcoat to control water contact angles and water containment during scanning, and the impact of the topcoat on the performance of the underlying resist.

3.2.1. Diffusion of Water into Photoresists

Water uptake into the resist film can change its properties or alter the kinetics of the chemical reactions that change

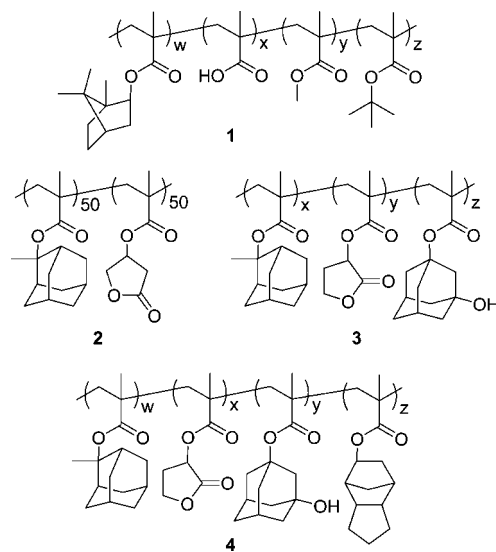


Figure 10. Typical 193 nm resists tested for water uptake and component leaching: IBM-V2 (1), Clariant T518 (2), TOK Poly-ILP01 (3), and TOK Poly-ILP04 (4).

the resist dissolution rate (especially for the acid-catalyzed hydrolysis of acetal protecting groups).^{82,87–90} The structures of typical resist materials examined in water interaction studies are shown in Figure 10.^{20,82,91}

All resists studied show measurable increases in mass and thickness when placed in contact with water.^{20,82,92–94} The kinetics of water diffusion into the resist material as derived by Crank is described by eq 4.^{82,95}

$$\frac{M(t)}{M_{\infty}} = 1 - \frac{8}{\pi^2} \sum_{n=0}^{\infty} \frac{1}{(2n+1)^2} \exp\left[-\frac{(2n+1)^2 \pi^2 D t}{L^2}\right] \quad (4)$$

wherein $M(t)$ is the mass uptake at time t , M_{∞} is the mass uptake at infinite time, D is the diffusion coefficient, and L is the film thickness. For short water-contact times, the solution is given by eq 5

$$\frac{M(t)}{M_{\infty}} = 2\sqrt{\frac{Dt}{L^2}} \left(\frac{1}{\pi^{1/2}} + 2 \sum_{n=1}^{\infty} (-1)^n \operatorname{ierfc}\left[\frac{nL}{\sqrt{Dt}}\right] \right) \quad (5)$$

wherein ierfc is the integrated complementary error function.^{82,95} The majority of water uptake occurs in the first few seconds of water contact (as seen in Figure 11).^{20,92,94} For example, finite element modeling indicated a resist film is over 50% saturated in 5 s and 93% saturated in 15 s.⁹² For short contact times ($M(t)/M_{\infty} < 0.6$), modeling the water uptake using a single diffusion coefficient provides a good fit to the experimental data.^{92,93} For longer contact times, water uptake has been described using time-dependent diffusion processes⁹⁴ or multiple diffusion processes.^{20,82}

Although swelling of 193 nm resist films by water is observed, the actual film thickness change is typically small.²⁰ The water uptake of a resist per unit thickness is roughly

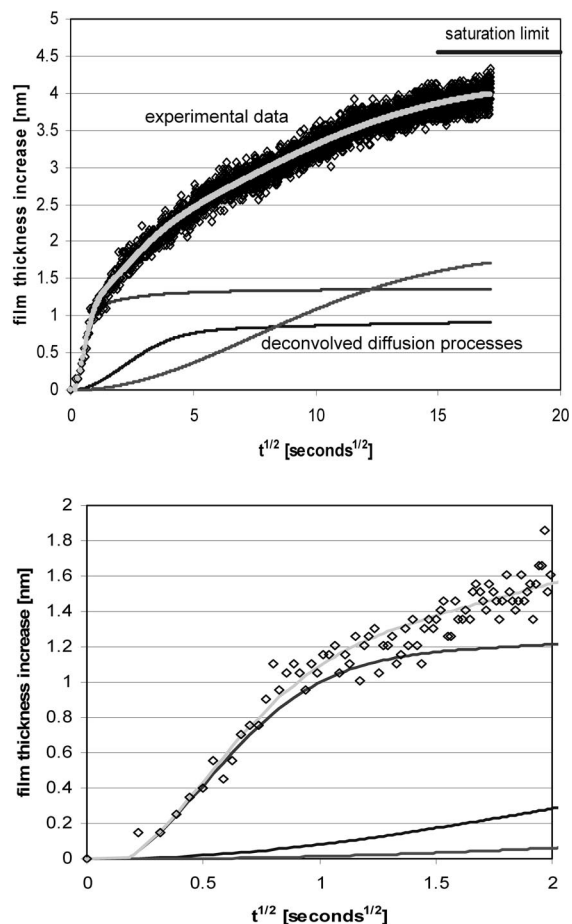


Figure 11. Water uptake of a 200 nm thick film of TOK ILP01 (3) for moderate (top figure) and short (bottom figure) immersion times. Open circles are experimental data points. The lighter solid line represents fitting to experimental data, and the darker solid lines represent the deconvolved contributions from three distinct diffusion processes. Reprinted with permission from ref 20. Copyright 2004 SPIE.

constant and increases with exposure and increased resist hydrophilicity.⁹⁶ In particular, the water uptake fraction of the fast diffusion process in Figure 11 was observed to be roughly equivalent of the molar fraction of polar hydroxyl- and lactone-containing monomers in the resist polymer.^{20,82} In addition to having a lower water diffusion coefficient than phenolic-based 248 nm resists,^{20,82} typical 193 nm methacrylate resists were found to absorb less water (~1.5–4 wt %) than hexafluoroisopropanol-functionalized norbornene addition polymers (5–8 wt %), poly(hydroxystyrene) (9–10 wt %), and novolac (2–5 wt %).^{91,93} Polymeric topcoats (whether alkali soluble or organic-developable) have been shown to be permeable to water by reflectance^{97,98} and quartz crystal microbalance^{90,91,99,100} measurements. Even though highly fluorinated organic-developable topcoats absorb very little water themselves (<0.1 wt %),^{88,100} water still permeates through them (albeit less than through more hydrophilic alkali-soluble topcoats) and is taken up into the underlying resist.⁹⁷ Interestingly, Foubert et al. showed that the uptake of water of a resist-topcoat stack is generally not the sum of the water uptake of the individual layers.⁹⁶ The presence of a topcoat could actually enhance the water uptake into the resist by up to a factor of 3. This was initially attributed to intermixing of the topcoat and resist;¹⁰¹ however, further

experiments indicated the additional water uptake was not localized at the topcoat–resist interface.⁹⁶

While the presence of water during immersion exposure has a measurable effect on the modulation transfer function (MTF) of 248 nm resists (an increase for UVII-HS and a decrease for KRS XE3), the presence of a topcoat had little to no impact.⁹⁷ The detrimental impact of water on the KRS resist is not surprising given its acid-catalyzed hydrolysis mechanism.^{87,88} There was little change in the intrinsic image blur of several 193 nm resists with or without topcoat under immersion conditions, presumably due to the aforementioned lower water uptake of 193 nm resists relative to 248 nm materials.⁹⁷ In addition, a topcoat was observed to suppress outgassing of deprotection fragments from the resist film^{97,102} as well as to reduce the effects of airborne environmental contamination.^{81,97}

3.2.2. Extraction of Photoresist Components into Water

While typical lens materials exhibit sufficient durability in the presence of ultrapure water,¹⁰³ growth of photogenerated contamination layers on the last lens element and other tool surfaces may result in increased absorbance, light scattering, or particle generation. Although such contamination deposits can be removed, additional cleaning processes would significantly affect tool uptime and wafer throughput.¹⁶ The outgassing of photoresists and its potential for lens contamination has been previously studied in the case of dry lithography.^{104,105} In immersion lithography, the risk of lens contamination is dependent upon the extraction rate of photoresist components into the immersion fluid, the structure and deposition efficiency of the contaminant, and the fluid dynamics in the immersion showerhead (fluid velocity, gap height, flow geometry, etc.).¹⁰⁶

A number of studies have been published on the controlled photocontamination of lens surfaces by organic contaminants including extracted resist components.^{107–110} Although typical solvents and plasticizer materials were not shown to induce lens contamination,¹⁰⁷ lens contamination due to iodonium and sulfonium-based PAGs has been observed at concentrations above 300 ppb, with a strong dependence upon the PAG cation structure.^{108–110} Ionic PAGs with high fluorine content preferentially enrich the air–resist interface (surface concentrations 20–70 times greater than the bulk concentration).¹¹¹ This high local concentration of PAG at the resist surface makes it particularly susceptible to leaching into the immersion fluid. For example, around 50% of the PAG was depleted from the top 25 nm of a IBM-V2 methacrylate resist (1) film as a result of water contact.²⁰ Various experimental measurements of PAG extraction indicate that 5–10% of the total PAG content can be leached from the resist film.^{20,102,112} Liquid scintillation counting (LSC) experiments with resists containing ¹⁴C-labeled components showed that 30–50 ng/cm² of PAG was extracted, with most of the extraction occurring in the first 10 s and minimal extraction after 30 s.⁹¹ Base extraction was found to be ~2 ng/cm² and to occur on the same time scale.⁹¹ Accordingly, tool vendors have established general leaching specifications based on maximum rates of PAG extraction (ASML: 1.6×10^{-12} mol/(cm² s), Nikon: 5×10^{-12} mol/(cm² s)).^{101,113}

Many experimental techniques have been devised to measure the kinetics of resist component extraction by water in order to meet these specifications. These techniques include simple contact of the resist surface to water confined in an O-ring or vial, flowing water through a specifically

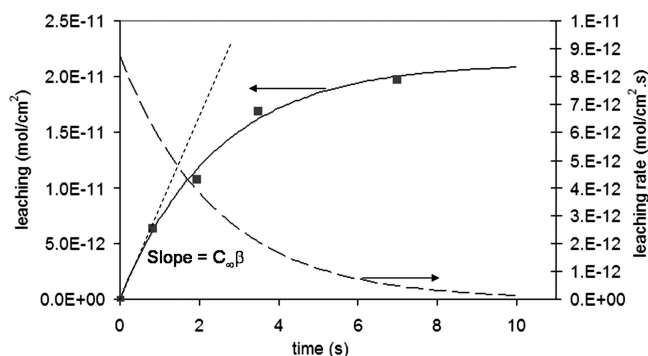


Figure 12. Dynamic measurement of PAG leaching from a dry 193 nm photoresist (Sumitomo PAR-817). Adapted with permission from ref 117. Copyright 2006 SPIE.

designed cell mounted on the wafer, or dragging a drop or puddle of fluid across the resist-coated wafer.^{20,82,86,114–119} In an attempt to standardize leaching measurements, many vendors now utilize a dynamic method employing a multi-channel flow cell (so-called dynamic WEXA).¹¹⁶

In order to accurately determine PAG leaching rates, Dammel et al. have modeled the kinetics of PAG leaching with a single exponential model

$$N = N_0 \cdot e^{-\beta t} \quad (6)$$

wherein N is the number of leached PAG molecules and N_0 is the total quantity of leachable PAG molecules.^{114,115} The time-dependent PAG concentration C in the fixed volume of immersion fluid is then given by

$$C = C_\infty(1 - e^{-\beta t}) \quad (7)$$

wherein C_∞ is the saturation concentration at infinite time.^{114,115} For short times, this equation can be approximated by

$$C \approx C_\infty \beta \cdot t \quad (8)$$

wherein the initial rate of PAG leaching at time zero is $C_\infty \beta$. An example of measured PAG leaching from a typical dry 193 nm photoresist is shown in Figure 12.

For longer soak times, a dual exponential model has been used to fit PAG leaching data, with the two leaching processes being attributed to rapid diffusion of PAG from the resist surface and much slower PAG diffusion from the bulk of the film.¹¹³ Rathsack et al. suggested that the leaching behavior of resists could be explained by a nonuniform initial PAG distribution and a nonuniform PAG diffusion coefficient.⁹² The use of a nonuniform PAG distribution reduced the calculated PAG depletion depth to ~ 3 nm, which is slightly shallower than the ~ 4 – 6 nm calculated by Taylor et al.⁹¹ (who assumed a uniform PAG distribution) and the depletion depths measured experimentally.^{20,102}

Prerinsing the wafer with water removes the easily leached PAG from the resist surface and reduces subsequent PAG leaching during the immersion process by roughly 80–90%.^{68,91,114,115,117,120,121} In order to explain why PAG leaching can still be observed from the supposedly PAG-depleted prerinsed surface, Dammel et al. proposed that additional PAG from within the film repopulates the resist surface during the drying process.¹¹⁴

Many groups have attempted to correlate the structure of photoacid generators and their photoacids with their leaching behavior. The leaching parameters for a variety of triphenylsulfonium-based photoacid generators are listed in Table 3.^{114,115} The time constant β of leaching typically ranges from

Table 3. Leaching Parameters for Triphenylsulfonium Salt Photoacid Generators (Reprinted with Permission from Ref 114; Copyright 2005 SPIE)

anion	C_∞ [mol/cm ²]	β [s ⁻¹]	τ [s]	$C_\infty \beta$ [mol/(cm ² s)]
CF ₃ SO ₃ ⁻	6.7×10^{-12}	0.23	3.0	1.56×10^{-12}
C ₄ F ₉ SO ₃ ⁻	6.3×10^{-12}	0.43	1.6	2.71×10^{-12}
C ₈ F ₁₇ SO ₃ ⁻	4.1×10^{-12}	0.68	1.0	2.75×10^{-12}

~ 0.1 – 1.3 s⁻¹.^{114,115,117,122} While triphenylsulfonium perfluorooctanesulfonate shows lower saturation concentrations than analogous triflate- or nonaflate-based PAGs, it exhibits a higher time constant β (presumably due a higher surface concentration).^{114,115} When selecting a PAG for immersion applications, however, it is important to take into account a number of other properties in addition to leaching behavior. For example, while triphenylsulfonium triflate shows the lowest rate of leaching ($C_\infty \beta$) of the PAGs listed in Table 3, the higher diffusivity of triflic acid in the resist film can lead to image blur.^{86,114,115} A few low-leaching PAGs shown in Figure 13 have bulky hydrophobic substituents that reduce their water solubility (**5**–**6**) or alternative anions such as the cyclic fluorinated disulfonylimidate in **7**.^{123,124}

In the case of exposed resist films, increased levels of photoacid leaching are commonly observed (both higher C_∞ and higher β),¹¹⁷ although this behavior is highly dependent upon the photoacid structure.^{121,124} In order to achieve low levels of photoacid leaching, Wada et al. developed PAGs that feature large hydrophobic anchoring groups connected by an acid-labile linkage to the anion.¹²⁵ While the wafer is being exposed in the immersion scanner, this large anchor group reduces photoacid leaching; however, cleavage of the linkage by the photoacid in the exposed regions during the postexposure bake (PEB) facilitates diffusion.

Despite the inability of the topcoats to prevent water penetration into the resist film, they are an effective means by which to prevent PAG leaching into the immersion fluid. Typically, greater than 90% reduction in the amount of PAG leaching is observed with the use of a topcoat.^{82,97,112,115,117,126} Interestingly, topcoats are unable to reduce PAG leaching levels in direct proportion to their thickness.^{99,115,117} In general, PAG leaching with a topcoat is predominantly from the topcoat surface with little PAG diffusion through the topcoat film itself.^{115,117,122} Analysis of topcoat–resist film stacks reveals that PAG and other resist components can migrate into the topcoat film during casting.^{102,112,122,127–129} For certain topcoat–resist pairs, this intermixing layer is substantial (see Figure 14).¹⁰² The intermixing of resist components with the topcoat is strongly dependent on the polarity of the topcoat casting solvent, with alcoholic solvents causing increased intermixing relative to less polar ethereal or hydrocarbon solvents.^{102,117,130} In addition, the presence of a strong intermixing layer generally results in a region

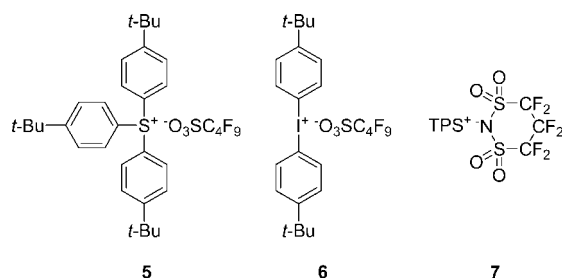


Figure 13. Photoacid generators with lower water solubility.

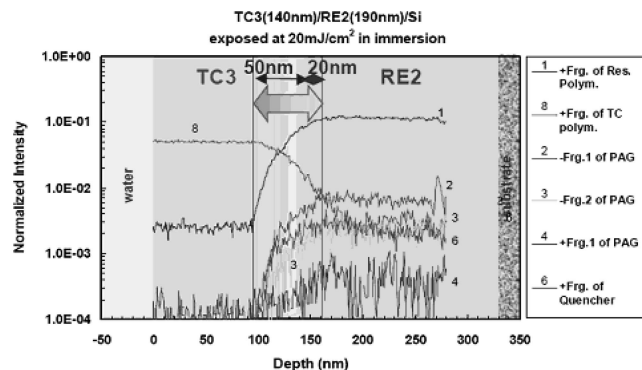


Figure 14. Depth profile of a topcoat (TC3)—photoresist (RE2) film stack by secondary ion mass spectroscopy. A 70 nm thick interdiffusion region between topcoat and resist components is indicated by the large double-headed arrow. Reprinted with permission from ref 102. Copyright 2005 SPIE.

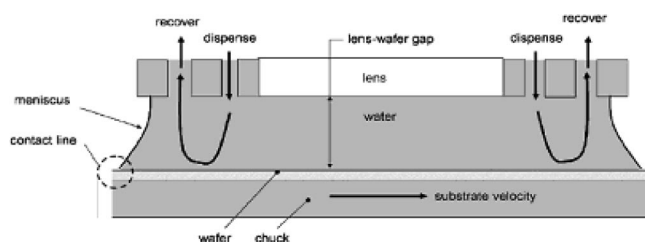


Figure 15. Schematic of an immersion showerhead. Reprinted with permission from ref 72a. Copyright 2006 SPIE.

with slower dissolution rate during development, increased surface roughness after development, and T-top formation in the final resist profiles.^{102,112}

3.2.3. Water Contact Angles, Film Pulling, And Fluid Handling

Three methods to contain the immersion fluid on the wafer have been explored: stage immersion, wafer immersion, and local delivery. In stage and wafer immersion, large pools of water are employed to submerge the entire wafer; however, these two approaches are not considered to be feasible due to long fluid fill/removal times and long relaxation times for fluid motion caused by stage movement.^{9,10} Instead, all commercial immersion scanners use a local delivery method in which water is circulated in a localized pool under the lens by a showerhead (also referred to as an immersion hood, immersion nozzle, etc.). (see Figure 15).^{8,10,72a} This configuration enables rapid fill and removal processes as well as allowing alignment, focusing, and leveling techniques to remain unchanged.⁷ In order to maintain fluid in the lens/wafer gap as the wafer is scanned rapidly, surface tension forces must be sufficient to counteract viscous and inertial forces. With any given imaging material, the fluid can no longer be contained when the wafer scan rate exceeds a critical velocity at which point liquid is left behind on the wafer. Controlling the water may be particularly difficult as the wafer edge moves under the pool of water.^{8,10} As will be discussed later, the evaporation of residual fluid droplets on the wafer has been strongly correlated with various patterning defects. Therefore, the critical velocity of the resist surface strongly influences both the maximum acceptable wafer scan rate (i.e., wafer throughput) and defectivity (i.e.,

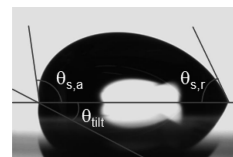


Figure 16. Measurement of static advancing ($\theta_{s,a}$) and receding ($\theta_{s,r}$) water contact angles by tilting sessile drop method (stage and camera tilted by θ_{tilt}).

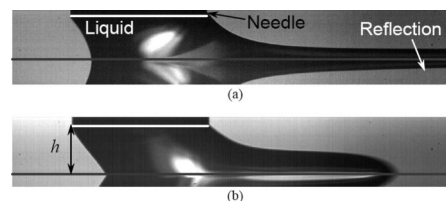


Figure 17. Meniscus shapes of a water droplet held under a needle during substrate scanning. Failure modes shown are (a) film pulling on a surface with a low SRCA and (b) inertial instability on a surface with higher SRCA. Reprinted with permission from ref 141. Copyright 2006 SPIE.

yield). Much additional work has focused on how to prevent fluid loss by improvements to showerhead design^{131,132} and stage speed, acceleration, and routing during exposure.¹³³

To study the fundamental interaction of water with immersion surfaces, contact angle measurements are made using commercially available systems.^{134–137} In the tilting sessile drop method shown in Figure 16, for example, a droplet of water is placed on a coated substrated that is tilted until the droplet begins to slide. The static advancing contact angle (SACA, $\theta_{s,a}$) and static receding contact angle (SRCA, $\theta_{s,r}$) are determined just before the drop begins to slide. The difference between the SACA and the SRCA is referred to as contact angle hysteresis and is a composite measure of the roughness, chemical heterogeneity, and reorientation/mobility of molecules on the surface.¹³⁸ In general, immersion materials with high SRCA values and low contact angle hysteresis are preferred for immersion lithography. Additional experimental apparatus have been designed to accurately determine the impact of substrate velocity and acceleration on the dynamic wetting and dewetting behavior of water on moving photoresist surfaces.^{134,139,140}

Fluid loss has been found to occur via two mechanisms: film pulling and inertial instability (as shown in Figure 17).^{134,140–142} Film pulling occurs when the dynamic receding contact angle approaches zero and a thin layer of fluid is pulled out behind the receding meniscus.¹⁴³ The film pulling velocity (v_{fp}) can be modeled by

$$v_{fp} = C_1 \bar{v}_{ca} \theta_{s,r}^3 \quad (9)$$

wherein C_1 is an empirical constant, $\theta_{s,r}$ is the static, receding contact angle, and the capillary velocity \bar{v}_{ca} is defined as

$$\bar{v}_{ca} = \frac{\gamma}{\mu} \quad (10)$$

wherein γ is the surface tension and μ is the dynamic viscosity of the fluid.^{137,141,144} Film pulling of water is frequently observed at low velocities on hydrophilic surfaces (i.e., those with low SRCA values).

Fluid loss by inertial instability occurs when the fluid surface tension is insufficient to counteract the inertial force

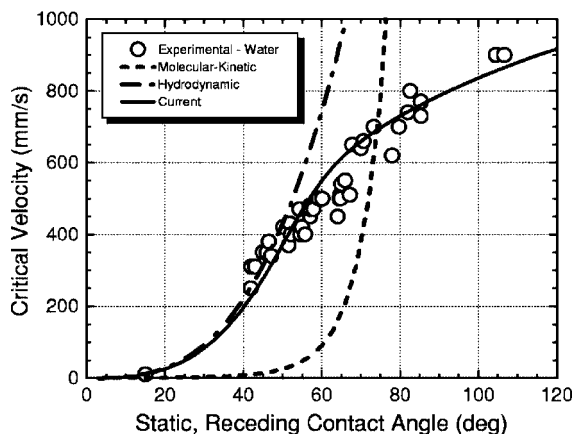


Figure 18. Comparison of various models with experimental measurements of the critical velocity for fluid loss with respect to static receding contact angle. Reprinted with permission from ref 137a. Copyright 2007 SPIE.

imposed by the fluid at the receding meniscus.^{134,137,140,141} In this case, bulk fluid loss occurs when droplets of fluid break off from the extended receding meniscus. Failure by inertial instability is frequently observed at high wafer accelerations and velocities on more hydrophobic surfaces (i.e., those with higher SRCA values). The inertial instability velocity (v_{in}) can be modeled by

$$v_{in} = C_2 \bar{v}_{in}^{3/4} \bar{v}_{ca}^{1/4} \sin^{3/4} \left(\frac{\theta_{s,r}}{2} \right) \quad (11)$$

wherein C_2 is an empirical constant and \bar{v}_{in} is given by

$$\bar{v}_{in} = \sqrt{\frac{\gamma}{\rho \kappa^{-1}}} \quad (12)$$

wherein ρ is the density of the fluid and κ^{-1} is

$$\kappa^{-1} = \sqrt{\frac{\gamma}{\rho g}} \quad (13)$$

wherein g is the acceleration due to gravity.^{137,141}

Shedd et al. fit the experimental critical velocities for fluid loss (v_{crit}) by asymptotically matching the terms describing the film pulling and inertial instability velocities (Figure 18).^{137,141}

$$v_{crit} = (v_{fp}^{-m} + v_{in}^{-m})^{-1/m} \quad (14)$$

An inflection point is observed near a static receding contact angle of 65° , where the failure mode switches from film pulling to inertial instability.

In reality, the velocity at which fluid containment fails is not solely determined by the immersion surface but is also heavily impacted by a number of factors including shower-

head design^{131,132} and stage speed, acceleration, and routing during exposure.¹³³ However, these simplified dynamic measurements of wetting and dewetting behavior and the accompanying empirical models have generally proved useful in immersion materials design and screening. According to Figure 18, a material with a SCRA of $\sim 60^\circ$ is necessary to enable commercially viable wafer scan rates of 500 mm/s without fluid loss.^{137,145} Typical dry 193 nm resists have static receding contact angles in the range of $43\text{--}53^\circ$ (see Table 4), rendering them unsuitable for high-speed scanning.¹³⁴ In order to have a margin of safety and to accommodate scan rates greater than 500 nm/s, immersion surfaces (particularly topcoats) with SRCA values $\geq 70^\circ$ are generally desired. As shown in Table 4, the SRCA values of a few representative commercial immersion topcoats and topcoat-free resists are currently at or above this level.

3.2.4. Defectivity Issues in Water Immersion Lithography

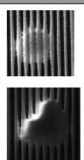
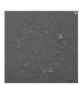
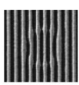
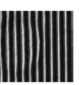
In order to achieve defectivity levels similar to that of dry lithography, an enormous effort was directed toward identifying, classifying, and determining the root cause of various defects associated with immersion lithography.^{60,73,78,96,99,101,108,110,132,147–156} As shown in Figure 19, typical defects can be classified into nonimmersion defects (particles, microbridging, and coating defects) and immersion-related defects (air bubbles, topcoat blister/resist swelling, drying stains, and watermarks). Since the mechanisms of defect formation in 193 nm immersion lithography and process-related defect reduction strategies have been recently reviewed by Wei and Brainard,^{60,155} only a brief overview will be presented here.

Nonimmersion Defects. Particles. Particles suspended in the immersion fluid near the wafer surface or lying on top of the resist/topcoat can be imaged into the underlying resist or transferred to the underlying resist during development.^{60,91,110,149} Although particles are not inherently immersion-related, immersion lithography introduces new mechanisms by which particles may interfere with imaging.¹²⁶ Particles generated by peeling/flaking of loosely adhered topcoat, resist, or bottom antireflective coating (BARC) material near the wafer bevel can be transferred elsewhere on the wafer or the surrounding stage (where they can contaminate future wafers).^{99,132,148,157} In order to reduce particle levels, engineering of the wafer bevel area (including optimized topcoat coating processes, immersion-specific edge bead removal processes, and wafer bevel cleaning processes) and improved tool hygiene procedures (such as automated stage cleaning processes) have been implemented as reviewed elsewhere.⁶⁰

Bridging. Microbridging between lines is a nonimmersion-specific defect typically attributed to resist nonuniformity (e.g., gels) or BARC defects, which may generally be

Table 4. Water Contact Angles of Various Lithographic Materials and Substrates

type	material	static CA	adv. CA	rec. CA	ref.
substrates	fused silica	48.6°	55.8°	39.5°	134
	quartz mask blank	41.5°	50.1°	34.9°	134
dry photoresists	Sumitomo PAR817	67.7°	76.8°	42.6°	134
	TOK TARF6111	66.8°	75.4°	52.7°	134
	JSR 237J	70.0°	79.3	52.6	134
	Sumitomo IM850			57°	99
immersion photoresist	Sumitomo IM850			57°	99
	alkali-soluble topcoats	TOK TILC-031	78.0°	67.1°	145
topcoat-free photoresists	JSR TCX-041	78.9° ¹⁴⁶		69°	119
	JSR AIM5570JN	90°		80°	119
	JSR AIM5120JN	95°		86° ¹⁵⁰	119
organic-developable topcoat	TOK TSP-3A	117.0°		115.0°	145

Class	Pattern expansion	Drying stains	Inverted attenuation	Pattern attenuation
examples				
Structure	Circular or irregular	round deposits	Circular shape	circular shape
Size	0.1 – 10 μm	1 – 1000 μm	Narrower pitch 0.1 – 1 μm	Wider pitch 0.5 – 2 μm
Root Cause	Droplet interaction with resist	Droplet drying after resist leaching	Droplet swelling topcoat/resist before exposure	Bubble on topcoat/resist

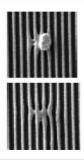
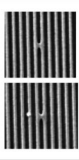
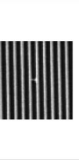
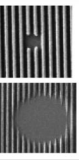
Class	Printed particle	Bridge	Micro Bridge	Missing Pattern
examples				
Structure	Irregular, Particle affecting pattern	Bridge between 2 lines	hair-like bridge between 2 lines	Circular, resist is gone
Size	0.1 – 5 μm	< 0.5 μm	< 0.2 μm	0.1 – 5 μm
Root Cause	Particles exposed	Resist process or small particle	Incomplete develop/rinse or small particle	solvent splash back in track

Figure 19. Characteristic patterning defects produced during immersion lithography and their root causes. Reprinted with permission from ref 132a. Copyright 2007 SPIE.

reduced by proper filtration.¹⁵⁵ Microbridging defects also increase as the resolution is pushed beyond the capability of the original dry photoresist.¹⁵¹ Immersion lithography, however, introduces potential new sources of bridging including the presence of low dissolution rate material in resist–topcoat intermixing layers.

Immersion-Related Defects. Air Bubbles. The impact of an air bubble on imaging performance depends upon the bubble lifetime¹⁵⁸ as fraction of exposure time and the relative distance⁹ of the bubble from the wafer. Bubbles closer to the wafer are more problematic due to their stronger shadow and the longer residence time over a position on the wafer (due to the slower fluid flow near the wafer surface).^{71,76} Many simulations have been performed to assess the impact of various free and surface-bound air bubbles on immersion lithography.^{71,76,159–162} Surface-bound air bubbles have been found to produce defects characterized by significant underexposure^{60,155,161,162} and geometry-dependent pattern distortion (i.e., magnification).¹⁵⁵ This class of defects has been largely addressed by fluid degassing¹⁶³ and improvements in tool and showerhead design, which have been reviewed elsewhere.⁶⁰

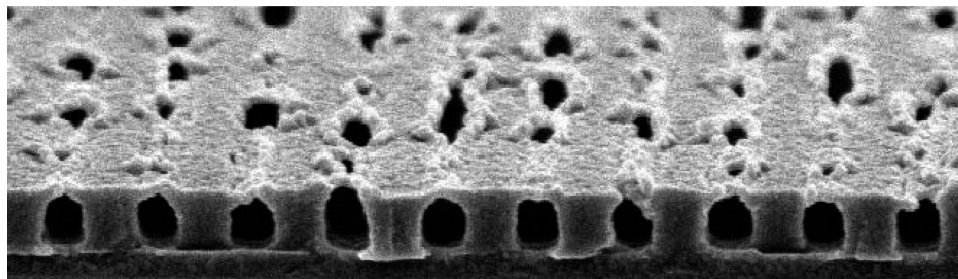


Figure 20. Cross-sectional scanning electron micrograph of a watermark defect formed by the evaporation of a water droplet on the surface of a photoresist during the postexposure bake process. Reprinted with permission from ref 169. Copyright 2005 SPIE.

Topcoat Blisters/Resist Swelling. Prior to exposure, water may penetrate the topcoat (often through small pinholes⁹⁸) and form circular blisters¹¹⁰ or induce swelling of the resist.¹⁶⁴ The blister or swelling causes a lensing defect during exposure, which is exhibited by a circular region with narrower pitch.^{110,132,151,152,155} The topcoat blister defect was predominantly observed with early base-soluble topcoats, and improvements in topcoat materials have largely eliminated this type of defect.^{60,155}

Drying Stains. Drying stains are the result of deposition of contaminants during droplet evaporation and can take the form of a singular island or well-known “coffee stain”¹⁶⁵ patterns depending upon the physics¹⁶⁶ of the droplet drying process.¹³² Controlled contamination studies have placed droplets of pure or contaminated water (containing photoacids, PAGs, and base quenchers) on model silicon, resist, and topcoat materials and observed the resultant staining and impact on resist performance.^{78,96,108,129,167} Frequently, drying stains from “pure” water droplets are observed¹⁰⁸ even on clean silicon wafers due to dissolved silica¹²⁸ or contaminants picked up from the environment such as dust, phthalates, or siloxanes.¹⁶⁸

Watermarks. If water droplets are left on the resist surface, they can induce so-called watermark defects, which are characterized by regions with t-topped or bridged resist profiles having a generally larger critical dimension (CD) (see Figure 20).¹⁶⁹ The probability of a defect being formed is related to the size and drying time of the droplet, the permeability of the topcoat, and the resist sensitivity to water.^{110,129,164,170} Intense research has endeavored to explain why water droplets on the resist surface cause defects whereas uniform extended soaking of the resist surface does not.¹⁴⁷ Watermark formation has been attributed to an inhibited region at the surface of the chemically amplified resist with little to no base dissolution rate¹⁰² due to a lower degree of deprotection¹²⁵ (see Figure 21). While the size of watermark defects has been correlated with the size of the water droplet during the final phase of evaporation (≤ 400 μm),^{101,164,171} the exact mechanism for this localized inhibition has not yet been definitively established.^{82,171} Empirically, it has been found that removing all water droplets from the wafer before they can dry can successfully reduce the number of watermark defects.^{60,164,168,171}

3.3. Topcoat Materials for Water Immersion Lithography

General strategies used in the design of topcoat materials are outlined in Figure 22. Topcoat materials are generally spun cast from low polarity organic (e.g., fluorocarbon, alcoholic, ethereal, or hydrocarbon-based) solvents into 30–120 nm thick films on top of conventional 193 nm photoresists. Typically, saturated hydrocarbon, fluorocarbon,

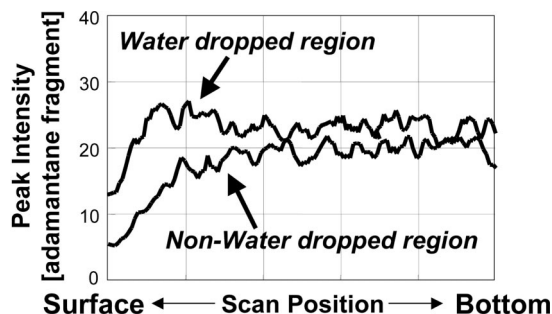


Figure 21. Time-of-flight secondary ion mass spectroscopy (TOF-SIMS) line scan of a gradient shaved resist film. A surface inhibition region is observed in a photoresist film exposed to water as indicated by the higher concentration of the adamantane-based protecting group. Reprinted with permission from ref 125. Copyright 2007 SPIE.

or organosilicon-containing groups are incorporated into the topcoat to reduce surface energy, increase water contact angles, and enable high wafer scan rates (>500 mm/s) without film pulling. After exposure, the topcoats can be removed using a separate topcoat remover (typically, a fluorinated organic solvent) or, more preferably, with standard 0.26 N aqueous tetramethylammonium hydroxide (TMAH) during the photoresist development process. Since it is desired that the topcoat be removed during the first second or so of photoresist development, typical dissolution rates of alkali-soluble topcoats range from one hundred to several hundred nanometers per second.

In addition to providing optimal water contact angles, PAG leaching levels, resist interactions, and defectivity levels, an immersion topcoat can serve as a top antireflective coating (TARC) if it has the appropriate optical properties and film thickness. TARCs have historically been used in dry lithography to minimize reflectivity and maximize lithographic performance.⁷⁹ The ideal refractive index of a nonabsorbing TARC is given by

$$n_{\text{TARC}} = \sqrt{n_{\text{immersion fluid}} n_{\text{resist}}} \quad (15)$$

and the ideal thickness (L) corresponds to a quarter wavelength.^{79,82}

$$L_{\text{TARC}} = \frac{\lambda_0}{4n_{\text{TARC}}} \quad (16)$$

The ideal optical properties and thicknesses of absorbing TARC materials are described elsewhere.¹⁷² While the refractive indices of air and typical 193 nm photoresists ($n_{\text{air}} = 1$, $n_{\text{resist}} \approx 1.7$) require that nonabsorbing TARCs for 193 nm dry lithography have a refractive index around 1.3,¹⁷³ the higher refractive index of water ($n_{\text{water}} = 1.437$) at 193 nm shifts the ideal refractive index of an immersion TARC to around 1.55. Reported refractive indices for commercial 193 nm water immersion topcoats range between 1.4 and 1.6.¹⁵⁷

The topcoat structures in the following section have been selected from recent publications and patents to give a representative overview of the materials design strategies and chemistries being employed in this area. Given the sensitivity of topcoat performance metrics such as defectivity to tooling, process, and resist specifics, only general performance behavior can be described. Readers interested in detailed contact angle data for the examples presented herein should consult the original literature.

3.3.1. Organic-Developable Topcoat Materials

The first reported topcoat materials were based on highly fluorinated polymers such as 2,2-bis(trifluoromethyl)-4,5-difluoro-1,3-dioxole copolymers (**8–9**, DuPont Teflon AF) and cyclopolymers of perfluorobutyl vinyl ether or perfluoroallyl vinyl ether (**10–11**, Cytop from Asahi Glass) shown in Figure 23. For example, one patent discloses a solvent-developable topcoat material based on a blend of Cytop and a perfluoroalkylpolyether (Demnum from Daikin Industries).¹⁷⁴ These materials offer extremely high water contact angles (see TOK TSP-3A in Table 4) but suffer from the aforementioned cost-of-ownership issues associated with the extra solvent-based topcoat-removal step.

3.3.2. Water-Castable Topcoat Materials

A number of topcoats capable of being cast from water were explored; however, the resulting topcoats must be rendered insoluble in water so they do not dissolve during

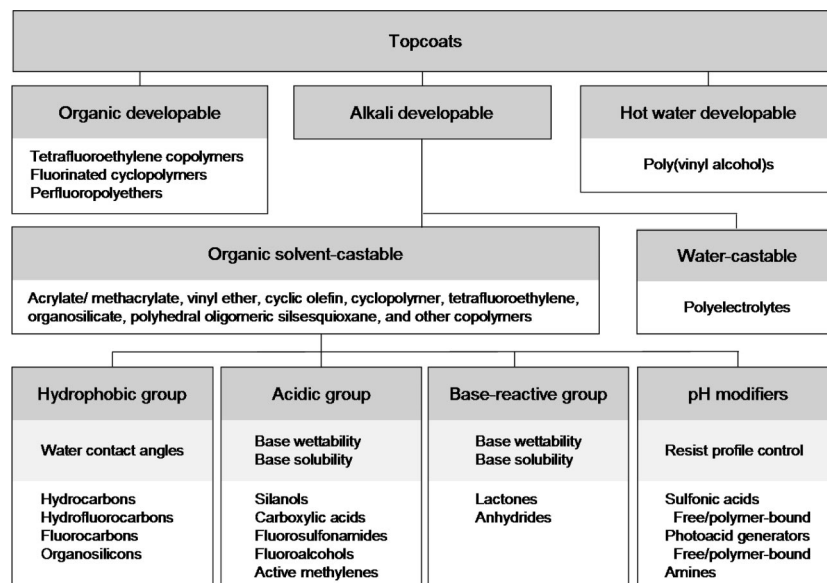


Figure 22. Design of topcoat materials for immersion lithography.

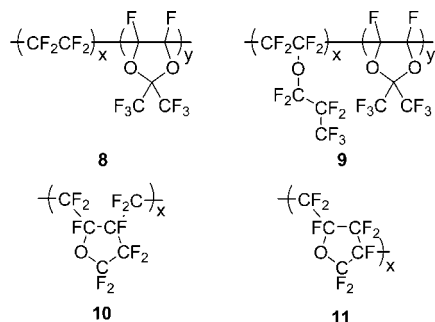


Figure 23. Organic-developable topcoat polymers.

the immersion process. Poly(vinyl alcohol) can be cast from water, rendered insoluble in room-temperature water by a postapplication bake (PAB), and later dissolved in hot water after the exposure process.¹⁷⁵ Alternatively, carboxylic acid-functionalized polymers such as poly(acrylic acid) or poly(methacrylic acid) copolymers can be solubilized in water as their ammonium salts. During the PAB, ammonia is driven off to regenerate the carboxylic acid-functionalized polymer, which is insoluble in water.¹⁷⁶ These early attempts at water-castable topcoats exhibited unacceptably low receding water contact angles and, therefore, have been abandoned in favor of alkali-soluble topcoats with higher contact angles, which are cast from organic solvents.

3.3.3. Alkali-Soluble Topcoat Materials

Alkali-soluble topcoat materials, which can be removed during the photoresist development process, have a significant cost-of-ownership advantage over topcoats requiring a separate topcoat-removal step. Alkali-soluble topcoats typically contain hydrophobic groups to control water contact angles and acidic groups such as carboxylic acids or base-reactive groups like lactones or anhydrides to impart base solubility. Unfortunately, most of these base-solubilizing groups are hydrophilic, lower receding water contact angles, and increase contact angle hysteresis. Fluoroalcohols and trifluoromethanesulfonamides are particularly well-suited for use in alkali-soluble immersion materials because the fluoroalkyl groups in these moieties make them considerably more hydrophobic.¹³⁶ Hexafluoroalcohol-based materials in particular exhibit good water contact angles, acceptable dissolution rates in TMAH developer, and high solubility in alcoholic casting solvents.

A number of reported water immersion topcoats are based on materials such as fluorine or silicon-containing polymers first explored for use in 157 nm lithography. For example, tetrafluoroethylene copolymers were explored for 157 nm pellicle¹⁷⁷ and resist¹⁷⁸ materials. A number of topcoat polymers (**12–13**) based on similar materials are shown in Figure 24.^{179,180} In another example, a fluoroalcohol-containing cyclopolymer (FPR, **14**) was one of the most transparent resist materials at 157 nm (see Figure 7); however, its water contact angle is insufficient for usage as a topcoat.¹⁸¹ A HFA-functionalized cyclopolymer (FUGU, **15**) and a copolymer (**16**) exhibit higher receding water contact angles.¹⁸² Interestingly, block copolymer versions of **16** were observed to have better contact angles than random copolymers.¹⁸³

Only a small number of topcoats based on silicon have been reported for immersion lithography. This is due to the fact that bilayer resists tend to be incompatible with (i.e., dissolve in) the solvents used to apply topcoat materials. Instead, multilayer patterning schemes using conventional

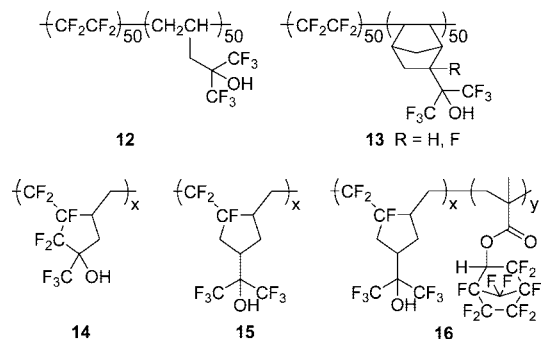


Figure 24. Topcoats based on tetrafluoroethylene and fluorinated cyclopolymer.

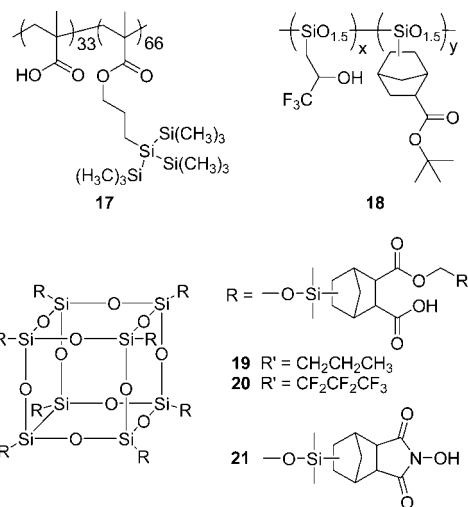


Figure 25. Topcoat materials containing silicon.

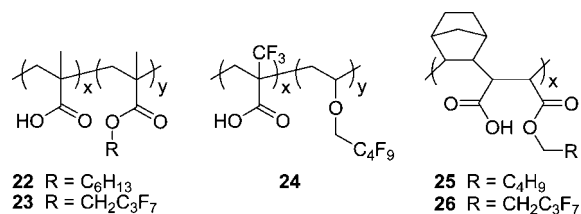


Figure 26. Topcoat polymers with carboxylic acid groups.

organic photoresists and inorganic hardmasks are more commonly used. In such applications, the orthogonal etch properties of a silicon-based topcoat could introduce additional defectivity concerns if some topcoat material remains on the wafer after development (e.g., as particles or as interdiffusion layers at the surface of the photoresist). Some examples of silicon-based topcoats are shown in Figure 25, including acrylic polymers with silicon-containing side chains (**17**),¹⁸⁴ fluoroalcohol-functionalized silsesquioxane polymers (**18**),¹⁸⁵ functionalized polyhedral oligomeric silsesquioxanes (**19–21**),¹⁸⁶ and partially condensed organosilicate resins.^{187,188}

Acrylic polymers form the basis of many 193 nm resist platforms and were quickly adapted for use as topcoats. Simple copolymers such as **22–24** (Figure 26) consisting of a hydrocarbon or hydrofluorocarbon-functionalized monomer with a (meth)acrylic acid variant were explored as early topcoat materials.^{180,189–191} Similarly, anhydride-containing copolymers can be ring-opened with various alcohols to form alcohol-soluble, alkali-developable topcoat polymers (**25–26**).¹⁹²

The water contact angles of side-chain fluorinated acrylic polymers are strongly dependent upon the length of the

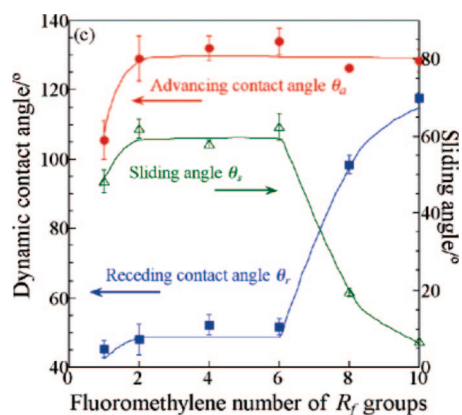


Figure 27. Dynamic contact angles and sliding angle for a water droplet on poly(fluoroalkyl acrylates) as a function of perfluorinated side chain length. Reprinted with permission from ref 193a. Copyright 2005 American Chemical Society.

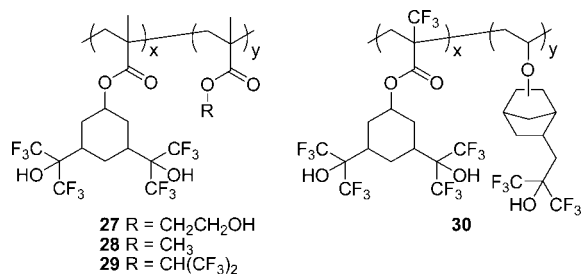


Figure 28. Topcoats containing 3,5-bis(1,1,1,3,3,3-hexafluoro-2-propanol)cyclohexyl groups.

fluorinated segment.^{136,193} For example, the dynamic contact angles of water droplets on poly(fluoroalkyl acrylate) polymers (i.e., $-\text{[CH}_2\text{CH(CO}_2\text{(CH)}_x\text{(CF}_2\text{))}_{y-1}\text{CF}_3\text{]}_n-$, wherein $x = 1$ for $y = 1-2$, and $x = 2$ for $y = 4-10$) are shown in Figure 27 as a function of the length of the perfluorinated side-chain length (y).^{193a} Takahara et al. attributed the very high receding contact angles of polymers having long ($y > 8$) perfluorinated segments to ordered, crystalline structures of the fluorinated side-chains at the surface. In contrast, polymer with shorter ($y < 6$) perfluorinated segments showed no crystalline organization of their side-chains. The increased mobility of the shorter perfluorinated side-chains allows reorientation in the presence of water to expose carbonyl groups to the surface and thereby lowers water contact angles.^{193a} It is likely that side-chains in topcoat materials such as those in Figure 26 will reorient in the presence of water due to the presence of the significant quantities of the acidic comonomers required to impart base-solubility. In addition, topcoat materials for immersion lithography tend to be amorphous to prevent issues with scattering and birefringence.

In order to improve water contact angles, acrylic topcoats featuring the more hydrophobic fluoroalcohol groups instead of the relatively hydrophilic carboxylic acid groups were developed. For example, the 3,5-bis(1,1,1,3,3,3-hexafluoro-2-propanol)cyclohexyl group provides moderate water contact angles and high TMAH dissolution rates. A variety of topcoats based on 3,5-bis(1,1,1,3,3,3-hexafluoro-2-propanol)cyclohexyl-functionalized methacrylate copolymers (such as **27–29**, Figure 28)^{86,194} and α,α,α -trifluoromethacrylate copolymers with vinyl ethers (**30**)¹⁹⁵ or cyclic olefins (e.g., norbornenes)¹⁹⁶ have been reported.

Acrylic polymers bearing a single hexafluoroalcohol group per repeat unit can offer contact angles superior to those

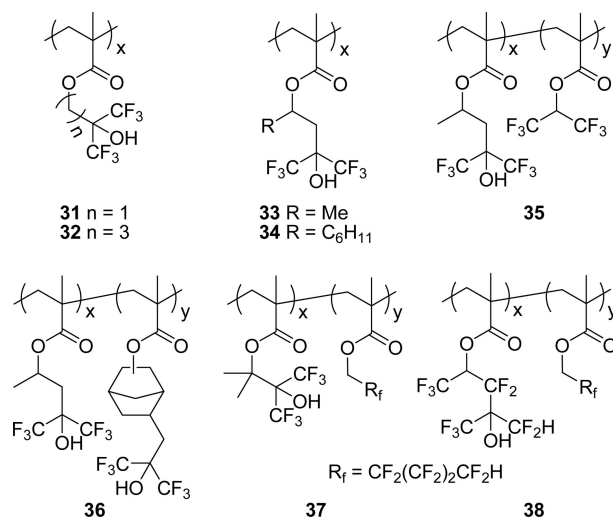


Figure 29. Acrylic topcoats bearing fluoroalcohol groups.

bearing 3,5-bis(1,1,1,3,3,3-hexafluoro-2-propanol)cyclohexyl groups, albeit with reduced base dissolution rates. While acrylate, methacrylate, α -fluoroacrylate, and α,α,α -trifluoromethacrylate variants of these monomers have all been reported, the methacrylate monomers have been most widely reported due to their low cost and acceptable glass transition temperatures. With HFA-based methacrylates, the contact angles and dissolution rates are strongly determined by the structure of the aliphatic linking group.^{197,198} For example, polymer **32** (Figure 29) with a linear linking group has a receding contact angle around 15 degrees lower than the analogous polymer (**33**) with a branched linking group.¹⁹⁷ A systematic study found that the receding contact angle increased with the size of the aliphatic group in the branched linking group; however, the dissolution rate decreased significantly more rapidly.¹⁹⁷ For example, incorporation of a cyclohexyl group (in **34**) rather than a methyl group (in **33**) increases the receding contact angle by ~ 15 degrees but renders the material virtually insoluble in TMAH developer. Copolymers with comonomers bearing more hydrophobic fluoroalkyl groups (**35**)¹⁸⁹ or less soluble HFA groups (**36**)^{190,199} have also been reported. Other fluoroalcohol-containing topcoats include variants with tertiary ester-based HFA groups (**37**)^{200,201} and fluoroalcohols with fluorinated linking groups (**38**).²⁰⁰

Alternatively, hydrophobic cyclic olefin polymers bearing fluoroalcohol groups have been reported for use as topcoats (**39–41**, Figure 30).^{194,202–204} Many of these norbornene-type polymers were initially developed for 157 and 193 nm photoresists due to their high etch resistance and were only later modified for potential use as topcoat materials.^{52,53} In order to avoid the complications and costs associated with removing the residual metallic impurities from transition metal-catalyzed norbornene addition polymers, topcoats based on free radical copolymerization of functionalized norbornenes with acrylate, methacrylate, or α,α,α -trifluoromethacrylate monomers have been reported (**42–43**).^{195,205}

In comparison with HFA groups, trifluoromethanesulfonamide groups impart higher alkali dissolution rates but lower receding contact angles. Some exemplary topcoats featuring trifluoromethanesulfonamide groups (**44–46**) are shown in Figure 31.^{204,206}

The structure and formulation of alkali-developable topcoat materials are frequently tailored to control the profiles of the final photoresist features formed during development. For

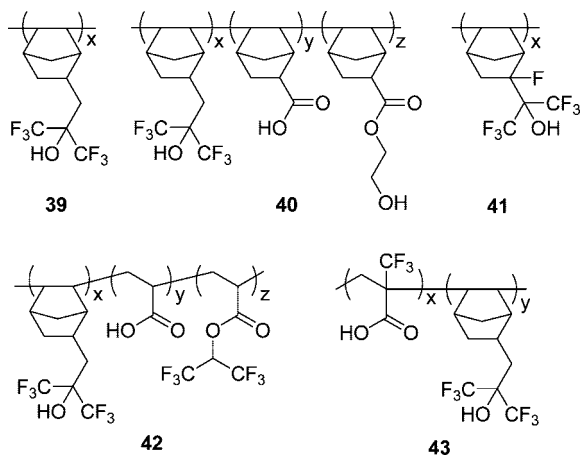


Figure 30. Cyclic olefin topcoats bearing fluoroalcohol groups.

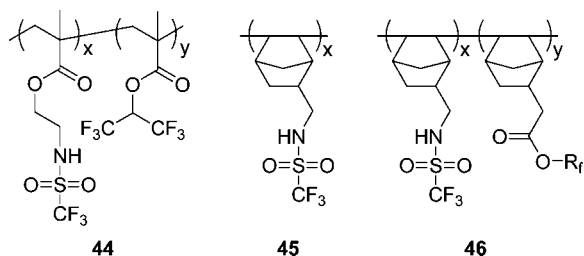


Figure 31. Topcoat materials based on trifluoromethanesulfonamide groups.

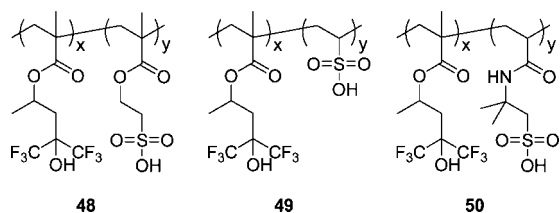
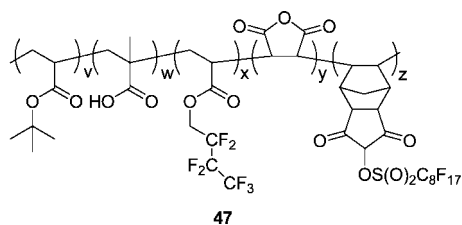


Figure 32. Topcoats containing polymer-bound PAG or sulfonic acid.

example, it has been shown that ethereal or hydrocarbon topcoat casting solvents cause less topcoat-resist interdiffusion and extract less PAG than alcoholic casting solvents.^{102,117,130} The addition of free sulfonic acid species or thermal acid generators into the topcoat formulation has been reported to induce some resist top-loss, eliminate t-topping, and improve profiles.^{81,114,115,207} Remarkably, the addition of photoacid generators into the topcoat formulation has been shown to alleviate profile issues (via the generation of additional photoacid above the exposed regions of the resist) without significantly increasing the amount of PAG leaching into the immersion fluid.^{81,115,208} Alternatively, small amounts of strongly acidic groups can be incorporated into the topcoat polymer itself as a polymer-bound PAG (**47**, Figure 32) or as a polymer-bound acid (**48–50**) to alleviate profile issues.^{126,209,210}

Topcoat material design must balance a number of structure–property trade-offs to achieve high water contact

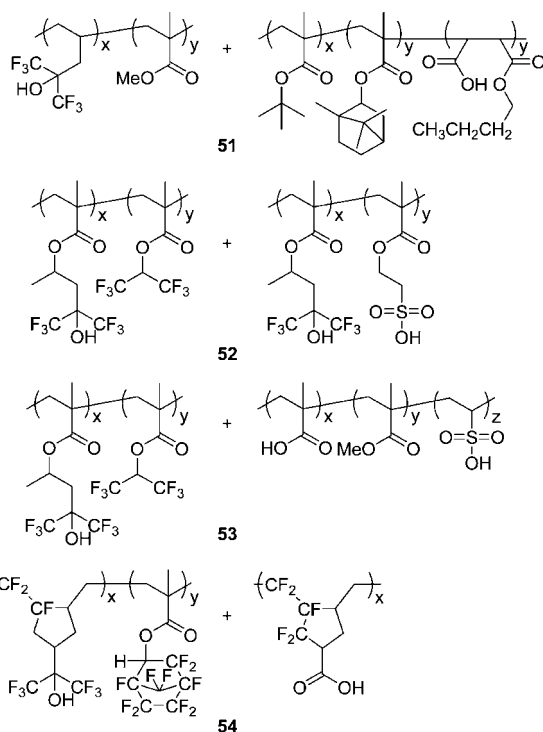


Figure 33. Topcoats based on polymer blends.

angles, high base dissolution rate, and good resist compatibility. In order to break these trade-offs and achieve higher water contact angles, topcoats based on polymer blends have been reported. In a blend of two polymers, it is common for wetting (or enrichment) layers to form at the air and substrate interfaces with the air/topcoat interface becoming enriched in the lower surface energy material.²¹¹ In this way, the requirements of low surface energy (for high water contact angles) and good resist interaction and high base dissolution rate can be separated between the two-component polymers. Thus, the traditional trade-offs associated with topcoat design can be broken in an effort to keep pace with the rapid advances in contact angle performance enabled by newer topcoat-free resists.

Examples of topcoats based on blends of acrylic polymers are shown in Figure 33. In example **51**, a fluorine-rich polymer with superior water contact angles is blended with a fluorine-free polymer.²¹² While the chemically similar polymers in blend **52** formed a homogeneous layer with averaged properties, a blend with a nonfluorinated sulfonic acid-containing polymer (example **53**) resulted in strong enrichment layers of the fluorinated polymer at the air/topcoat interface and of the strongly acidic polymer at the topcoat/resist interface.¹⁴⁶ A similar blend system was disclosed in a JSR patent.²¹³ In another example, blends of the cyclo-polymer **21** with the less hydrophobic, faster dissolving carboxylic acid-functionalized cyclo-polymer (blend **54**) exhibited receding water contact angles above 70 degrees with moderate dissolution rates ($\sim 250\text{--}450$ nm/s).^{182,183}

3.3.4. Performance of Immersion Topcoat Materials

Many researchers have attempted to correlate immersion defectivity with some easily measured property of topcoat materials. In general, defectivity has found to decrease with increasing SRCA.^{98,99,118,127,152} For example, Nikon showed that defectivity was markedly reduced with topcoats having receding water contact angles near 70° (Figure 34).^{152c} This

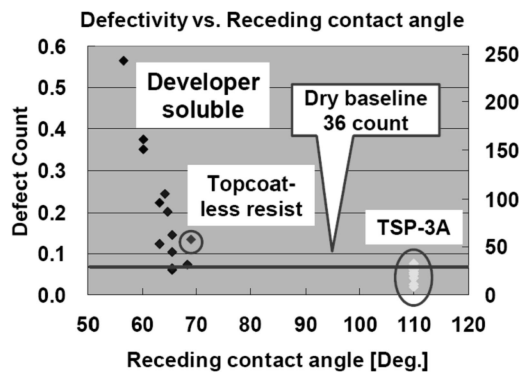


Figure 34. Defectivity as a function of receding contact angle of alkali developer soluble topcoats and an organic soluble topcoat. The baseline defectivity level for dry lithography is 0.083 defects/cm² (36 counts). Reprinted with permission from ref 152c. Copyright 2006 SPIE.

transition from high to low defectivity occurs above the critical velocity for film pulling ($\sim 50^\circ$ – 60°) discussed previously.⁹⁹ While a topcoat with a high contact angle may reduce the number of residual water droplets and thereby improve defectivity, some water droplets can still be left behind and cause defects. Co-optimization of a number of process parameters including resist–topcoat pairing, topcoat casting solvents, postapplication and postexposure bake temperatures, and various pre-exposure, postexposure, and postdevelopment rinse processes has been found to reduce defectivity levels of topcoat–resist stacks (see ref 60 and references therein). Over the last several years, immersion-specific defectivity levels have decreased to levels equivalent to or below that of conventional dry lithography (<0.06 defects/cm²).^{16,110,132,151,152,214,215} Current research into topcoat materials is focused on further reducing defectivity levels and increasing the water contact angles further to match those of topcoat-free photoresists and enable future increases in wafer scan rates.

3.4. Topcoat-Free Photoresists for Water Immersion Lithography

Protective topcoat layers have been effective in reducing the leaching of PAG into the immersion fluid while maintaining high wafer throughput and acceptable defectivity levels; however, the use of topcoats has increased process costs (due to extra topcoat spin-coating and postapplication bake steps) as well as material costs. In addition, it has been argued that the additional process steps and materials required by topcoat-based immersion processes inherently lead to additional defectivity.^{101,150} In recent years, the industry has begun developing immersion-capable photoresists that do not require a topcoat. Efforts to produce topcoat-free photoresists have largely fallen into two approaches: the use of hydrophobic resists with nonleaching PAGs and the incorporation of surface-segregating additives (Figure 9).

3.4.1. Hydrophobic Resists with Low Leaching PAGs

Increasing the water contact angles of a conventional photoresist through the incorporation of low surface energy (usually fluorine-based) monomers seems straightforward; however, this approach often requires redesign of both the resist polymer and the formulation package. Conventional methacrylate-based 193 nm photoresists typically have a significant number of polar functionalities such as hydroxyl

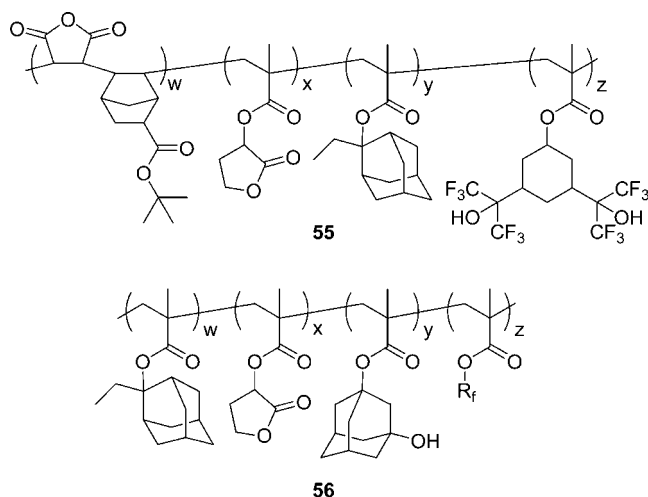


Figure 35. Incorporation of fluorinated groups into the photoresist polymer.

or lactone groups.^{52,53} In order to compensate for these hydrophilic polar groups, a highly hydrophobic (e.g., fluorinated) monomer must be incorporated into the resist polymer. For example, 3,5-bis(1,1,1,3,3,3-hexafluoro-2-propanol)cyclohexyl methacrylate was incorporated into resist **55**²¹⁶ and a fluorinated alicyclic methacrylate was incorporated into resist **56**²¹⁷ as shown in Figure 35. However, when changing the resist polymer structure through the use of additional hydrophobic monomers or end groups,²¹⁸ one must consider the impact on the physical and chemical properties (glass transition temperature, etch resistance, adhesion to substrate, etc.) of the resist, lithographic performance, and defectivity.^{216,219} In addition, the use of high contact angle base resins in the photoresist does not address the problem of PAG leaching because only a weak correlation exists between the hydrophobicity of the resist resin and the PAG leaching.²²⁰ In order to achieve low levels of PAG leaching, the resist must be reformulated with PAGs having lower water solubility, such as those discussed previously.

3.4.2. Surface-Segregating Additives Containing Silicon or Fluorine

Low surface energy materials such as organosilicon and fluorine-containing polymers have long been known to segregate to the surface of polymer blends during film formation.²¹¹ To take advantage of this phenomenon, small loadings (~ 1 – 5 wt %) of tailored surface-active materials have been used to convert conventional 193 nm dry photoresists into immersion-compatible versions.^{119,221–227} During spin-casting of the photoresist, these additives segregate to the resist surface to form a thin enrichment layer of the additive, which serves as an in situ topcoat barrier to reduce PAG leaching and control the water contact angles of the resist. These additives are sometimes also referred to as embedded barrier layers (EBLs)²²² or water shedding agents (WSAs).²²³ In contrast to a topcoat process where steps were taken to minimize interdiffusion of the topcoat and resist to reduce patterning defects, the surface-active additives in these topcoat-free resists are inherently intermixed with the photoresist and must be specifically designed to not degrade the imaging performance of the resist.

As shown in Figure 36, additives based on a wide variety of 193 nm transparent polymer backbones have been reported. Surface-active additives must have low surface energies to facilitate surface-segregation during film forma-

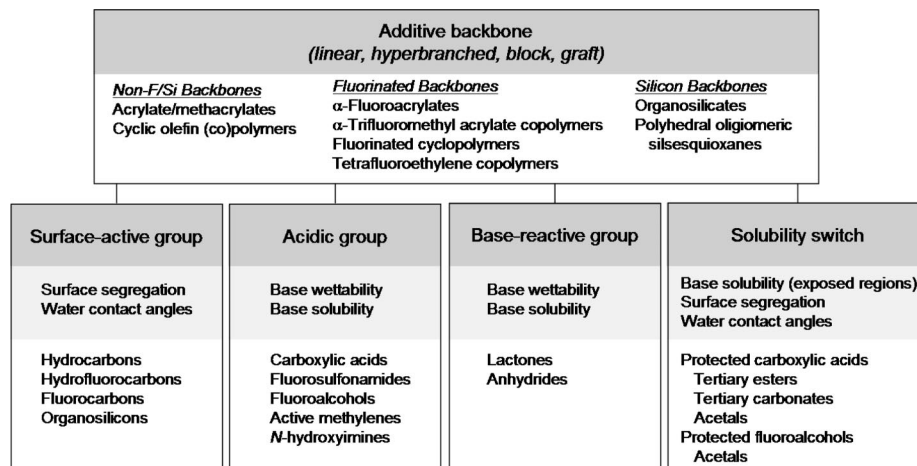


Figure 36. Design of additives for topcoat-free photoresists.

Table 5. Additive Design Strategies

additive type	additive solubility in TMAH developer after PEB		challenges
	unexposed	exposed	
topcoat-type	insoluble	insoluble	development defects
	soluble	soluble	water contact angles, leaching
resist-type	insoluble	soluble	developer wettability, blob defects

tion as well as to provide high water contact angles. Similar to topcoat materials, hydrocarbon, hydrofluorocarbon, and fluorocarbon groups are commonly used for this purpose. The surface-active fluorine and silicon groups can be incorporated either as part of the polymer backbone or as pendant side groups. Several strategies for designing additives based on when (or if) the additive becomes soluble in aqueous tetramethylammonium hydroxide photoresist developer are outlined in Table 5. Although patterns can still be imaged in topcoat-free photoresists using additives that are insoluble in aqueous base developer, defectivity levels can be very high due to incomplete lift-off of the additive-rich layer during development and/or redeposition of the additive back onto the wafer. Alternatively, base-soluble topcoat-type additives were designed containing acidic groups such as carboxylic acids, trifluoromethanesulfonamides, and fluoroalcohols or base-reactive groups such as lactones or anhydrides. For use as additives, however, the structure and quantity of these more polar, base-soluble groups, which impart base-solubility, must be balanced against the needs for high surface-segregation, high water contact angles, and low PAG leaching.¹⁵⁶ Unlike materials designed for use as topcoat films, the surface-segregating additives for topcoat-free resists can effectively employ protected acidic groups to ensure both high levels of hydrophobicity during exposure and high levels of developer wettability and alkali solubility in the exposed regions during development. The acid-catalyzed deprotection reactions, which convert the hydrophobic, protected acidic group into a hydrophilic, base-soluble group, occur primarily during the postexposure bake and, therefore, do not significantly lower SRCA values and induce film pulling during the exposure process.^{221,222} Challenges with these resist-type additives include developer wettability in the unexposed regions and bridging and blob defects.²²⁸

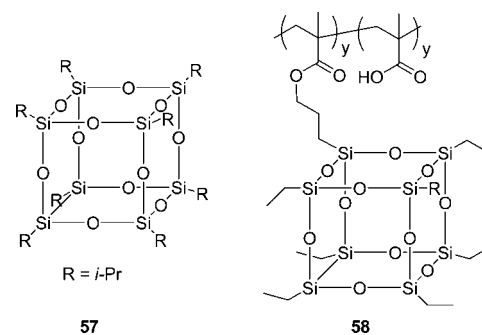


Figure 37. Polyhedral oligomeric silsesquioxane-based additives.

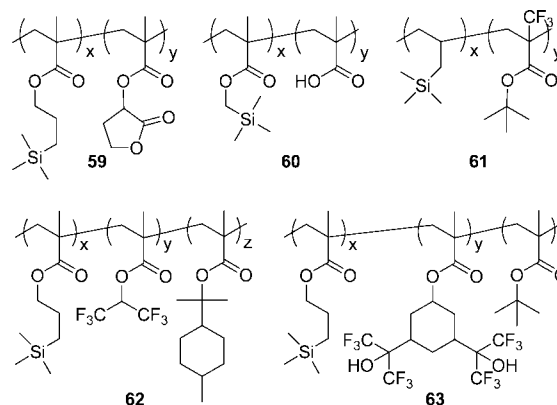


Figure 38. Silicon-containing additives.

3.4.2.1. Silicon-Based Additives for Topcoat-Free Resists.

Some silicon-based additives are shown in Figures 37 and 38. Photoresists bearing pendant polyhedral oligomeric silsesquioxane (PSS) groups have been shown to have enrichment layers of PSS groups at the surface.²²⁹ Examples of PSS additives for use in topcoat-free resists include both base-insoluble (**57**, Figure 37)^{230,231} and base-soluble (**58**,²³¹ Figure 37 and **19–21**,^{186,232} Figure 25) additives. Figure 38 shows some representative silicon-containing acrylic additives such as **59** and **60**, which employ base-reactive lactone and methacrylic acid groups, and **61–63**, which rely on protected methacrylic acid moieties to serve as a solubility switches.^{231,233} In addition, the leaching of PAG and silicon-containing resist components from topcoat-free silicon-containing bilayer resists for immersion lithography have been examined by Malik et al.²³⁴

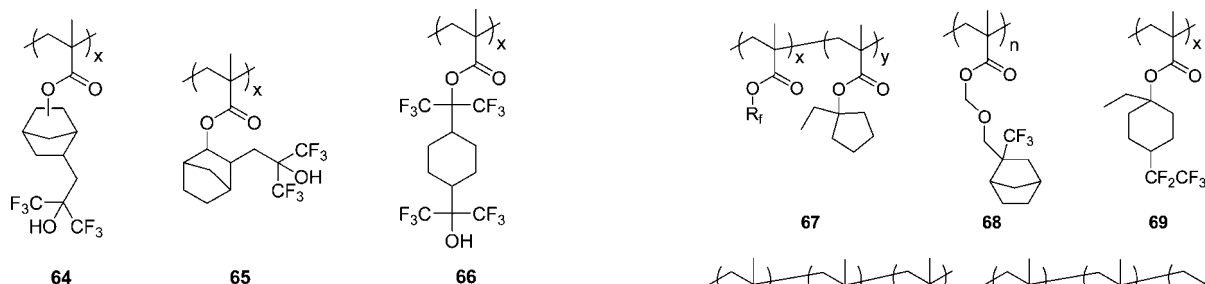


Figure 39. TMAH-insoluble fluoroalcohol-based additives.

3.4.2.2. Fluorine-Based Additives for Topcoat-Free Resists. Many early topcoat-type additives consist of simple copolymers of methacrylic acid with comonomers featuring hydrocarbon or fluorocarbon groups (such as those shown in Figure 26).^{230,232,235} These carboxylic acid-based additives generally afford low static receding contact angles (with high hysteresis) and poor leaching performance. In order to improve both surface segregation and contact angle performance, more hydrophobic acidic groups with higher water contact angles were desired.

As discussed previously, fluoroalcohol and trifluoromethanesulfonamide-based materials have been found to be particularly useful in immersion topcoat materials due to their good receding contact angles, low hysteresis, and good development properties. Jablonski et al. reported that fluoroalcohol-based resist polymers could surface segregate²³⁶ in resist blends developed by Ito et al.²³⁷ Later, fluoroalcohol-based methacrylate homopolymers such as **64–66** (Figure 39) were explored as additives for topcoat-free immersion resists.^{221,225,238} Loading norbornane hexafluoroalcohol methacrylate into a photoresist as a homopolymer additive (**64**) was significantly more effective at increasing water contact angles than incorporation into the resist polymer itself.^{225,239} TOF-SIMS on gradient-shaved²⁴⁰ films confirmed that the fluoroalcohol-based additive segregates to the air interface while the fluorine concentration remains uniform throughout a film of resist containing the fluoroalcohol as a comonomer. Although adequate resist profiles can be obtained using resists containing additives such as **64**, its lack of solubility in TMAH developer can result in increased surface roughness and large

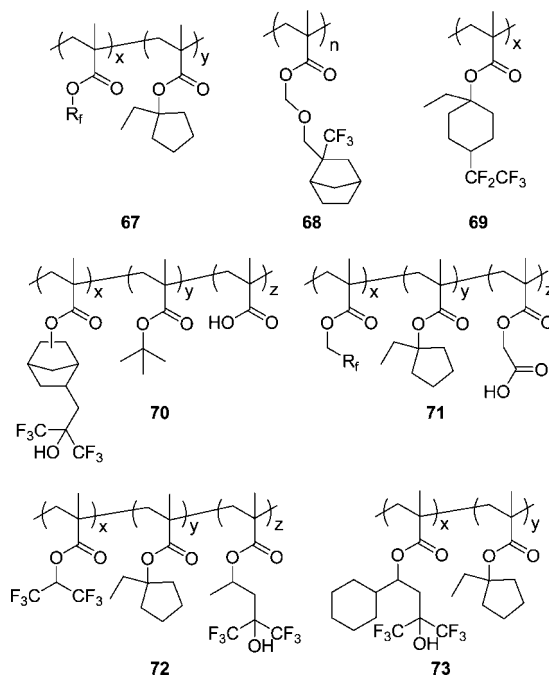


Figure 41. Fluorinated additives with protected acidic groups.

numbers of blob/residue defects.^{225,239} Alternatively, topcoat-type alkali-soluble additives based on copolymers of fluoroalcohol- and trifluoromethanesulfonamide-containing monomers have been reported, such as materials **35** and **36** (Figure 29) and **44** (Figure 31).^{230,232} For example, Figure 40 shows the higher receding contact angles and lower contact angle hysteresis enabled by the replacement of methacrylic acid with trifluoromethanesulfonamide- and fluoroalcohol-based methacrylate comonomers in a series of additives.¹³⁶ In practice, the HFA-based additive shown in Figure 40 is insoluble in TMAH developer, and higher loadings of the HFA-containing monomer are required to ensure base solubility, which in turn limits the achievable contact angles.

Simple resist-type copolymer additives such as **67** (Figure 41) consist solely of a surface-active monomer and a protected methacrylic acid.^{241,242} The use of fluorine-containing protecting groups such as a fluorinated acetal in **68**²⁴³ or

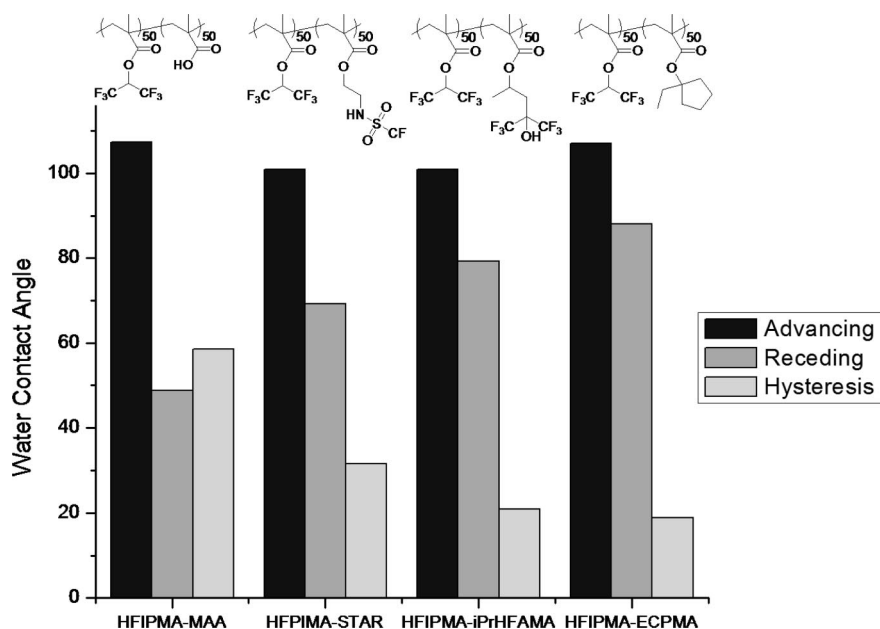


Figure 40. Water contact angles of topcoat- and resist-type additives (5 wt % in a 193 nm photoresist).

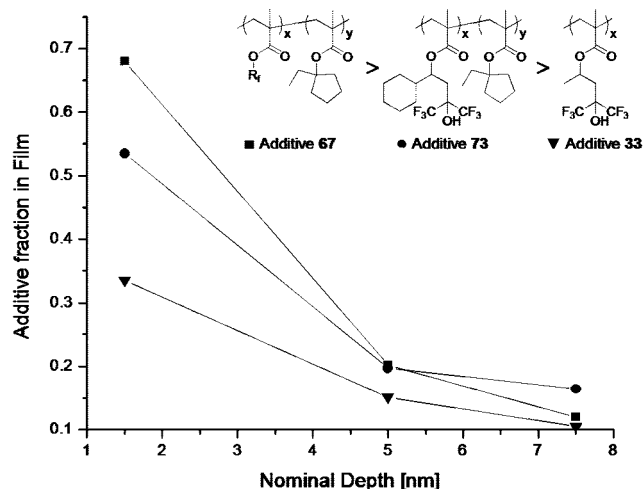


Figure 42. Surface-segregation of various additives in a 193 nm photoresist as measured by X-ray photoelectron spectroscopy.

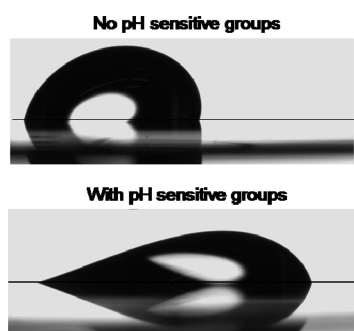


Figure 43. Tilted drops of aqueous TMAH developer on topcoat-free resists with and without pH-sensitive groups. Reduced contact angles and improved wetting of surface by developer observed with materials having acidic functional groups.

tertiary ester in **69**²⁴⁴ allows a single structure to perform both roles. While these resist-type additives exhibit higher levels of surface segregation relative to many topcoat-type additives (as shown in Figure 42) and afford very low PAG leaching, the extremely hydrophobic nature of fully protected resist-type additives can result in large advancing contact angles and base wettability issues in the nonexposed regions.²²¹ To overcome this issue, small amounts of an acidic group can be added to the additive in order to ensure good base wettability in the unexposed regions. These pH-sensitive groups, including carboxylic acid (**70** and **71**) or more hydrophobic groups such as fluoroalcohols (examples **72** and **73**), are readily deprotonated under the alkaline conditions of development.^{221,222,230,232} Figure 43 illustrates the impact of additives containing acidic functional groups on the developer contact angles of topcoat-free resists. Similarly, base-reactive groups like lactones have been incorporated into additives to impart base solubility (**74–78**, Figure 44).^{238,245,246}

Many of the fluorinated cyclopolymer topcoat materials discussed previously have been also screened for use as additives; however, the unprotected FUGU material (**15**, Figure 24) exhibited insufficient surface segregation to afford good contact angle and low leaching performance. Acetal-protection of the fluoroalcohol groups of **79** (Figure 45) increased surface segregation and contact angles; however, performance still lagged methacrylate-based additives.^{247,248} Copolymers with methacrylates bearing fluorinated alicyclic groups (**80**) showed increased surface segregation and water

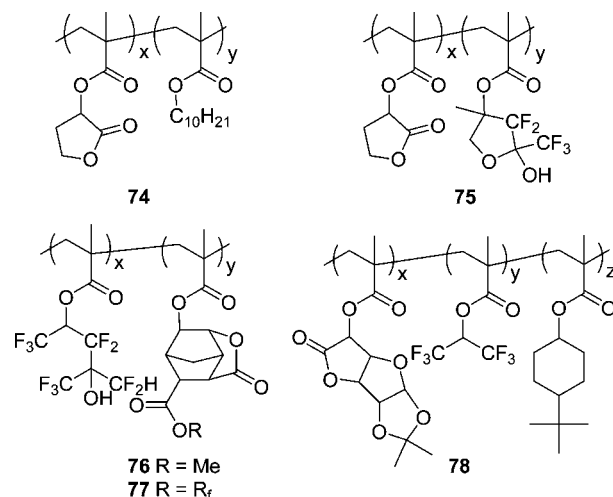
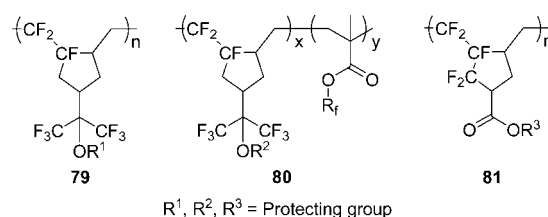


Figure 44. Additives containing lactone groups.



$R^1, R^2, R^3 =$ Protecting group

Figure 45. Additives based on fluorinated cyclopolymers.

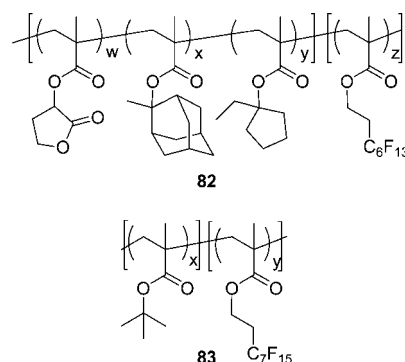


Figure 46. Additives based on block copolymers.

contact angles; however, only a limited amount of comonomer could be introduced before the material became base-insoluble. Alternatively, the carboxylic acid-functionalized cyclopolymer (**81**, FIT, $R^3 = H$) offers higher dissolution rate and base-wettability; however, protected versions of **81** segregated to the resist surface more poorly than **79**. Copolymerization of a tertiary ester-protected FIT monomer with a FIT monomer bearing a fluorinated ester group resulted in adequate surface segregation performance at low additive loadings.²⁴⁷ Branched tertiary ester groups such as *t*-amyl were found to be more effective than cyclic protecting groups like 1-ethyl cyclopentyl or 1-methyl cyclohexyl in increasing surface segregation.²⁴⁹

Although additives based on random linear polymers have been the most widely reported, a variety of other polymer architectures have also been explored. For example, hyperbranched additives have been synthesized using a trifunctional acrylate monomer.²³⁰ Block copolymer additives such as **82**²⁵⁰ and **83**²⁵¹ have been reported as well (Figure 46). Additive **82** features one block of an identical composition as the resist material for optimum resist compatibility and a fluorinated block for surface activity and water contact angles.²⁵⁰

3.4.3. Performance of Topcoat-Free Photoresists

Topcoat-free photoresists have demonstrated a significant advantage over base-soluble topcoat materials in terms of receding contact angle as shown in Table 4. While the elimination of a topcoat reduces materials cost, reduces the number of process steps, and improves water contact angles, the use of surface-segregating additives in topcoat-free resists has been viewed with caution as a potential source for new defectivity issues. Numerous studies have since reduced this concern. The surfaces of topcoat-free resist films show similar surface roughness as standard 193 nm photoresists and undergo negligible roughening upon exposure to developer.^{221,252} Surface segregation of the additive has been shown to occur uniformly across the wafer as measured by contact angles,²⁵² PAG leaching,²⁵² and TOF-SIMS depth profiling.²⁴⁸ In addition, segregation has been found to occur during the spin-casting step with little dependence upon the postapplication bake time or temperature.^{146b,242,248}

Hagiwara et al. explored the surface-segregation process of cyclopolymer-based additives in more detail and found that the contact angle increased with the thickness of the film; however, the contact angle was independent of the spin speed or solution concentration used to achieve that film thickness.²⁴⁸ For a single solution, the use of a higher spin speed (to obtain a thinner film) afforded a reduced concentration of additive at the surface, while the use of a lower spin speed (to obtain a thicker film) afforded a thicker and more enriched region of additive at the surface of the resist film, albeit with a significant amount of additive remaining in deeper regions of the film.²⁴⁸

The defectivity of topcoat-free resists was found to increase with increasing wafer scan rate, and a resist based on a hydrophilic polymer showed much higher defect levels than one based on a hydrophobic polymer.²⁵³ While higher molecular weight additives are generally more effective at increasing the water contact angles of the resist surface at lower loadings,^{225,239,254,255} higher concentrations of the additive can result in poor line width roughness (LWR) performance.^{254,255}

Frequently, so-called blob defects of precipitated material (similar to that previously seen in dry lithography)²⁵⁶ have been observed in dark-field imaging of topcoat-free immersion resists.¹⁰¹ During development, suspended gel or clusters that have lower solubility in the developer can easily reattach to the surface and form blob defects, especially during the sudden pH change accompanying the DI water rinse.^{157,256} Lower numbers of blob defects have been correlated with more negative zeta potential of the additive²⁵⁴ and decreased static water contact angle of the resist surface after development,^{257,258} lower water contact angles after postexposure bake,²³⁹ and lower water²¹⁴ or developer²⁵⁵ contact angles of the unexposed resist surface. Most of these correlations are consistent with the hypothesis that hydrophobic aggregates can precipitate and attach to a hydrophobic resist surface during development to create blob defects, while the more hydrophilic aggregates of resist-type additives would be more easily rinsed away from a hydrophilic resist surface during development.²³⁹ Accordingly, rinse treatments and alternative development processes have been found to be effective means to reduce the numbers of blob defects.^{119,150,214,215,228,257–260} Alternatively, Hagiwara et al. explored removing the hydrophobic additive material from the surface of the resist using an organic solvent in a

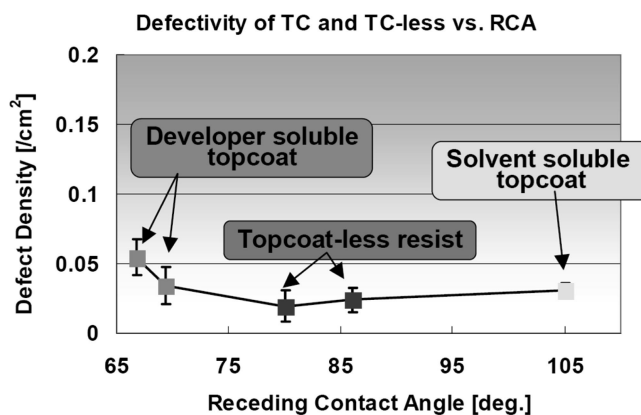


Figure 47. Defectivity of various immersion patterning materials solutions versus receding contact angle. Reprinted with permission from ref 150. Copyright 2008 SPIE.

“selective segregation removal” (SSR) process prior to development of the resist pattern.²⁶¹

Studies comparing the lithographic performance of topcoat-free 193 nm immersion resists relative to that of standard topcoat/resist stacks have shown that optimized topcoat-free resist processes can achieve equivalent or superior lithographic performance, including resolution, process windows, sidewall angle/resist profiles, CD uniformity, line edge roughness (LER)/LWR, postexposure delay stability, and defectivity levels (see Figure 47).^{119,150,152,221,252,262}

Current work in topcoat-free immersion resists is now focused on further increasing contact angles, lowering defectivity levels, and expanding their capabilities to other resist platforms. For example, negative-tone resist materials have some advantages in double patterning schemes since they do not require any hardening²⁶³ and can allow very high resolution trench patterns to be formed.²⁶⁴ Unfortunately, negative-tone resists have not been widely used in immersion lithography, partially due to their incompatibility with common alcoholic casting solvents of topcoats. Recently, Ando et al. developed a topcoat-free negative-tone photoresist for use in trench-based double patterning schemes.²⁶⁵ The topcoat-free negative-tone resist included a base-soluble fluorinated additive and a nonleaching PAG that was soluble in TMAH developer in its salt form.²⁶⁵

4. Materials for 193 nm High-Index Immersion Lithography

At the limit of water immersion lithography (~ 1.3 – 1.35 NA), 55 nm half-pitch features can be printed at a k_1 of 0.38 (required for aggressive dual-orientation patterning) and 40 nm half-pitch features with a k_1 of 0.28 (required for aggressive single-orientation patterning) (see Table 6). In order to extend 193 nm immersion lithography to 45 nm ($k_1 = 0.38$) and 32 nm ($k_1 = 0.28$) half-pitch, an NA of about 1.7 is required (see Table 6).^{61–63,266} With a planar last lens element, the NA of an immersion lithography tool is limited by the lowest refractive index in the optical stack (i.e., last lens element, immersion fluid, topcoat, and photoresist). In 193 nm water immersion lithography, the immersion fluid presents the first limiting refractive index ($n_{\text{water}} \approx 1.44$, $n_{\text{LLE}} \approx 1.50$ – 1.56 , $n_{\text{topcoat}} \approx 1.5$ – 1.66 , $n_{\text{resist}} \approx 1.7$).²⁶⁷ Replacing water with a second-generation immersion fluid with a higher refractive index can increase the NA, although the lens material soon becomes the next limiting index. The ultimate progression of this approach is the elimination of the

Table 6. High Index Immersion System Capabilities and Requirements^{61–63,266}

	numerical aperture of immersion tool			
	1.35 NA	1.45 NA	1.55 NA	1.65–1.70 NA
$k_1 \approx 0.38$ resolution (half-pitch)	55 nm	51 nm	47 nm	44–45 nm
$k_1 \approx 0.28$ resolution (half-pitch)	40 nm	38 nm	35 nm	32–33 nm
$n_{\text{last lens element}}$	1.56 (SiO ₂)	1.64 (BaLiF ₃)	2.14 (LuAG)	2.14 (LuAG)
$n_{\text{immersion fluid}}$	1.44 (water) (1st-gen. fluid)	~ 1.64 (2nd-gen. fluid)	~ 1.64 (2nd-gen. fluid)	> 1.8 (3rd-gen. fluid)
$n_{\text{photoresist}}$	1.7 (standard resist)	1.7 (standard resist)	1.7 (standard resist)	> 1.8 (high index resist)

Table 7. Optical Properties of Lens Materials

material		bandgap [eV]	$n_{193 \text{ nm}}$	$\alpha_{10} [\text{cm}^{-1}]$	IBR [nm/cm]	SBR [nm/cm]	ref.
target		≥ 6.41	≥ 1.8	≤ 0.005	≤ 10	≤ 0.5	
BaLiF ₃			1.64	0.003	25.4	0.7 (111) 1.7 (100)	271
MgAl ₂ O ₄	crystalline spinel	7.75	1.87		52		269
	ceramic spinel		1.9203	≥ 1.5	–	≥ 5	
MgO		7.6	1.96	3.9	~ 70		269
Al ₂ O ₃	sapphire	9.0–9.1	1.932 (n_o) 1.918 (n_c)	0.11	high	low	273
Mg ₃ Al ₂ Si ₃ O ₁₂	pyrope	≤ 8.3	2.0	25	~ 10	~ 5	269
CaLu ₂ Mg ₂ Ge ₃ O ₁₂	germanate garnets	5.17–5.52	1.9–2.2	high		~ 5	269
Mg ₃ Al ₂ Ge ₃ O ₁₂							
Lu ₃ Al ₅ O ₁₂	LuAG	~ 6.9	2.1435	0.035	30.1	0.73 (YAG)	269, 272

immersion fluid entirely by placement of the lens either in direct contact with the photoresist stack (contact lithography) or in close enough proximity that the evanescent fields can be transmitted into the photoresist. Laboratory demonstrations of such solid immersion or evanescent-wave lithography have imaged at effective NAs greater than 1.8;²⁶⁸ however, these techniques are not practical for high-volume manufacturing and will not be discussed further in this review.

For commercial applications, research has focused on increasing the refractive indices of the materials in the optical stack (LLE, fluids, topcoats, and resists) to increase the NA of liquid immersion lithography tools to 1.7 and beyond.^{61–63,266} A 1.7 NA immersion tool would require a new high-index lens material, a high-index immersion fluid, and a high-index photoresist (see Table 6). Lower NA tools (1.45 NA and 1.55 NA) using lower refractive index fluids and lens materials were proposed as development targets while research progressed on third-generation ($n > 1.8$) immersion fluids and the high-index lens material.

4.1. High Refractive Index Lens Materials

Beyond taking maximum advantage of the refractive index of the immersion fluid, a high-index lens material reduces the overall size and complexity of the lens.²⁶⁹ While a concave final lens element would alleviate the need for a high refractive index lens material, this geometry increases the path length through the immersion fluid and consequently requires extreme fluid optical properties (transmission, dn/dT , etc.).²⁷⁰

The refractive index of the ideal material for the last lens element should be significantly higher than fused silica ($n_{193 \text{ nm}} \approx 1.56$) or calcium fluoride ($n_{193 \text{ nm}} \approx 1.50$), while having high transparency, low intrinsic birefringence (IBR), low stress birefringence (SBR), and good homogeneity. Potential lens materials were screened by Burnett et al., and a summary of their findings is shown in Table 7.²⁶⁹ Many

candidate materials were easily eliminated because of their insufficient bandgap at 193 nm or their anisotropic optical properties.

While falling short of the refractive index target, BaLiF₃ ($n_{193 \text{ nm}} = 1.64$) merited early attention since large boules (~ 150 mm diameter) with high transparency could be fabricated, whereas other high-index lens materials were still struggling with transparency (purity) and manufacturing issues.²⁷¹ The most promising high-index lens material proved to be Lu₃Al₅O₁₂. Lutetium aluminum oxide (LuAG) has both a sufficient bandgap at 193 nm and a highly symmetric crystal structure that reduces intrinsic birefringence.^{269,272} Initial measurements on samples of LuAG revealed the refractive index to be 2.14 at 193 nm. After an intense development process to remove absorbing impurities and improve the transparency of LuAG, a final absorbance of 0.035 cm^{-1} was achieved (see Table 7).²⁷²

Since polarized illumination is used in most low k_1 imaging processes, the potential use of uniaxial crystals of sapphire as a last lens element material has been proposed.²⁷³ Although the current transparency of sapphire at 193 nm is not as high as LuAG, the higher thermal conductivity and lower dn/dT of sapphire may allow slightly higher absorbance (perhaps 0.04 cm^{-1}) to be accommodated.²⁷³

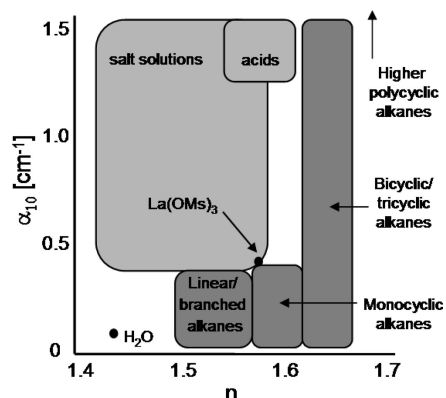
4.2. High Refractive Index Immersion Fluids

As delineated in Table 6, a second-generation immersion with a fluid refractive index of ~ 1.64 is required to enable 1.55 NA, and a third-generation immersion fluid with a refractive index greater than 1.8 is required to enable 1.7 NA. Beyond having sufficient refractive indices, the high-index immersion fluids should retain all of the properties that make water a successful immersion fluid (see Table 8). In general, high-index immersion fluid candidates fall into one of two classes: nonpolar saturated hydrocarbons or aqueous salt solutions. Within these two classes, a wide

Table 8. Fluid Requirements for High Index Immersion Lithography

property	1st generation (water) ⁴³	2nd generation	3rd generation
refractive index	1.437	≥1.64	≥1.8
absorbance	0.036 cm ⁻¹	<0.15 cm ⁻¹ ^a	<0.15 cm ⁻¹ ^a
dn/dT	-93 ppm/K	<250 ppm/K ^a	<250 ppm/K ^a
viscosity	1 cP	≤3 cP	≤3 cP
surface tension	72.8 mN/m	~70 mN/m	~70 mN/m

^a A concave last lens element would require a fluid absorbance < 0.03 cm⁻¹ and dn/dT < 50 ppm/K.²⁶⁷

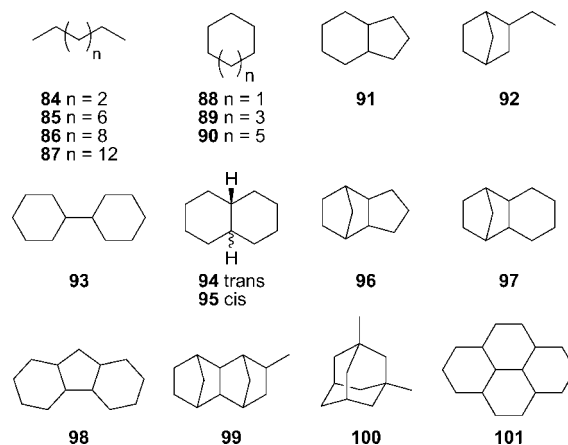
**Figure 48.** Optical properties of second-generation immersion fluid candidates.

variety of potential second-generation immersion fluids have been explored, and their optical properties are summarized in Figure 48.

4.2.1. Second-Generation Organic Immersion Fluids

The oblique path length of radiation through the immersion fluid is much larger than that in a photoresist layer, which requires the absorbance of an immersion fluid ($\alpha_{10} \leq 0.15 \text{ cm}^{-1}$) to be many orders of magnitude smaller than that of photoresists ($\alpha_{10} \leq 2 \mu\text{m}^{-1}$). Consequently, many organic functional groups that contain electrons in nonbonding or π molecular orbitals have absorption bands in the deep UV and are too absorbing for use in an immersion fluid. Saturated hydrocarbons are the most promising candidates for high-index immersion fluids because their absorption bands typically fall below 193 nm.²⁷⁴ In fact, hydrocarbons have a long history as immersion fluids for lithography with demonstrations by Shank and Schmidt in 1973 (xylene at 325 nm),²² Kawata et al. in 1989 (high-index oil at 453 nm),²⁶ and Hoffnagle et al. in 1999 (cyclooctane at 257 nm).²⁸ However, even trace contaminants such as oxidized or unsaturated impurities significantly increase the absorbance of hydrocarbons at 193 nm ($\alpha_{10} > 2\text{--}10 \text{ cm}^{-1}$).^{275,276} Fluid transparency can be improved by removal of these impurities by a number of purification procedures including hydrogenation, reaction with sulfuric acid, distillation, and chromatography through activated silica, alumina, or other media.^{275,276}

A number of hydrocarbon liquids screened for use as high-index immersion fluids are shown in Figure 49, and their properties are listed in Table 9. In general, there is a strong correlation between the degree of alicyclic unsaturation and the fluid refractive index. A related linear trend between hydrocarbon density and refractive index is shown in Figure 50.²⁷⁷ With these correlations in mind, the search for organic immersion fluids can simplistically be described as a search for liquid polycyclic hydrocarbons with the highest possible

**Figure 49.** Saturated hydrocarbons for high-index immersion fluids.**Table 9. Optical Properties of Saturated Hydrocarbons at 193 nm**

name	<i>n</i>	α_{10} [cm ⁻¹]	ref.
2,2-dimethyl butane	1.481	0.23	276
2-methyl pentane	1.495	0.05	276
<i>n</i> -hexane (84)	1.493	0.11	304
<i>n</i> -decane (85)	1.549	0.19	284
<i>n</i> -dodecane (86)	1.564	0.29	276
<i>n</i> -hexadecane (87)	1.581	0.41	284
cyclohexane (88)	1.571	0.09	284
cyclooctane (89)	1.615	0.17	284
cyclododecane (90)	1.621	0.18	277
octahydroindene (91)		0.89	276
2-ethyl norbornane (92)	1.615	0.17	284
1,1'-bicyclohexyl (93)	1.634	0.09	280, 276
<i>trans</i> -decahydronaphthalene (94)	1.643	0.46	276
<i>cis</i> -decahydronaphthalene (95)	1.656	0.75	276
<i>exo</i> -tetrahydrodicyclopentadiene (96)	1.660	0.42	276
tricyclo[6.2.1.0 ^{2,7}]undecane (97)	1.664	1.71	276
perhydrofluorene (98)	1.668	>2	277
3-methyl tetracyclo[4.4.0.1.2 ^{5,7,10}]dodecane (99)	1.687	>2	279
1,3-dimethyl adamantane (100)		>2	277
perhydropyrene (101)	1.701	>2	277

densities that remain transparent at 193 nm. Numerous second-order structural effects on refractive index, absorbance onset, and fluid properties have been characterized.^{277–280} For example, the refractive index was found to generally increase with the number of carbon atoms and transoid-connected cyclohexane rings; however, the concomitant shifting of the absorption edge from below 190 nm to above

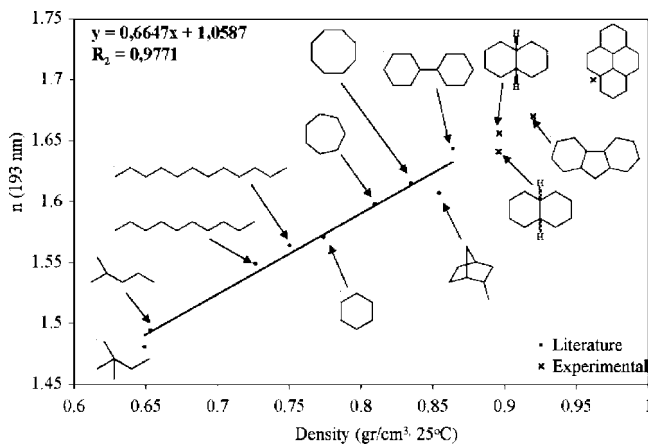
**Figure 50.** Refractive index versus density of selected hydrocarbons. Reprinted with permission from ref 277a. Copyright 2007 American Chemical Society.

Table 10. Properties of Commercial Organic Second-Generation Immersion Fluids

supplier	fluid	$n_{193\text{ nm}}$	α_{10} [cm^{-1}]	dn/dT [ppm/K]	viscosity [cP]	surface tension [mN/m]	vapor pressure (25 °C) [Pa]
	Water ^{43,288}	1.437	0.036	-93	1	72.8	3200
DuPont	IF131 ²⁷⁸	1.639	0.116	-570	2.4 ²⁷⁰	30 ²⁷⁰	
	IF132 ²⁷⁸	1.644	0.036	-550	3.3 ²⁷⁰	32 ²⁷⁰	
	IF138 ²⁷⁸	1.610	0.055	-690			
	IF169 ²⁷⁸	1.655	0.06	-560	2.6 ²⁷⁰	30 ²⁷⁰	
JSR	HIL-001 ²⁸⁸	1.64	0.038	-560	2.1	30 ²⁷⁰	160
	HIL-002 ²⁸⁸	1.65	0.032	-560	2.9	30 ²⁷⁰	—
	HIL-203 ²⁸⁹	1.64	0.020	-540	3.7		5.9
	HIL-204 ²⁸⁹	1.65	0.011		2.9		56
Mitsui	Delphi ²⁹⁰	1.635	0.08	-565	2	30 ²⁷⁰	150
	Babylon ²⁹⁰	1.642	0.022	-526	4		10

193 nm renders the absorbance of polycyclic compounds **97–101** too high to be useful immersion fluids.^{277–280} On the basis of these findings, practical immersion fluid candidates can be narrowed down to bicyclic and tricyclic hydrocarbons composed of 9–12 carbon atoms, such as octahydroindene (**91**), ethyl norbornane (**92**, 1,1'-bicyclohexyl (**93**), decahydronaphthalene (trans (**94**) and cis (**95**)), and *exo*-tetrahydrodicyclopentadiene (tricyclo[5.2.1.0^{2,6}]decane) (**96**).^{277–280} Some of these saturated polycyclic hydrocarbons are used commercially in applications such as high-temperature process fluids (bicyclohexyl **93**)²⁸¹ or high-energy fuels (*exo*-tetrahydrodicyclopentadiene **96** is the primary component of JP-10 missile fuel²⁸²). Air Products,²⁸³ DuPont,^{276,278,284} JSR,^{285–289} and Mitsui²⁹⁰ have all produced commercial high-index immersion fluids based on saturated hydrocarbons with refractive indices ~ 1.64 – 1.65 (listed in Table 10) and transparencies sometimes exceeding that of water. Early interferometric immersion lithography patterning efforts with these fluids show that they are capable of imaging 32 nm half-pitch features and beyond.^{267,284,286,287}

Another contribution to the absorbance of saturated alkanes in the deep ultraviolet region is the formation of contact charge transfer complexes between alkanes and oxygen in the deep UV.^{277,291} The oxygen-induced absorbance of JSR HIL-203 at 193 nm was measured to be $0.018\text{ cm}^{-1}\text{ ppm}^{-1}$.²⁹² For this reason, the measurements of fluid optical properties listed in Tables 9 and 10 were carried out using rigorously deoxygenated samples. Several groups have reported the formation of oxygenated products by irradiation of oxygen–hydrocarbon mixtures at wavelengths in the charge-transfer band.²⁹³ Additional studies with model immersion fluids such as cyclohexane show the production of a variety of photodecomposition products including unsaturated and oxidized species as well as polymeric material.^{294,295} Radiation-induced fluid darkening for a number of saturated hydrocarbons is shown in Figure 51. In addition to increasing the absorbance of the immersion fluid, photodecomposition products also form highly absorbing graphitic deposits on the surface of the lens that can generate particles in the fluid.^{292,295} In situ cleaning methods using UV–ozone^{295–297} or UV–aqueous hydrogen peroxide²⁹⁸ have been shown to rapidly and effectively remove lens contaminants. More recently, the addition of small amounts of water to the immersion fluid has been found to effectively suppress lens contamination.^{292c}

In order to maintain acceptable fluid transparency and prolong fluid lifetimes, in-line systems have been developed to remove photodecomposition products, extracted photoresist components, particles, and dissolved gases (especially oxygen) in order to allow continuous on-site recycling of the immersion fluid.^{288,289,296,299,300} The introduction of such active recycling systems results in a significant reduction in the rate of fluid darkening. With an active recycling system,

a 200 L batch of fluid is estimated to last ~ 8 – 10 days in a scanner at typical scan rates and wafer throughput.²⁹⁷

With respect to thermal aberrations from exposure-induced fluid heating, organic high index immersion fluids are ~ 10 times as thermally sensitive as water due to their larger thermo-optic coefficients, lower specific heat capacities, smaller thermal conductivities, and higher viscosities.^{62,63,270,297} Fortunately, the substantially lower volatilities and lower heats of vaporization of the hydrocarbons decreases the impact of evaporative cooling.⁶¹ Other techniques to reduce thermal aberrations include alternative fluid nozzle design,⁶³ fluid thickness reduction,^{62,270} and optical and stage corrections.^{62,297}

From eqs 10 and 11, film pulling of organic immersion fluids at low scan rates is expected given their lower surface tension-to-viscosity ratios and lower contact angles on typical resist and topcoat surfaces.^{77,280,301,302} In agreement with the models, film pulling of these fluids on commercial photoresist and topcoat materials is observed at very low scan rates

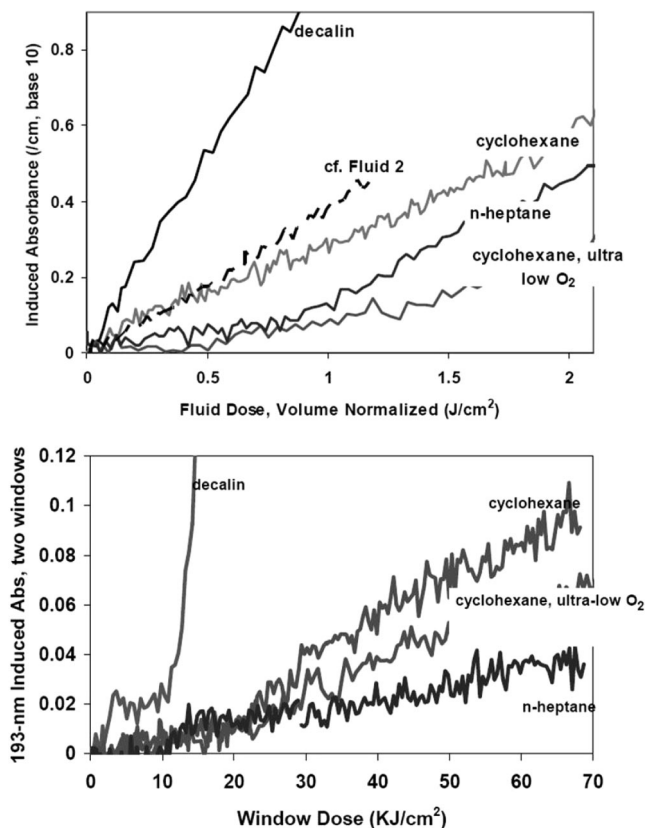


Figure 51. Radiation-induced darkening of various organic immersion fluids: (upper) bulk absorbance of hydrocarbon fluids, (lower) window-induced absorbance. Reprinted with permission from ref 295. Copyright 2007 SPIE.

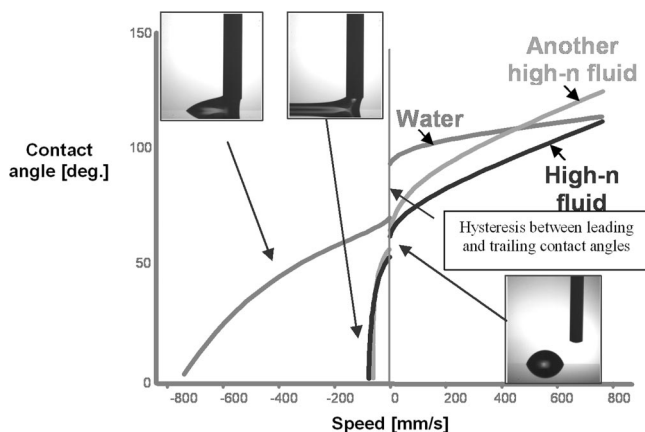


Figure 52. Comparison of contact angles of organic and aqueous immersion fluids as a function of wafer scan rate. Receding contact angles are plotted at negative velocities, while advancing contact angles are plotted at positive velocities. Fluid loss is observed when the receding contact angle reaches zero. Reprinted with permission from ref 61a. Copyright 2007 SPIE.

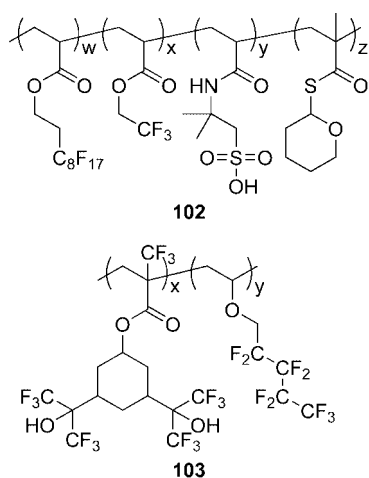


Figure 53. High-index topcoat (**102**) and additive for topcoat-free resist (**103**) designed for use with organic high-index immersion fluids.

(<200 mm/s) (see Figure 52).^{61,270,292,297,301} JSR reported a high refractive index ($n = 1.64$) topcoat (**102**, Figure 53)^{286,288,303} with improved contact angle performance ($\theta_{\text{static}} \approx 70^\circ$) with organic immersion fluids that enables scan rates up to ~ 350 mm/s without film pulling.²⁹⁷ The incorporation of fluorine into a side chain was found to be more effective in raising the contact angles with organic immersion fluids than incorporation of fluorine into the main chain.²⁸⁹ Alternatively, topcoat-free photoresists tailored for high-index immersion using additive (**103**) can achieve moderate receding contact angle with organic immersion fluids (SRCA ≈ 42 – 48° with JSR HIL-001).⁷⁷ Since high index fluids cannot be contained by conventional immersion showerheads at 500+ mm/s scan rates on existing materials, alternative fluid-handling schemes were considered, including flooding the entire wafer with fluid (the wafer wet approach) or simply allowing film pulling and removing the fluid afterward.^{63,292,297} Even if film pulling cannot be prevented, controlling the surface energy of the resist facilitates removal of the immersion fluid prior to postexposure bake.

The prospect of increasing defectivity due to the interaction of organic immersion fluids with the photoresist is partially mitigated by the lower evaporation rate of the immersion fluid²⁹⁷ and the lower leaching^{286,290,296,299,302} (due to lower

solubility) of ionic photoacid generators into organic fluids. Quartz crystal microbalance experiments showed that hydrocarbon fluids swell photoresists slightly more than water, but the effect was very small.^{77b,296} Pre- and postexposure soak experiments have shown that the impact of the fluid on the CD of patterned features depends upon the fluid and the resist. For example, resists soaked in water generally show increased inhibition (and larger CD) compared to a control, while resists soaked in high index fluids often exhibit reduced inhibition (and smaller CD) compared to the control, although this behavior is strongly dependent upon the resist.^{61,296,297} Misting experiments generally show fewer defects with high index fluids than with water.^{61,270,287,296}

4.2.2. Second-Generation Aqueous and Other Immersion Fluids

In order to develop aqueous second-generation immersion fluids, aqueous solutions of water-soluble organic molecules, inorganic salts and acids, heavy metal salts, and surfactants were explored.^{283,284,304–311} The optical properties of a variety of aqueous solutions of various acids and salts are listed in Table 11. Charge-transfer-to-solvent (CTTS) transitions of the anions dominate the absorption behavior (and refractive index via the Kramers–Kronig relationship) of these ionic solutions in the deep-UV region.^{305,306} For instance, different cations have little influence on the optical properties of chloride salt solutions (entries 8–12, Table 11) whereas differing anions significantly impact the optical properties of sodium salt solutions (entries 8 and 13–17). Unfortunately, few of these acid or salt solutions are sufficiently transparent at 193 nm. Smith et al. were able to use solutions of 85% phosphoric acid, sodium sulfate, and 50% $\text{AlCl}_3 \cdot 6 \text{H}_2\text{O}$ as immersion fluids to image sub-80 nm half-pitch features using a 193 nm immersion interferometric tool, although the low refractive indices of these fluids limited the NA to ~ 1.5 in the best case.³⁰⁵

With metal ions and halides being prohibited in electronic-grade materials used in semiconductor fabs and the corrosivity of acid solutions posing risks to tooling, more semiconductor-friendly ionic additives based on ammonium salts were explored.³⁰⁶ In particular, the methylsulfonate anion is significantly more transparent than acetate at 193 nm.^{283,284,306,307} For example, saturated solutions of $\text{La}(\text{OMs})_3$ exhibit a refractive index of 1.577 with low absorbance ($\sim 0.3 \text{ cm}^{-1}$). Alternative alkylsulfonate structures unfortunately exhibit increased absorbance at 193 nm and tend to form micelles at higher concentrations.³⁰⁸ Similarly, ammonium salts based on multifunctional sulfonates (such as methanedisulfonate and methanetrilsulfonate) increase fluid absorbance far more rapidly than the refractive index.³⁰⁹

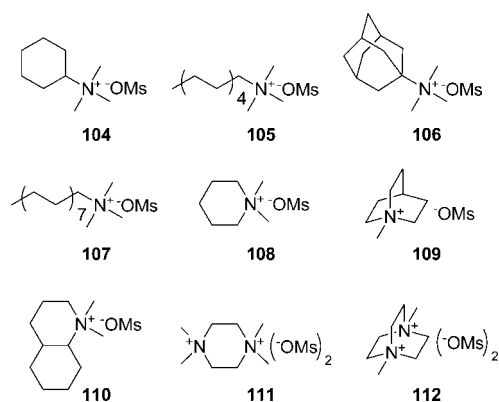
Modification of the structure of the quaternary ammonium cation rather than the methylsulfonate anion proved to be more successful (as shown in Figure 54 and Table 12). The refractive index and absorbance of ammonium methylsulfonate solutions increase with the size of the pendant aliphatic group in the monovalent (**104**–**107**), cyclic monovalent (**108**–**110**), and cyclic divalent (**111**–**112**) ammonium cations.³⁰⁸ A 3.4 M solution of cyclohexyl(dimethyl)ammonium methylsulfonate (**104**) has the best balance of properties with a refractive index of 1.58 and an absorbance of 1.43 cm^{-1} .³⁰⁸

Micellar solutions of anionic surfactants such as sodium dodecyl sulfate (SDS) or cationic surfactants such as cetyl trimethylammonium chloride with a wide range of inor-

Table 11. Optical Properties of Selected Aqueous Solutions

entry	fluid	data from Smith et al. ³⁰⁵					data from Willson et al. ³⁰⁶				
		refractive index		absorbance			refractive index		absorbance		
		$n_{193\text{ nm}}$	conc. [%]	α_c [mm ⁻¹]	λ_0^a [nm]	conc. [%]	$n_{193\text{ nm}}$	conc. [M]	α_{10} [cm ⁻¹]	λ_{edge}^b [nm]	conc. [mM]
1	H ₂ O	1.436					1.4379		0.0902	185.9	
2	H ₃ PO ₄	1.452	20	0.0575	192	20	1.4545	2	0.184	186.3	0.1
3		1.538	85	0.2444	192	85					
4	H ₂ SO ₄	1.472	20	0.5658	197	20	1.4558	2	0.183	186.3	0.1
5	HCl	1.583	37	sat'd	210	20	1.4631	2	0.240	187.4	0.1
6	HBr						1.5409	2	1.61	202.7	0.1
7	HNO ₃						1.4906	2	1.31	212.5	0.1
8	NaCl		20	sat'd	208	20	1.4892	2	0.427	190.2	1
9	KCl		20	sat'd	209	20	1.4853	2	0.478	190.4	1
10	CsCl	1.561	60	sat'd	206	20	1.4772	2	0.481	190.4	1
11	NH ₄ Cl						1.4784	2	0.480	190.4	1
12	Me ₄ NCl						1.495	2	0.437	190.1	1
13	NaClO ₄						1.4538	2	0.199	186.2	0.1
14	NaHSO ₄	1.473	44				1.4651	2	0.184	186.3	0.1
15	NaOAc						1.4744	2	0.646	190.6	1.0
16	NaSCN						1.5531	2	1.25	195.6	0.1
17	NaBr						1.5353	2	1.27	199.8	0.1

^a λ_0 determined by extrapolating straight-line fit of the absorption band to zero absorbance. ^b λ_{edge} is the wavelength at which $\alpha_{10} = 1\text{ cm}^{-1}$.

**Figure 54.** Quaternary ammonium methylsulfonates.

ganic salts were also explored.³¹⁰ A 6.5 M aqueous solution of CdCl₂ with 8.2 mM SDS exhibited a refractive index of ~1.6. In order to overcome solubility limitations, crown ethers were used to increase the aqueous solubility of the less toxic BaCl₂,³¹¹ however, it was found that the highest refractive indices were obtained with neat crown ether (in which barium chloride is insoluble). While a refractive index of ~1.68 at 193 nm was measured for 12-crown-4 and 15-crown-5 ethers, the absorbance levels were very high due to impurities as well as absorption by the oxygen lone pair electrons.³¹¹

Other aqueous fluids based on water-soluble organic compounds suffer from similar issues. Glycerol, for example, has a refractive index of 1.615 but its absorption coefficient ($\alpha_{10} = 2.3\text{ mm}^{-1}$) at 193 nm is too high to be useful.³⁰⁴ A diluted (50%) solution of glycerol in water ($n = 1.573$) still has an absorption of greater than 6 cm^{-1} .²⁸³ On the basis of computations^{312,313} that predicted some cyclic sulfone, sulfonate, and sulfate compounds would have refractive indices up to 1.67 at 193 nm, a number of water-soluble sulfones including dimethyl sulfone and sulfolane were investigated; however, the low solubility of dimethyl sulfone (~20%) in water, the high absorbance of sulfolane, and their photoinstability to 193 nm radiation prevent these systems from being useful.³⁰⁹

To date, 2.82 M La(OMs)₃ and 3.4 M cyclohexyl-(dimethyl)ammonium methylsulfonate offer the best properties of the aqueous salt-based immersion fluids, although they still fall short of the best organic second-generation immersion fluids (see Table 13). Immersion interference lithography using these aqueous fluids has imaged 32 nm half-pitch features at 1.5 NA.³⁰⁸ While the low cost, low toxicity, and low sensitivity to oxygen of the aqueous immersion fluids are promising, these salt solutions possess lower surface tension-to-viscosity ratios than organic second-generation immersion fluids and would likely exhibit film pulling at similarly low wafer scan rates.³¹⁴ Further increases in the

Table 12. Optical Properties of Quaternary Ammonium and Methylsulfonate Salt Solutions^{306,308}

salt	refractive index		absorbance		
	$n_{193\text{ nm}}$	conc. [M]	α_{10} [cm ⁻¹]	λ_{edge} [nm]	conc. [M]
(CH ₃) ₄ N(OAc)	1.472	1.5	0.767	191.5	0.001
(C ₄ H ₉) ₄ N(OAc)	1.533	1.5	1.095	193.5	0.001
Ba(OMs) ₂	1.493	2	0.314	188.4	2
La(OMs) ₃	1.522	~2.82	0.541	191.0	2
	1.577	~2.82	0.314	188.4	2
104	1.477	1	0.51	<190	1
	1.58	3.4	1.43		3.4
105	1.503	1	1.23	195.2	1
106	1.508	1	>2	196.5	1
107	1.493	0.8	>2	235.9	0.8
108	1.467	1	0.68	<190	1
109	1.472	1	1.29	196.1	1
110	1.485	1	1.25	202.0	1
111	1.490	1	0.79	190.2	1
112	1.493	1	1.75	204.8	1

Table 13. Comparison of Aqueous and Organic Second-Generation Immersion Fluids

fluid	concentration [M]	$n_{193\text{ nm}}$	α_{10} [cm^{-1}]	surface tension (γ) [mN/m]	viscosity (μ) [cP]	γ/μ
water ^{43,308}		1.437	0.036	72.8	1.0	72.8
La(OMs) ₃ ³⁰⁸	2.8	1.577	0.314	28.2	92.8	0.30
(C ₆ H ₁₁)(Me) ₃ N(OMs) (104) ³⁰⁸	3.4	1.58	1.43	52.5	21.4	2.45
DuPont IF-132 ^{270,278}		1.644	0.036	30	3.3	9.1

refractive indices, transparency, and physical properties of aqueous high-index fluids are required.

4.2.3. Third-Generation Fluids Based on Boron, Silicon, And Germanium

Unfortunately, the property requirements required for third-generation immersion fluids eliminate most known materials. For example, increasing the refractive index of polycyclic hydrocarbons by adding additional cyclic structures shifts the absorption edge to higher wavelengths and increases the absorbance at 193 nm to unacceptable levels. Methyl cubane was predicted to have one of the highest densities of any polycyclic hydrocarbon that would still be a liquid at room temperature. Unfortunately, UV measurements on a small sample of purified methyl cubane showed a UV cutoff at ~ 240 nm.³¹⁵

Alternative fluids such as borates,³¹⁶ tetraalkoxysilanes and trialkoxysilyl chlorides,³¹⁷ and oligomeric or polymeric siloxanes^{318,319} have been proposed as immersion fluids with potentially higher refractive indices. Computational studies of organosilicon and organogermanium fluids indicate that organosilicon fluids have lower ultimate refractive indices but higher transparencies than their organogermanium counterparts.³¹³ 5-Silacyclo[4.4]nonane has a D-line refractive index of 1.49 (similar to that for organic second-generation immersion fluids).²⁸⁵ Although DuPont has reported the synthesis of a pure organosilicon fluid with $n_D^{20} = 1.52$,²⁹⁹ there is little indication that organosilicon or organogermanium fluids will be viable third-generation immersion fluids.

3.2.4. Third-Generation Nanoparticle-Based Immersion Fluids

Inorganic materials such as Al₂O₃ ($n \approx 1.95$), MgO ($n \approx 2$), and LuAG ($n = 2.14$) have far higher refractive indices and transparencies at 193 nm than the best second-generation immersion fluids. Dispersions of nanoparticles of such high refractive index inorganic materials in water have been proposed as aqueous second-generation immersion fluids.^{315,320,321} Likewise, nanocomposite fluids based on saturated hydrocarbons are proposed for use as third-generation immersion fluids ($n \geq 1.8$).^{315,322–324} Similar stabilized dispersions of submicrometer diameter inorganic nanoparticles in organic solvents (e.g., silica in cyclohexane,³²⁵ alumina in toluene³²⁶ or decalin^{327,328}) have been extensively studied as model colloidal systems. Many practical and theoretical aspects of nanoparticle-based immersion fluids are discussed in depth elsewhere,^{323,324} and only a brief synopsis will be presented here.

The refractive index of a nanocomposite fluid is dependent upon the refractive index and volume fraction of the nanoparticle cores.^{315,321–324} However, in order to provide stable dispersions of nanoparticles at high concentrations, stabilizing layers are often required to prevent flocculation and sedimentation.^{326–328} The thickness of the stabilizer shell increases the effective volume fraction of the nanoparticle.³²⁹ In order to maximize the refractive index and minimize the

viscosity of the nanocomposite fluid, it is important to utilize a nanoparticle with the highest refractive index possible (to minimize the required volume fraction) and to employ the thinnest stabilizer required to maintain stability at the desired loading (to minimize the excluded volume fraction). For example, the use of hafnia would reduce the required volume fraction of nanoparticles due to its extremely high refractive index at 193 nm ($n \approx 2.9$); however, its transmission cutoff is higher than 193 nm.³¹⁵ It has been proposed that, by reducing the particle size below 10 nm, the quantum confinement effect may be able to shift the absorption edge of hafnia from 225 nm for the bulk to below 193 nm.^{315,322,323}

Another challenge faced by nonhomogeneous immersion fluids is light scattering. Scattered light that does not reach the photoresist is lost (similar to if it had been simply absorbed by the fluid), while scattered light that reaches the wafer degrades image contrast. In order to control scattering, very small nanoparticles with narrow polydispersity will be required.^{323,324} Early aqueous dispersions of alumina nanoparticles (~ 40 wt %) achieved a D-line (589.3 nm) refractive index of 1.455 (extrapolated to ~ 1.6 at 193 nm); however, this fluid was almost completely opaque at 193 nm due to absorption from impurities and scattering from large particles.³²⁰ Jahromi et al. was able to image 130 nm half-pitch patterns using 248 nm interferometric immersion lithography with an aqueous dispersion of silica nanoparticles.^{321,323} Zimmerman et al. have prepared aqueous dispersions of 1 nm diameter HfO₂ nanoparticles (19 vol %, ~ 69 wt %) with a refractive index of 1.418 at 589 nm (extrapolated to 1.59 at 193 nm); however, this system has an absorption cutoff around 240 nm.^{315,322}

Only a few nanoparticle dispersions in hydrocarbon fluids for third-generation immersion fluids have been reported to date. Early work with dispersions of α -Al₂O₃, γ -Al₂O₃, MgAl₂O₄, and MgO in decane showed that refractive indices up to 1.72 at 193 nm were possible in the case of 40 vol % of MgO nanoparticles.³²¹ Subsequent work has focused on the use of higher refractive index nanoparticles like LuAG and HfO₂ in decalin.³²³ Zimmerman et al. produced 5 vol % dispersions of HfO₂ nanoparticles in decalin with a refractive index of 1.492 at 589 nm.³²² However, little transparency data at 193 nm has been reported for these third-generation nanocomposite immersion fluids because of absorption issues. A significant amount of work still remains before a final assessment of the viability of third-generation nanocomposite immersion fluids can be made.

4.3. High Refractive Index Photoresists

Early simulations suggested that photoresists with higher refractive indices ($n \approx 1.8–1.9$) could afford increased process windows and reduced mask error enhancement factor (MEEF) in conventional 193 nm water immersion lithography.³³⁰ Increasing the refractive index of the photoresist restores image contrast by improving the coupling of TM polarized radiation into the photoresist at high NAs.³³¹ Subsequent computational work indicated the benefits of

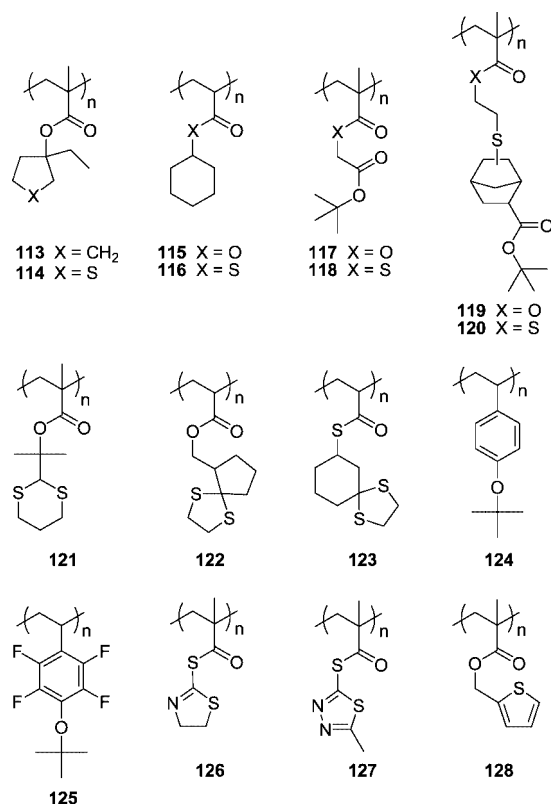


Figure 55. High refractive index homopolymers.

using a high refractive index photoresist with water immersion lithography ($NA \leq 1.35$) may be insufficient compared to the challenges and costs associated with developing a suitable high refractive index photoresist.³³² However, beyond 1.35 NA, the refractive index of the fluid should be greater than or equal to the refractive index of the immersion fluid. Since many commercial 193 nm photoresists have refractive indices around 1.66–1.70, which are sufficient for use with second-generation immersion fluids, work focused on developing photoresists with refractive indices greater than 1.8 and absorption coefficients (α_{10}) less than $3 \mu\text{m}^{-1}$ to enable 1.7 NA imaging.

4.3.1. Organic High Refractive Index Photoresists

The requirements of 193 nm lithography and chemically amplified photoresists eliminate much of the periodic table from consideration when designing high refractive index (RI) photoresists.^{331,333} The most heavily explored approaches toward high-index photoresist materials for 193 nm lithography include increasing the sulfur content of resists to boost RI,^{333–341} manipulating the absorption bands of higher RI aromatic or heteroaromatic structures to improve their transparency,^{333–339,342} incorporating metalloid elements like silicon or germanium into the polymer (i.e., bilayer-type resists),³³³ and blending functionalized inorganic nanoparticles into conventional 193 nm photoresists.^{331,343}

Figure 55 and Table 14 show a variety of polymers developed as part of exploring the first two approaches. Polymer pairs **113/114**, **115/116**, and **117/118** demonstrate the increase in RI by the incorporation of a single sulfur atom into the polymer structure. The thioesters **116** and **118** have significantly improved RI, albeit at the cost of lower transparency. Additional increases in the refractive index can be achieved by incorporating two (**120–122**) or three (**123**) sulfur atoms. Since the absorbance increases more signifi-

Table 14. Optical Properties of High Refractive Index Homopolymers

polymer	$n_{193 \text{ nm}}$	$\alpha_{10} [\mu\text{m}^{-1}]$	ref
113	1.69	0.14	333
114	1.71	1.51	333
115	1.66	0.08	340
116	1.84	3.15	340
117	1.64	0.03	344
118	1.81	2.83	337, 338
119	1.74	1.13	337, 338
120	1.86	2.12	338
121	1.82	3.29	333
122	1.84	3.28	340
123	1.94	5.29	340
124	1.63	19.25	333
125	1.82	10.47	333
126	2.01	7.35	335, 336, 338
127	1.98		335, 336
128	1.86	5.28	333

cantly than the refractive index with each additional sulfur atom, there is a practical limit to how much sulfur can be incorporated into the polymer structures.

Aromatic (or phenolic) structures like **124** used in 248 nm resists have high absorbance at 193 nm; however, the incorporation of fluorine can blue-shift the absorption band of aromatic structures. For example, the fluorinated analogue **125** has a higher refractive index and higher transparency than **124**. Heteroaromatic structures such as **126–128** feature high refractive indices as well, although they share the same high absorbance issues as the other aromatic polymers.

A number of photoresist copolymers based on high refractive index sulfur- or heteroaromatic-based monomers are shown in Figure 56, and their optical properties are listed in Table 15. Many of these materials (**131–132** and **138–140**) suffer from high absorbance or insufficient glass transition temperatures. To date, the high-index photoresists with the best reported balance of refractive index and absorbance include those based on sulfone-containing thiomethacrylate monomers (**135–136**)³⁴⁰ or a thiocarbonate structure (**137**).³⁴¹ Dry 193 nm lithography of a formulated resist based on **136** yielded 100 nm half-pitch L/S patterns, while JSR reported imaging 80 nm half-pitch L/S patterns using **137**.^{340,341} However, even the best of these materials offers only a modest refractive index increase over that of model 193 nm resist materials such as **129** and **130** and cannot currently compete with the lithographic performance of state-of-the-art 193 nm photoresists that have been designed and optimized under far fewer constraints.

Photoresist additives such as photoacid generators, base quenchers, etc. can significantly influence the final optical properties as well. Gonsalves et al. sought to exploit the refractive-index boosting power of both a thiophene-based monomer as well as a polymer-bound PAG to create high refractive index photoresists such as **141** with refractive indices of 1.72–1.78 (Figure 57).³⁴²

4.3.2. Silicon-Based High Refractive Index Photoresists

Silicon and germanium-based polymers have long been used to make thin-layer photoresists suitable for bilayer imaging.^{2,52} With respect to high-index immersion lithography, higher silicon or germanium content desirably improves the refractive index while simultaneously boosting etch resistance. In addition, the high etch resistance of a bilayer resist allows very thin layers of photoresist to be employed and may relax the transparency requirements.

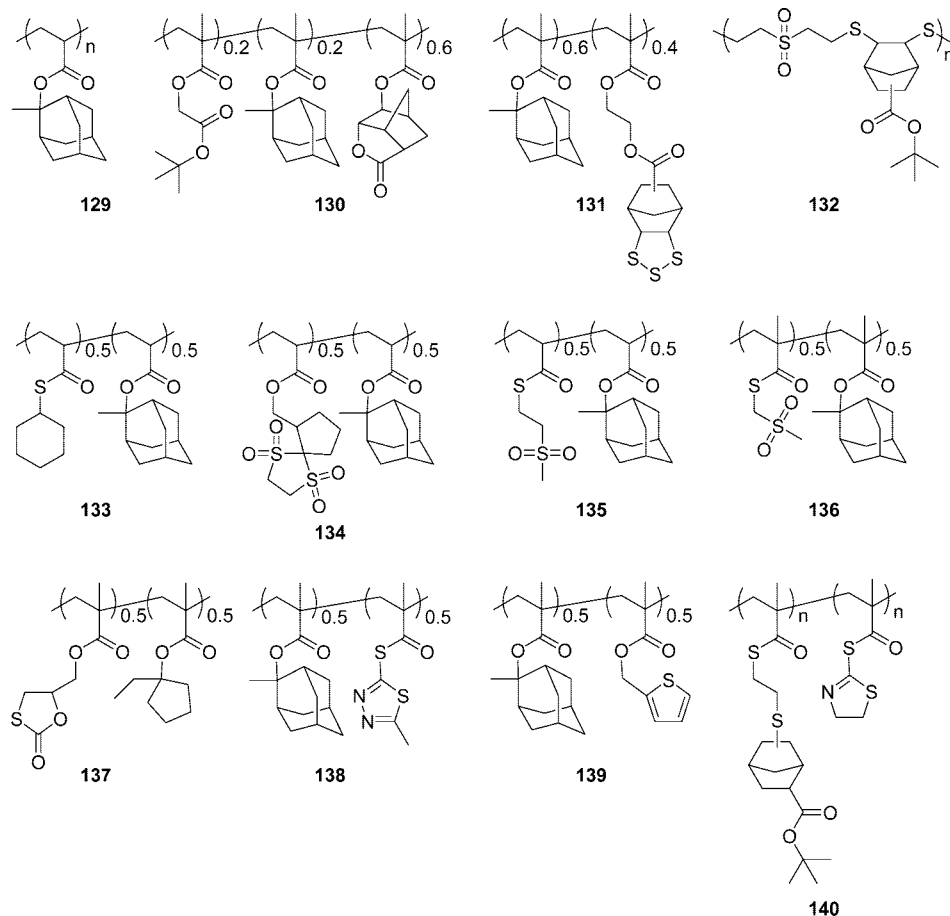


Figure 56. High refractive index photoresist polymers.

Table 15. Optical Properties of High Refractive Index Photoresist Polymers

polymer	$n_{193\text{ nm}}$	$\alpha_{10} [\mu\text{m}^{-1}]$	ref
129	1.73	0.13	340
130	1.71		334, 339
131	1.86		334, 339
132	1.80	7.2	335, 336
133	1.78	1.19	340
134	1.74	0.17	340
135	1.82	1.25	340
136	1.78	1.15	340
137	1.76	1.70	341
138	1.70	5.22	335, 336
139	1.76	5.22	335, 336
140	1.82	10.7	331, 335

Typical bilayer resist backbones such as silsesquioxanes (and polyhedral oligomeric silsesquioxane cage materials) have only moderate refractive indices; therefore, polysilane (142) and polycarbosilane (143–144) materials were screened as potential high-index photoresist backbone materials (Figure 58 and Table 16).³³³ Polycarbosilanes featuring a methylene linkage (143) provided the best balance of refractive index and absorbance; however, the commercially

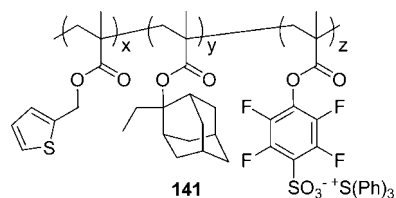


Figure 57. High refractive index photoresist incorporating a polymer-bound PAG.

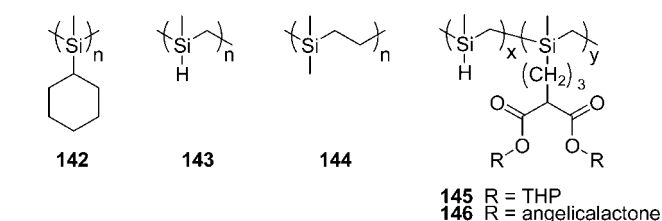


Figure 58. Silicon-based high refractive index polymers.

Table 16. Optical Properties of Silicon-Based High Refractive Index Polymers³³³

polymer	$n_{193\text{ nm}}$	$\alpha_{10} [\mu\text{m}^{-1}]$
142	1.82	5.88
143	1.92	3.88
144	1.71	0.80
145	1.83	1.99
146	1.79	1.36

available highly branched poly(carbomethylsilane) proved difficult to fully functionalize via metal-catalyzed hydrosilylation. Functionalization using tetrahydropyranyl (THP) or angelicalactone-protected difunctional groups (such as allylmalonic acid) was required to produce working polycarbosilane resists (145–146) capable of resolving 130 nm half-pitch L/S patterns.³³³

4.3.3. Nanocomposite-Based High Refractive Index Photoresists

Rather than developing a new high refractive index bilayer resist, nanocomposite resists based on blending functionalized nanoparticles of a high-index inorganic oxide into state-of-

the-art 193 nm photoresists have been proposed as a simpler alternative.³³¹ The proof-of-concept for this approach was demonstrated in 2000 when silica nanoparticles were added to resists in order to improve their transparency for 157 nm lithography.³⁴⁵

The challenges of developing a nanocomposite-based high refractive index photoresist are similar to those described previously for nanoparticle-based third-generation 193 nm immersion fluids, albeit with relaxed absorption requirements due to the shorter optical path length in a photoresist. Unsurprisingly, the candidate materials tend to be identical, with hafnia being the foremost material under consideration.³³¹ Initial films of hafnia nanorods showed $n \approx 2.0$ and $\alpha_{10} \approx 2.5 \mu\text{m}^{-1}$; however, solubility in typical resist casting solvents was poor.³³³ The use of phosphonate- and carboxylic acid-based ligands can increase the solubility of hafnia nanoparticles in propylene glycol methyl ether acetate to over 50 wt % in the best cases.³⁴³ Spun-cast films of nanocomposite systems (methacrylate resist + nanoparticles) exhibited surface roughness comparable to the resist alone.³³¹ Loading 0.7 wt % hafnia nanoparticles into TOK TARF-P6111ME increased the refractive index at 193 nm from 1.7 to 1.73.³⁴³ Work continues on improving the nanoparticle synthesis (size, purity) as well as increasing the nanoparticle loadings in 193 nm photoresists in order to achieve higher refractive indices and increased dry etch resistance.

4.4. Status of High-Index Immersion Lithography

Delays in the fabrication of LuAG lens elements pushed back the delivery dates of the first high-index immersion tools to 2011 at the earliest, nearly two years after their capability was required by the flash memory manufacturers. Eventually, Nikon dropped high-index immersion from their tool roadmap in May 2008³⁴⁶ and was soon followed by the other scanner manufacturers in October 2008.^{292c} Although high-index immersion double-patterning lithography could potentially extend water immersion double-patterning lithography, the abandonment of LuAG development for the high-index last lens element renders the future development of any high-index immersion tools unlikely. Despite this setback for high-index immersion lithography, it is hoped that some of the high-index materials research will impact future patterning materials efforts in a manner similar to how the fluorinated materials originally developed for 157 nm lithography eventually found use in 193 nm immersion topcoats and topcoat-free resists.

5. Summary

The increased numerical aperture and greater depth-of-focus provided by water immersion lithography has enabled the extension of 193 nm optical lithography beyond the 65 nm node. The rapid progress in 193 nm exposure tooling, immersion fluids, topcoats, and resists helped seal the fate of 157 nm lithography. The development and adoption of 193 nm water immersion lithography into high-volume manufacturing was only achieved through tremendous efforts at understanding the impact of water on photoresist materials and imaging and designing materials (e.g., topcoats and topcoat-free resists) to address these issues. High-index immersion lithography was explored as a potential way to further extend the patterning capabilities of 193 nm immersion lithography. High-index immersion lithography employing a lutetium aluminum garnet high-index last lens element

and alicyclic hydrocarbon high-index immersion fluids was shown to be capable of sub-30 nm half-pitch imaging; however, high-index immersion lithography did not meet the necessary insertion point in the semiconductor roadmap timeline.

With high-index immersion lithography at 193 and 157 nm being limited to research project status, 193 nm water immersion lithography will remain the state-of-the-art manufacturing solution until a next-generation lithographic technique (such as EUV lithography, nanoimprint lithography, or parallel e-beam direct write lithography) is available.⁶ To extend the performance of 193 nm optical lithography to further lithographic nodes, industry is now attempting to circumvent the single-exposure resolution limit by moving to double-exposure and double-patterning processes. It is certain that, if implemented, many of these double-exposure and double-patterning processes will be carried out using immersion lithography. In order to design double-exposure materials and double-patterning processes that are compatible with immersion lithography, chemists and engineers will rely on the accumulated knowledge of the interaction of water with lithographic materials and will build upon the available materials and process-based mitigation strategies discussed herein. While the various materials challenges presented by these new double-patterning or double-exposure schemes are currently at the forefront of current lithographic materials research, the continued development of patterning materials for 193 nm immersion lithography will be critical to the future of the semiconductor industry for years to come.

6. Acknowledgments

The author would like to thank Dr. Ratnam Sooriyakumaran (IBM) and Dr. Thomas I. Wallow (GlobalFoundries) for their helpful comments and suggestions and Dr. Carl E. Larson and Dr. Gregory M. Wallraff for contributions to Figure 8. The author would like to dedicate this review to the memory of Dr. Hiroshi Ito, a pioneer in the field of photoresist chemistry, valued colleague, mentor, and friend who will be dearly missed.

7. References

- (1) Wallraff, G. M.; Hinsberg, W. D. *Chem. Rev.* **1999**, *99*, 1801.
- (2) (a) Mack, C. *Fundamental Principles of Optical Lithography: The Science of Microfabrication*; Wiley: West Sussex, England, 2008. (b) Sheats, J. R., Smith, B. W., Eds. *Microolithography: Science and Technology*; Marcel Dekker, Inc.: New York, 1998.
- (3) (a) Thompson, L. F., Willson, C. G., Bowden, M. J., Eds. *Introduction to Microolithography*; American Chemical Society: Washington, DC, 1994. (b) Reichmanis, E.; Thompson, L. F. *Chem. Rev.* **1989**, *89*, 1273. (c) Stepan, H.; Buhr, G.; Vollmann, H. *Angew. Chem., Int. Ed. Engl.* **1982**, *21*, 455.
- (4) (a) Trybula, W. J. *J. Microolith., Microfab., Microsyst.* **2005**, *4*, 011007. (b) Benschop, J. ASML 157 nm program. SEMATECH Litho Forum, Los Angeles, CA, 27–29 January 2004. (c) Wiesner, J. C. Nikon's 157 nm technology—Status and plans. SEMATECH Litho Forum, Los Angeles, CA, 27–29 January 2004. (d) Takahashi, K. Current status and future plan for 157nm lithography. SEMATECH Litho Forum, Los Angeles, CA, 27–29 January 2004.
- (5) Lin, B. J. *J. Microolith., Microfab., Microsyst.* **2002**, *1*, 7.
- (6) (a) Lin, B. *Microelectron. Eng.* **2006**, *83*, 604. (b) Lin, B. C. R. *Physique* **2006**, *7*, 858.
- (7) (a) Lin, B. J. *J. Microolith., Microfab., Microsyst.* **2004**, *3*, 377. (b) Lin, B. J. *Proc. SPIE* **2004**, *5377*, 46.
- (8) Mulken, J.; Flagello, D.; Streefkerk, B.; Graeupner, P. *J. Microolith., Microfab., Microsyst.* **2004**, *3*, 104.
- (9) Streefkerk, B.; Baselmans, J.; Gehoel-van Ansem, W.; Mulken, J.; Hoogendam, C.; Hoogendorp, M.; Flagello, D.; Sewell, H.; Graeupner, P. *Proc. SPIE* **2004**, *5377*, 285.

- (10) (a) Owa, S.; Nagasaka, H. *J. Microlith., Microfab., Microsyst.* **2004**, *3*, 97. (b) Owa, S.; Nagasaka, H.; Ishii, Y.; Hirakawa, O.; Yamamoto, T. *Proc. SPIE* **2004**, *5377*, 264. (c) Owa, S.; Nagasaka, H. *Proc. SPIE* **2003**, *5040*, 724.
- (11) Gil, D.; Brunner, T. A.; Fonseca, C.; Seong, N.; Streefkerk, B.; Wagner, C.; Stavenga, M. *J. Vac. Sci. Technol. B* **2004**, *22*, 3431.
- (12) Chen, J.-H.; Chen, L.-J.; Fang, T.-Y.; Fu, T.-C.; Shiu, L.-H.; Huang, Y.-T.; Chen, N.; Oweyang, D.-C.; Wu, M.-C.; Wang, S.-C.; Lin, J. C. H.; Chen, C.-K.; Chen, W.-M.; Gau, T.-S.; Lin, B. J.; Moerman, R.; Gehol-van Ansem, W.; van der Heijden, E.; de Jong, F.; Oorshot, D.; Boom, H.; Hoogendorp, M.; Wagner, C.; Koek, B. *Proc. SPIE* **2005**, *5754*, 13.
- (13) (a) Smith, B. W.; Kang, H.; Bourov, A.; Cropanese, F.; Fan, Y. *Proc. SPIE* **2003**, *5040*, 679. (b) Smith, B. W.; Bourov, A.; Kang, H.; Cropanese, F.; Fan, Y.; Lafferty, N.; Zavyalova, L. *J. Microlith., Microfab., Microsyst.* **2004**, *3*, 44.
- (14) (a) Wong, A. K. *Resolution Enhancement Techniques in Optical Lithography*; SPIE Press: Bellingham, WA, 2001. (b) Capodiecchi, L. *Proc. SPIE* **2006**, *6154*, 615401. (c) Ronse, K. C. R. *Physique* **2006**, *7*, 844. (d) Mack, C. A. *Proc. SPIE* **2004**, *5374*, 1. (e) Schellenberg, F. *Proc. SPIE* **2004**, *5377*, 1.
- (15) Ito, T.; Okazaki, S. *Nature* **2000**, *406*, 1027.
- (16) Chibana, T.; Kobayashi, M.; Nakano, H.; Arawaka, M.; Matsuoka, Y.; Kawasaki, Y.; Tanabe, M.; Oda, H. *Proc. SPIE* **2008**, *6924*, 69241B.
- (17) 2001 International Technology Roadmap for Semiconductors. Available for download at <http://www.itrs.net>.
- (18) (a) Wu, B.; Kumar, A. *J. Vac. Sci. Technol. B* **2007**, *25*, 1743. (b) Wurm, S.; Jeon, C.-U.; Lercel, M. *Proc. SPIE* **2007**, *6517*, 651705. (c) Kinoshita, H. *J. Vac. Sci. Technol. B* **2005**, *23*, 2584.
- (19) Rothschild, M.; Bloomstein, T. M.; Kunz, R. R.; Liberman, V.; Switkes, M.; Palmacci, S. T.; Sedlacek, J. H. C.; Hardy, D.; Grenville, A. *J. Vac. Sci. Technol. B* **2004**, *22*, 2877.
- (20) Hinsberg, W.; Wallraff, G.; Larson, C.; Davis, B.; Deline, V.; Raoux, S.; Miller, D.; Houle, F.; Hoffnagle, J.; Sanchez, M.; Rettner, C.; Sundberg, L.; Medeiros, D.; Dammel, R.; Conley, W. *Proc. SPIE* **2004**, *5376*, 21.
- (21) Stix, G. *Sci. Am.* **2005**, *7*, 64.
- (22) Shank, C.; Schmidt, R. *Appl. Phys. Lett.* **1973**, *23*, 154.
- (23) Lin, B. *Microelectron. Eng.* **1987**, *6*, 31.
- (24) Takanashi, A.; Harada, T.; Akeyama, M.; Kondo, Y.; Kurosaki, T.; Kuniyoshi, S.; Hosaka, S.; Kawamura, Y. U.S. Pat. 4480910, 1984.
- (25) Tabarelli, W.; Lobach, E. W. U.S. Pat. 4509852, 1985.
- (26) (a) Kawata, H.; Carter, J. M.; Yen, A.; Smith, H. I. *Microelectron. Eng.* **1989**, *9*, 31. (b) Kawata, H.; Matsumura, I.; Yoshida, H.; Murata, K. *Jap. J. Appl. Phys.* **1992**, *31*, 4174.
- (27) Owen, G.; Pease, R. F. W.; Markle, D. A.; Grenville, A.; Hsieh, R. L.; von Bunau, R.; Maluf, N. I. *J. Vac. Sci. Technol. B* **1992**, *10*, 3032.
- (28) Hoffnagle, J. A.; Hinsberg, W. D.; Sanchez, M.; Houle, F. A. *J. Vac. Sci. Technol. B* **1999**, *19*, 3306.
- (29) Smith, R. *Microscopy and Photomicrography: A working manual*; CRC Press: Boca Raton, FL, 1990; pp 1–2.
- (30) (a) Flagello, D.; Milster, T.; Rosenbluth, A. E. *J. Vac. Sci. Technol. B* **1992**, *10*, 2997. (b) Flagello, D.; Milster, T.; Rosenbluth, A. E. *J. Opt. Soc. Am. A* **1996**, *13*, 53.
- (31) Mack, C. A.; Byers, J. D. *Proc. SPIE* **2004**, *5377*, 428.
- (32) Lin, B. *J. Microlith., Microfab., Microsyst.* **2004**, *3*, 21.
- (33) Bruning, J. H. *Proc. SPIE* **2007**, *6520*, 652004.
- (34) (a) Owa, S.; Nagasaka, H.; Nakano, K.; Ohmura, Y. *Proc. SPIE* **2006**, *6154*, 615408. (b) McCallum, M.; Kameyama, M.; Owa, S. *Microelectron. Eng.* **2006**, *83*, 640.
- (35) Mulkens, J.; Streefkerk, B.; Hoogendorp, M.; Moerman, R.; Leenders, M.; de Jong, F.; Stavenga, M.; Boom, H. *Proc. SPIE* **2005**, *5754*, 710.
- (36) Bloomstein, T. M.; Fedynshyn, T. H.; Pottebaum, I.; Marchant, M. F.; Deneault, S. J.; Rothschild, M. *J. Vac. Sci. Technol. B* **2006**, *26*, 2789.
- (37) Switkes, M.; Rothschild, M. *J. Vac. Sci. Technol. B* **2001**, *19*, 2353.
- (38) Hagiwara, T.; Tsuji, S.; Fujii, K.; Moriya, M.; Wakabayashi, O.; Sumitani, A.; Saito, Y.; Maeda, K. *Proc. SPIE* **2006**, *6154*, 61544H.
- (39) (a) Fujii, K.; Hagiwara, T.; Matsuura, S.; Ishimaru, T.; Matsubara, Y.; Wakamiya, W. *SPIE* **2005**, *5754*, 226. (b) Ishimaru, T.; Matsuura, S.; Seki, M.; Fujii, K.; Koizumi, R.; Hakataya, Y.; Moriya, A. *Proc. SPIE* **2005**, *5754*, 1260. (c) Tsuji, S.; Hagiwara, T.; Fujii, K.; Moriya, M.; Wakabayashi, O.; Sumitani, A. Feasibility of liquid immersion lithography at 157-nm. 2nd International Symposium on Immersion Lithography, Bruges, Belgium, 12–15 September, 2005. (d) Furukawa, T.; Hagiwara, T.; Kawaguchi, E.; Matsunaga, K.; Suganaga, T.; Itani, T.; Fujii, K. *Proc. SPIE* **2004**, *5376*, 1064.
- (40) (a) Switkes, M.; Rothschild, M. *Proc. SPIE* **2002**, *4691*, 459. (b) Switkes, M.; Rothschild, M. *J. Microlith., Microfab., Microsyst.* **2002**, *1*, 225.
- (41) (a) Kunz, R. R.; Switkes, M.; Sinta, R.; Curtin, J. E.; French, R. H.; Wheland, R. C.; Chai Kao, C.-P.; Maun, M. P.; Lin, L.; Wetmore, P.; Krukonsis, V.; Williams, K. *J. Microlith., Microfab., Microsyst.* **2004**, *3*, 73. (b) Switkes, M.; Kunz, R. R.; Sinta, R. F.; Rothschild, M.; Gallagher-Wetmore, P. M.; Krukonsis, V. J.; Williams, K. *Proc. SPIE* **2003**, *5040*, 690. (c) Switkes, M.; Kunz, R. R.; Rothschild, M.; Sinta, R. F.; Yeung, M.; Beak, S.-Y. *J. Vac. Sci. Technol. B* **2003**, *21*, 2794.
- (42) French, R. H.; Yang, M. K.; Lemon, M. F.; Synowicki, R. A.; Pribil, G. K.; Cooney, G. T.; Herzinger, C. M.; Green, S. E.; Burnett, J. H.; Kaplan, S. *Proc. SPIE* **2004**, *5377*, 1689.
- (43) Burnett, J. H.; Kaplan, S. G. *J. Microlith., Microfab., Microsyst.* **2004**, *3*, 68.
- (44) (a) Switkes, M.; Rothschild, M. *Proc. SPIE* **2002**, *4691*, 459. (b) Switkes, M.; Kunz, R. R.; Sinta, R. F.; Rothschild, M.; Gallagher-Wetmore, P. M.; Krukonsis, V. J.; Williams, K. *Proc. SPIE* **2003**, *5040*, 690.
- (45) Smith, B. W.; Bourov, A.; Fan, Y.; Zavyalova, L.; Lafferty, N.; Cropanese, F. *Proc. SPIE* **2004**, *5377*, 273.
- (46) Raub, A.; Brueck, S. *Proc. SPIE* **2003**, *5040*, 667.
- (47) (a) Raub, A. K.; Frauenglass, A.; Brueck, S. R. J.; Conley, W.; Dammel, R.; Romano, A.; Sato, M.; Hinsberg, W. *J. Vac. Sci. Technol. B* **2004**, *22*, 3459. (b) Raub, A. K.; Frauenglass, A.; Brueck, S. R. J.; Conley, W.; Dammel, R.; Romano, A.; Sato, M.; Hinsberg, W. *Proc. SPIE* **2004**, *5377*, 306.
- (48) Smith, B.; Kang, H.; Bourov, A.; Copranese, F.; Fan, Y. *Proc. SPIE* **2003**, *5040*, 679.
- (49) (a) Gil, D.; Bailey, T.; Corliss, D.; Brodsky, M. J.; Lawson, P.; Rutten, M.; Chen, Z.; Lustig, N.; Niguissie, T.; Petrillo, K.; Robinson, C. *Proc. SPIE* **2005**, *5754*, 119. (b) Gil, D.; Brunner, T. *Microlith. World* **2005**, *14*, 4.
- (50) Kono, T.; Higashiki, T.; Ito, S.; Inoue, S.; Azuma, T.; Hashimoto, K.; Ishigo, K.; Sato, K.; Hatano, M.; Mukai, H.; Mimotoji, S.; Kawano, K.; Ishii, Y.; Fujiwara, T.; Wakamoto, S.; Owa, S. Implementation of immersion lithography to NAND/CMOS device manufacturing. 4th International Symposium on Immersion Lithography, Keystone, CO, 8–11 October, 2007.
- (51) (a) Dammel, R. *Diazonaphthoquinone-based Resists*; SPIE Press: Bellingham, WA, 1993. (b) Dammel, R. R. *J. Photopolym. Sci. Technol.* **1998**, *11*, 687. (c) Wanat, S. F.; Plass, R. R.; Dahman, M. D. *J. Micro/Nanolith. MEMS MOEMS* **2008**, *7*, 033008.
- (52) Ito, H. *Adv. Polym. Sci.* **2005**, *172*, 37.
- (53) (a) Ito, H. *Proc. SPIE* **2008**, *6923*, 692302. (b) Ito, H. *J. Photopolym. Sci. Technol.* **2008**, *21*, 475. (c) Ito, H. *J. Photopolym. Sci. Technol.* **2007**, *20*, 319. (d) Mortini, B. C. R. *Physique* **2006**, *7*, 924. (e) Moon, S.-Y.; Kim, J.-M. *J. Photochem. Photobiol. C: Photochem. Rev.* **2007**, *8*, 157.
- (54) (a) MacDonald, S. A.; Willson, C. G.; Frechet, J. M. *Acc. Chem. Res.* **1994**, *27*, 153. (b) Reichmanis, E.; Houlihan, F. M.; Nalamasu, O.; Neenan, T. X. *Chem. Mater.* **1991**, *3*, 394. (c) Ito, H. *IBM J. Res. Dev.* **1997**, *41*, 69. (d) Ito, H. *J. Polym. Sci. A: Polym. Chem.* **2003**, *41*, 3863.
- (55) Gokan, H.; Esho, S.; Ohnishi, Y. *J. Electrochem. Soc., Solid State Sci. Technol.* **1983**, *130*, 143.
- (56) (a) Kaimoto, Y.; Nozaki, K.; Takechi, S.; Abe, N. *Proc. SPIE* **1992**, *1672*, 66. For more examples, see (b) Reichmanis, E.; Nalamasu, O.; Houlihan, F. M. *Acc. Chem. Rec.* **1999**, *32*, 659. (c) Stewart, M. D.; Patterson, K.; Somervell, M. H.; Willson, C. G. *J. Phys. Org. Chem.* **2000**, *13*, 767. (d) Okoranyanwu, U.; Byers, J.; Shimokawa, T.; Willson, C. G. *Chem. Mater.* **1998**, *10*, 3328. (e) Houlihan, F. M.; Wallow, T. I.; Nalamasu, O.; Reichmanis, E. *Macromolecules* **1997**, *30*, 6517.
- (57) (a) Kunz, R. R.; Bloomstein, T. M.; Hardy, D. E.; Goodman, R. B.; Downs, D. K.; Curtin, J. E. *J. Vac. Sci. Technol. B* **1999**, *17*, 3267. (b) Kunz, R. R.; Bloomstein, T. M.; Hardy, D. E.; Goodman, R. B.; Downs, D. K.; Curtin, J. E. *J. Photopolym. Sci. Technol.* **1999**, *12*, 561.
- (58) Gandler, J. R.; Jencks, W. P. *J. Am. Chem. Soc.* **1982**, *104*, 1937.
- (59) Ito, H.; Truong, H. D.; Allen, R. D.; Li, W.; Varanasi, P. R.; Chen, K.-J.; Khojasteh, M.; Huang, W.-S.; Burns, S. D.; Pfeiffer, D. *Polym. Adv. Technol.* **2006**, *17*, 104.
- (60) Wei, Y.; Brainard, R. L. *Advanced Processes for 193-nm Immersion Lithography*; SPIE Press: Bellingham, WA, 2009.
- (61) (a) Sewell, H.; Mulkens, J.; Graeupner, P.; McCafferty, D.; Markoya, L.; Donders, S.; Samarakone, N.; Duesing, R. *Proc. SPIE* **2007**, *6520*, 65201M. (b) Sewell, H.; Mulkens, J.; Wagner, C.; McCafferty, D.; Markoya, L.; Lipson, M.; Samarakone, N. *J. Photopolym. Sci. Technol.* **2007**, *20*, 651. (c) Sewell, H.; Mulkens, J.; McCafferty, D.; Markoya, L.; Wagner, C.; Graeupner, P. High-n immersion lithography. 4th International Symposium on Immersion Lithography, Keystone, CO, 8–11 October, 2007.
- (62) (a) Sekine, Y.; Kawahima, M.; Sakamoto, E.; Sakai, K.; Yamada, A.; Honda, T. *Proc. SPIE* **2007**, *6520*, 65201Q. (b) Watanabe, Y.;

- Sakai, K.; Iwasaki, Y.; Mori, S.; Yamashita, K.; Ogusu, M.; Nishikawara, T. Feasibility study of immersion system using a high index fluid. 4th International Symposium on Immersion Lithography, Keystone, CO, 8–11 October, 2007.
- (63) (a) Ohmura, Y.; Nakashima, T.; Nagasaka, H.; Sukegawa, A.; Ishiyama, S.; Kamijo, K.; Shinkai, M.; Owa, S. *Proc. SPIE* **2007**, *6520*, 652006. (b) Ohmura, Y.; Nagasaka, H.; Sukegawa, A.; Matsuyama, T.; Nakashima, T.; Kobayashi, T.; Ueda, M.; Owa, S. Development progress of high index immersion lithography. 4th International Symposium on Immersion Lithography, Keystone, CO, 8–11 October, 2007.
- (64) (a) El-Morsi, M.; Nellis, G.; Schuetter, S.; Van Peski, C.; Grenville, A. *J. Vac. Sci. Technol. B* **2005**, *23*, 2596. (b) Baek, S.; Wei, A.; Cole, D.; Nellis, G.; Yeung, M.; Abdo, A.; Engelstad, R. *Proc. SPIE* **2004**, *5377*, 415. (c) Wei, A.; Abdo, A.; Nellis, G.; Engelstad, R.; Lovell, E.; Beckman, W. *J. Vac. Sci. Technol. B* **2003**, *21*, 2788.
- (65) (a) Robinson, C.; Corliss, D.; Barns, J.; Cummings, K.; Jansen, H.; Lee, B.; Watson, R.; Woodbeck, J.; Goodwin, F.; Wei, Y.; Benson, P.; Housley, R.; Okoroanyanwu, U. Immersion lithography water quality learning at Albany. 2nd International Symposium on Immersion Lithography, Bruges, Belgium, 12–15 September, 2005. (b) Tittnich, M.; Hartley, J.; Denbeaux, G.; Okoroanyanwu, U.; Levinson, H.; Petrillo, K.; Robinson, C.; Gil, D.; Corliss, D.; Back, D.; Brandl, S.; Schwarz, C.; Goodwin, F.; Wei, Y.; Martinick, B.; Housley, R.; Benson, P.; Cummings, K. *Proc. SPIE* **2006**, *6151*, 615101.
- (66) (a) Parekh, B.; Xia, A.; Clarke, M. *Controlled Environ.* **2008**, *11*, 18. (b) Parekh, B.; Xia, A.; Clarke, M. E.; Smith, J. *Ultrapure Water* **2007**, *24*, 31. (c) Clarke, M. E.; Xia, A.; Smith, J.; Parekh, B. Proceedings of the 17th IEEE/SEMI Advanced Semiconductor Manufacturing Conference, Boston, MA, 22–24 May, 2006; p 238. (d) Clarke, M. E.; Xia, A.; Smith, J.; Parekh, B. Point-of-use ultrapure water for immersion lithography. 2nd International Symposium on Immersion Lithography, Bruges, Belgium, 12–15 September, 2005.
- (67) Nakano, H.; Hata, H.; Takahashi, K.; Arakawa, M.; Chibana, T.; Honda, T.; Chiba, K.; Mori, S. *Proc. SPIE* **2005**, *5754*, 693.
- (68) (a) Wei, Y.; Stepanenko, N.; Laessig, A.; Voelkel, L.; Sebald, M. *J. Microlith., Microfab., Microsyst.* **2006**, *5*, 033002. (b) Wei, Y.; Stepanenko, N.; Laessig, A.; Voelkel, L.; Sebald, M. *Proc. SPIE* **2006**, *6153*, 615305.
- (69) (a) Hinsberg, W.; Houle, F. *J. Vac. Sci. Technol. B* **2005**, *23*, 2427. (b) Hinsberg, W.; Houle, F. *Proc. SPIE* **2006**, *6153*, 615303. (c) Hinsberg, W.; Houle, F. *J. Photopolym. Sci. Technol.* **2006**, *19*, 623.
- (70) (a) Herrmann, H.; Reese, A.; Wictor, F.; Zellner, R. *J. Mol. Struct.* **1997**, *408/409*, 539. (b) Sauer, M. C.; Crowell, R. A.; Shkrob, I. A. *J. Phys. Chem. A* **2004**, *108*, 5490.
- (71) Switkes, M.; Bloomstein, T. M.; Kunz, R. R.; Rothschild, M.; Ruberti, J. W.; Shedd, T. A.; Yeung, M. *Proc. SPIE* **2004**, *5377*, 469.
- (72) (a) Burnett, H. B.; Wei, A. C.; El-Morsi, M. S.; Shedd, T. A.; Nellis, G. F.; Van Peski, C.; Grenville, A. *J. Microlith., Microfab., Microsyst.* **2006**, *5*, 013008. (b) Wei, A.; El-Morsi, M.; Nellis, G.; Abdo, A.; Engelstad, R. *J. Vac. Sci. Technol. B* **2004**, *22*, 3444. (c) Wei, A.; Nellis, G.; El-Morsi, M.; Engelstad, R. Predicting air entrapment and liquid recovery due to topography for immersion lithography. International Symposium on Immersion and 157nm Lithography, Vancouver, Canada, 2–5 August, 2004.
- (73) (a) Kocsis, M.; De Bisschop, P.; Maenhout, M.; Kim, Y.-C.; Wells, G.; Light, S.; DiBiase, T. *Proc. SPIE* **2005**, *5754*, 154. (b) Kocsis, M.; Wagner, C.; Donders, S.; DiBiase, T.; Wei, A.; El-Morsi, M.; Nellis, G.; Engelstad, R.; De Bisschop, P. Experimental characterization of topography induced immersion bubble defects. International Symposium on Immersion and 157nm Lithography, Vancouver, Canada, 2–5 August, 2004. (c) Donders, S.; Moerman, R.; Boom, H. Bubble investigation for immersion lithography. International Symposium on Immersion and 157nm Lithography, Vancouver, Canada, 2–5 August, 2004.
- (74) (a) Tyrrell, J. W. G.; Attard, P. *Phys. Rev. Lett.* **2001**, *87*, 176104/1. (b) Attard, P.; Moody, M. P.; Tyrrell, J. W. G. *Physica A* **2002**, *314*, 696. (c) Inshida, N.; Inoue, T.; Miyahara, M.; Higashitani, K. *Langmuir* **2000**, *16*, 6377. (d) Budhlall, B.; He, X.; Hyder, I.; Mehta, S.; Parris, G. Thermodynamic and kinetic stability of nanobubbles at the water–solid interface: A modeling and AFM study. International Symposium on Immersion and 157nm Lithography, Vancouver, Canada, 2–5 August, 2004.
- (75) (a) Kawai, A.; Niyama, T.; Endo, H.; Yamanaka, M.; Ishikawa, A.; Suzuki, K.; Tamada, O.; Sanada, M. *Proc. SPIE* **2006**, *6153*, 61531S. (b) Kawai, A. *J. Photopolym. Sci. Technol.* **2005**, *18*, 349. (c) Niyama, T.; Kawai, A. *J. Photopolym. Sci. Technol.* **2005**, *18*, 373. (d) Kawai, A.; Suzuki, K. *J. Photopolym. Sci. Technol.* **2007**, *20*, 673. (e) Suzuki, K.; Kawai, A. *J. Photopolym. Sci. Technol.* **2007**, *20*, 805. (f) Endo, H.; Kawai, A. *J. Photopolym. Sci. Technol.* **2004**, *17*, 713.
- (76) (a) Switkes, M.; Rothschild, M.; Shedd, T. A.; Burnett, H. B.; Yeung, M. *J. Vac. Sci. Technol. B* **2005**, *23*, 2409. (b) Switkes, M.; Rothschild, M.; Shedd, T. A.; Burnett, H. B. Bubbles in immersion lithography. International Symposium on Immersion and 157nm Lithography, Vancouver, Canada, 2–5 August, 2004.
- (77) (a) Sanders, D. P.; Sundberg, L. K.; Brock, P. J.; Ito, H.; Truong, H. D.; Allen, R. D.; McIntyre, G. R.; Goldfarb, D. L. *Proc. SPIE* **2008**, *6923*, 692309. (b) Sanders, D.; Hinsberg, W.; Truong, H.; Sundberg, L. Fluid–resist interactions for high index immersion lithography. 2008 SEMATECH Litho Forum, Bolton Landing, NY, 12–14 May, 2008. (c) Sanders, D.; Sundberg, L.; Ito, H.; Brock, P.; Sooriyakumaran, R.; Truong, H.; Allen, R. New materials for surface energy control of 193 nm photoresists. 4th International Symposium on Immersion Lithography, Keystone, CO, 8–11 October, 2007.
- (78) (a) Wallraff, G. M.; Larson, C. E.; Breyta, G.; Sundberg, L.; Miller, D.; Gil, D.; Petrillo, K.; Person, W. *Proc. SPIE* **2006**, *6153*, 61531M. (b) Gil, D.; Larson, C.; Wallraff, G.; Allen, R.; Robinson, C.; Corliss, D. The role of evaporation in defect formation in immersion lithography. 2nd International Symposium on Immersion Lithography, Bruges, Belgium, 12–15 September, 2005.
- (79) (a) Tanaka, T.; Hasegawa, N.; Shiraichi, H.; Okazaki, S. *J. Electrochem. Soc.* **1990**, *137*, 3900. (b) Tanaka, T.; Hasegawa, N.; Okazaki, S. *J. App. Phys.* **1990**, *67*, 2617. (c) Brunsvold, W. R.; Hefferon, G. J.; Lyons, C. F.; Moreau, W. M.; Wood, R. L. Eur. Pat. 522990 B1, 1996.
- (80) (a) Nalamasu, O.; Reichmanis, Cheng, M.; Pol, V.; Kometani, J.; Houlihan, F.; Neenan, T.; Bohrer, M.; Mixon, D.; Thompson, L. *Proc. SPIE* **1991**, *1466*, 13. (b) Kumeda, T.; Tanaka, Y.; Ueyama, A.; Kubota, S.; Kozuka, H.; Hanawan, T.; Morimoto, H. *Proc. SPIE* **1993**, *1925*, 31. (c) Oikawa, A.; Santoh, N.; Miyata, S.; Hatakenaka, Y. *Proc. SPIE* **1993**, *1925*, 392.
- (81) (a) Houlihan, F.; Kim, W.; Sakamuri, R.; Hamilton, K.; Simerli, A.; Abdallah, D.; Romano, A.; Dammel, R. R.; Pawlowski, G.; Raub, A.; Brueck, S. *Proc. SPIE* **2005**, *5753*, 78. (b) Houlihan, F.; Sakamuri, R.; Hamilton, K.; Dimerli, A.; Rentkiewicz, D.; Romano, A.; Dammel, R. R.; Wei, Y.; Stepanenko, N.; Sebald, M.; Hohle, C.; Conley, W.; Miller, D.; Itani, T.; Shigematsu, M.; Kawaguchi, E. *Proc. SPIE* **2005**, *5753*, 1136.
- (82) (a) Dammel, R. R.; Houlihan, F. M.; Sakamuri, R.; Rentkiewicz, D.; Romano, A. *J. Photopolym. Sci. Technol.* **2004**, *17*, 587. (b) Dammel, R. R.; Romano, A.; Pawlowski, G.; Houlihan, F.; Sakamuri, R.; Rentkiewicz, D.; Kim, W.-K.; Hamilton, K. The PAG leaching phenomenon in 193 nm immersion lithography. International Symposium on Immersion and 157nm Lithography, Vancouver, Canada, 2–5 August, 2004.
- (83) (a) Ohmori, K.; Ando, T.; Tsuji, H.; Yoshida, M.; Ishizuka, K.; Hirano, T.; Yukawa, H. Top coat investigation for immersion specific issue prevention. 2nd International Symposium on Immersion Lithography, Bruges, Belgium, 12–15 September, 2005. (b) Ishizuka, K.; Endo, K.; Tsuji, H.; Yoshida, M.; Hirano, T.; Sato, M. New cover material development status for immersion lithography. International Symposium on Immersion and 157nm Lithography, Vancouver, Canada, 2–5 August, 2004. (c) Sato, M. TOK resist & material development status for immersion lithography. SEMATECH Litho Forum, Los Angeles, CA, 27–29 January, 2004.
- (84) (a) Slezak, M.; Hung, R.; Liu, Z. *Solid State Technol.* **2004**, *7*, 91. (b) Yoshida, M.; Endo, K.; Ishizuka, K.; Sato, M. *J. Photopolym. Sci. Technol.* **2004**, *17*, 603.
- (85) Kusumoto, S.; Shima, M.; Wang, Y.; Shimokawa, T.; Sato, H.; Hieda, K. *Polym. Adv. Technol.* **2006**, *17*, 122.
- (86) (a) Allen, R. D.; Brock, P. J.; Sundberg, L.; Larson, C. E.; Wallraff, G. M.; Hinsberg, W. D.; Meute, J.; Shimokawa, T.; Chiba, T.; Slezak, M. *J. Photopolym. Sci. Technol.* **2005**, *18*, 615. (b) Wallraff, G. M.; Larson, C. E.; Sundberg, L. K.; Breyta, G.; Sanchez, M.; Truong, H.; Davis, B.; Allen, R. D.; Gil, D.; Prabhu, V.; Sambasivan, S. Topcoats for immersion lithography. 2nd International Symposium on Immersion Lithography, Bruges, Belgium, 12–15 September, 2005.
- (87) (a) Burns, S.; Medeiros, D.; Johnson, H.; Wallraff, G.; Hinsberg, W.; Willson, G. *Proc. SPIE* **2002**, *4690*, 313. (b) Bruce, J. A.; Dupuis, S. R.; Gleason, R.; Linde, H. *J. Electrochem. Soc.* **1997**, *144*, 3169.
- (88) (a) Wallraff, G. M.; Medeiros, D. M.; Larson, C. E.; Sanchez, M.; Petrillo, K.; Huang, W.-S.; Rettner, S.; Davis, B.; Sundberg, L.; Hinsberg, W. D.; Houle, F. A.; Hoffnagle, J. A.; Goldfarb, D.; Temple, K.; Bucchignano, J. *Proc. SPIE* **2005**, *5753*, 309. (b) Wallraff, G. M.; Medeiros, D. R.; Sanchez, M.; Petrillo, K.; Huang, W.-S.; Rettner, S.; Davis, B.; Larson, C. E.; Sundberg, L.; Brock, P. J.; Hinsberg, W. D.; Houle, F. A.; Hoffnagle, J. A.; Goldfarb, D.; Temple, K.; Wind, S.; Bucchignano, J. *J. Vac. Sci. Technol. B* **2004**, *22*, 3479.
- (89) Kishimura, S.; Endo, M.; Sasago, M. *Proc. SPIE* **2004**, *5376*, 44.
- (90) Sekiguchi, A.; Sensu, Y.; Minami, Y. *Proc. SPIE* **2005**, *5753*, 778.

- (91) (a) Taylor, J. C.; LeSuer, R. J.; Chambers, C. R.; Fan, F. F.; Bard, A. J.; Conley, W. E.; Willson, C. G. *Chem. Mater.* **2005**, *17*, 4194. (b) Taylor, J. C.; Chambers, C. R.; Deschner, R.; LeSuer, R. J.; Conley, W. E.; Burns, S. D.; Willson, C. G. *Proc. SPIE* **2004**, *5376*, 34.
- (92) Rathsack, B. M.; Scheer, S.; Kuwahara, Y.; Kitano, J.; Gronheid, R.; Baerts, C. *Proc. SPIE* **2008**, *6923*, 692315.
- (93) (a) Hoskins, T.; Roman, P. J.; Ludovice, P. J.; Henderson, C. L. *Proc. SPIE* **2005**, *5753*, 851. (b) Berger, C. M.; Henderson, C. L. *Polymer* **2003**, *44*, 2101. (c) Berger, C.; Henderson, C. *Proc. SPIE* **2003**, *5039*, 984.
- (94) Toriumi, M.; Matsubara, C.; Otoguro, A.; Itani, T. *Proc. SPIE* **2006**, *6153*, 615311.
- (95) Crank, J. *The Mathematics of Diffusion*; Oxford University Press: New York, 1975; Chapter 4.3, p 47.
- (96) Foubert, P.; Kocsis, M.; Gronheid, R.; Kishimura, S.; Soyano, A.; Nafus, K.; Stepanenko, N.; De Backer, J.; Vandenbroeck, N.; Ercken, M. *Proc. SPIE* **2007**, *6519*, 65190E.
- (97) (a) Hinsberg, W. D.; Hoffnagle, J. A.; Wallraff, G. M.; Larson, C. E.; Houle, F. A.; Sundberg, L.; Truong, H. D.; Davis, B. W.; Allen, R. D. *Proc. SPIE* **2005**, *5753*, 508. (b) Hinsberg, W.; Hoffnagle, J.; Wallraff, G.; Larson, C.; Sundberg, L.; Truong, H.; Davis, B.; Allen, R. Influence of water immersion on properties of lithographic materials. International Symposium on Immersion and 157 nm Lithography, Vancouver, Canada, 2–5 August, 2004.
- (98) Terai, M.; Kumada, T.; Ishibashi, T.; Hagiwara, T.; Hanawa, T.; Ando, T.; Matsunobe, T.; Okada, K.; Yuichi, M.; Yoshikawa, K.; Man, N. *Proc. SPIE* **2007**, *6519*, 65191S.
- (99) (a) Kocsis, M.; Van Den Heuvel, D.; Gronheid, R.; Maenhoudt, M.; Vangooidsenhoven, D.; Wells, G.; Stepanenko, N.; Benndorf, M.; Kim, H. W.; Kishiura, S.; Ercken, M.; Van Roey, F.; O'Brien, S.; Fyen, W.; Foubert, P.; Moerman, R.; Streefkerk, B. *Proc. SPIE* **2006**, *6154*, 615409. (b) Maenhoudt, M.; Kocsis, M.; Stepanenko, N.; O'Brien, S.; Can Den Heuvel, D.; Vangooidsenhoven, D.; Gronheid, R.; Benndorf, M.; Nafus, K.; Fyen, W.; Kim, H.-W.; Kishimura, S.; Ronse, K. *J. Photopolym. Sci. Technol.* **2006**, *19*, 585. (c) Kocsis, M.; Gronheid, R.; Soyano, A.; Foubert, P.; Nafus, K.; Maenhoudt, M.; Stepanenko, N.; Kishimura, S. Watermark defects: Underlying mechanisms and recommendations for their control. 3rd International Symposium on Immersion lithography, Kyoto, Japan, 2–5 October, 2006.
- (100) Otoguro, A.; Lee, J.-W.; Itani, T.; Fujii, K.; Funakoshi, T.; Sakai, T.; Watanabe, K.; Arakawa, M.; Nakano, H.; Kobayashi, M. *Proc. SPIE* **2006**, *6153*, 61531P.
- (101) (a) Stepanenko, N.; Kim, H.-W.; Kishimura, S.; Van den Heuvel, D.; Vandenbroeck, N.; Kocsis, M.; Foubert, P.; Maenhoudt, M.; Ercken, M.; Van Roey, F.; Gronheid, R.; Pollentier, I.; Vangooidsenhoven, D.; Delvaux, C.; Baerts, C.; O'Brien, S.; Fyen, W.; Wells, G. *Proc. SPIE* **2006**, *6153*, 615304. (b) Stepanenko, N.; Kishimura, S.; Gronheid, R.; Maenhoudt, M.; Ercken, M.; Kocsis, M.; Vandenbroeck, N.; Van den Heuvel, D.; Benndorf, M. Studies of the defectivity formation mechanisms between the top coats and resists in immersion lithography. 2nd International Symposium on Immersion Lithography, Bruges, Belgium, 12–15 September, 2005.
- (102) Kishimura, S.; Gronheid, R.; Ercken, M.; Maenhoudt, M.; Matsuo, T.; Endo, M.; Sasago, M. *Proc. SPIE* **2005**, *5753*, 20.
- (103) (a) Liberman, V.; Switkes, M.; Rothschild, M.; Palmacci, S. T.; Sedlacek, J. H.; Hardy, D. E.; Grenville, A. *Proc. SPIE* **2005**, *5754*, 646. (b) Liberman, V.; Switkes, M.; Rothschild, M.; Palmacci, S. T.; Sedlacek, J. H. C.; Hardy, D. E. Long-term 193-nm laser irradiation of thin-film-coated CaF₂ in the presence of water. International Symposium on Immersion and 157nm Lithography, Vancouver, Canada, 2–5 August, 2004.
- (104) (a) Kunz, R. R.; Downs, D. K. *J. Vac. Sci. Technol. B* **1999**, *17*, 3330. (b) Kunz, R. R.; Liberman, V.; Downs, D. K. *J. Vac. Sci. Technol. B* **2000**, *18*, 1306. (c) Kunz, R. R.; Liberman, V.; Downs, D. K. *Proc. SPIE* **2000**, *4000*, 474. (d) Houlihan, F. M.; Rushkin, I. L.; Hutton, R. S.; Gabor, A. H.; Medina, A. N.; Malik, S.; Niesser, M.; Kunz, R. R.; Downs, D. K. *Proc. SPIE* **1999**, *3678*, 264. (e) Bloomstein, T. M.; Sedlacek, J. H. C.; Palmacci, S. T.; Hardy, D. E.; Liberman, V.; Rothschild, M. *Proc. SPIE* **2003**, *5040*, 650.
- (105) (a) Kunz, R. R. *Proc. SPIE* **2004**, *5376*, 1. (b) Barclay, G.; Kanagasabapathy, S.; Pholers, G.; Mattia, J.; Xiong, K.; Ablaza, S.; Cameron, J.; Zampini, A.; Zhang, T.; Yamada, S.; Huby, F.; Wiley, K. *Proc. SPIE* **2003**, *5039*, 433.
- (106) (a) Nellis, G. F.; El-Morsi, M. S.; Van Peski, C.; Grenville, A. *J. Microlith. Microfab., Microsyst.* **2006**, *5*, 013007. (b) Nellis, G.; Engelstad, R.; Lovell, E.; Wei, A.; El-Morsi, M.; Van Peski, C. Contamination transport for wafer to lens. International Symposium on Immersion and 157nm Lithography, Vancouver, Canada, 2–5 August, 2004.
- (107) (a) Liberman, V.; Palmacci, S. T.; Hardy, D. E.; Rothschild, M.; Grenville, A. *Proc. SPIE* **2005**, *5754*, 148. (b) Liberman, V.; Palmacci, S.; Rothschild, M.; Grenville, A. Controlled contamination studies with photoacid generators in 193-nm immersion lithography. 2nd International Symposium on Immersion Lithography, Bruges, Belgium, 12–15 September 2005.
- (108) (a) Liberman, V. L.; Rothschild, M.; Palmacci, S. T.; Grenville, A. *J. Micro/Nanolit. MEMS MOEMS* **2007**, *6*, 013001. (b) Liberman, V.; Switkes, M.; Rothschild, M.; Palmacci, S. T.; Grenville, A. *Proc. SPIE* **2006**, *6154*, 615416.
- (109) Owa, S.; Nagasaka, H.; Ishii, Y.; Shiraiishi, K.; Hirukawa, S. *Proc. SPIE* **2005**, *5754*, 655.
- (110) (a) Streefkerk, B.; Mulken, J.; Moerman, R.; Stavenga, M.; vd Hoeven, J.; Grouwstra, C.; Bruls, R.; Leenders, M.; Wang, S.; van Dommelen, Y.; Boerema, M.; Jansen, H.; Cummings, K.; Riepen, M.; Boom, H.; Suddendorf, M.; Huisman, P. *Proc. SPIE* **2006**, *6154*, 61540S. (b) Streefkerk, B.; Mulken, J.; Moerman, R.; v Dommelen, Y.; Grouwstra, C.; Wang, S.; Blanco Mantecon, M.; Maas, J.; Bruls, R.; van der Graaf, S.; Groenewold, J. Immersion defect performance for volume manufacturing. 3rd International Symposium on Immersion Lithography, Kyoto, Japan, 2–5 October, 2006.
- (111) Lenhart, J. L.; Jones, R. L.; Lin, E. K.; Soles, C. L.; Wu, W.; Fischer, D. A.; Sambasivan, S.; Goldfarb, D. L.; Angelopoulos, M. *J. Vac. Sci. Technol. B* **2002**, *20*, 2920.
- (112) (a) Kanna, S.; Inabe, H.; Yamamoto, K.; Tarutani, S.; Kanda, H.; Mizutani, K.; Kitada, K.; Uno, S.; Kawabe, Y. *Proc. SPIE* **2005**, *5753*, 40. (b) Kanna, S.; Inabe, H.; Yamamoto, K.; Tarutani, S.; Kanda, H.; Mizutani, K.; Kitada, K.; Uno, S.; Kawabe, Y. *J. Photopolym. Sci. Technol.* **2005**, *18*, 603.
- (113) Ercken, M.; Gronheid, R.; Foubert, P.; Stepanenko, N.; Vandeweyer, T.; Pollentier, I.; Kim, H. W.; Kishimura, S.; Tenaglia, E.; Delvaux, C.; Vandenbroeck, N.; Moelants, M.; Baerts, C. *J. Photopolym. Sci. Technol.* **2006**, *19*, 539.
- (114) Dammel, R. R.; Pawlowski, G.; Romano, A.; Houlihan, F. M.; Kim, W.-K.; Sakamuri, R.; Abdallah, D. *Proc. SPIE* **2005**, *5753*, 95.
- (115) Dammel, R. R.; Pawlowski, G.; Romano, A.; Houlihan, F. M.; Kim, W.-K.; Sakamuri, R.; Abdallah, D.; Padmanaban, M.; Rahman, M. D.; McKenzie, D. *J. Photopolym. Sci. Technol.* **2005**, *18*, 593.
- (116) (a) Gronheid, R.; Baerts, C.; Caporale, S.; Alexander, J.; Rathsack, B.; Scheer, S.; Ohmori, K.; Rice, B. World wide standardization efforts on leaching measurement methodology. 4th International Symposium on Immersion Lithography, Keystone, CO, 8–11 October, 2007. (b) Gronheid, R.; Colburn, M. E.; Petrillo, K.; Tenaglia, E.; Ercken, M.; Larson, C. E.; Wallraff, G. M. Towards a standardized leaching measurement methodology. 3rd International Symposium on Immersion Lithography, Kyoto, Japan, 2–5 October, 2006.
- (117) Gronheid, R.; Tenaglia, E.; Ercken, M. *Proc. SPIE* **2006**, *6154*, 615411.
- (118) Nakagawa, H.; Hoshiko, K.; Shima, M.; Kusumoto, S.; Shimokawa, T.; Nakano, K.; Fujiwara, T.; Owa, S. *Proc. SPIE* **2006**, *6153*, 61530D.
- (119) (a) Matsumura, N.; Sugie, N.; Goto, K.; Fujiwara, K.; Yamaguchi, Y.; Tanizaki, H.; Nakano, K.; Fujiwara, T.; Wakamizu, S.; Takeguchi, H.; Arima, H.; Kyoda, H.; Yoshihara, K.; Kitano, J. *Proc. SPIE* **2008**, *6923*, 69230D. (b) Goto, K.; Yamaguchi, Y.; Fujiwara, T.; Nakano, K.; Ishii, Y.; Hyouda, H.; Kitano, J. Adapting non-topcoat process to high volume manufacturing. 4th International Symposium on Immersion Lithography, Keystone, CO, 8–11 October, 2007.
- (120) (a) Conley, W.; LeSuer, R. J.; Fan, F. F.; Bard, A. J.; Taylor, C.; Tsiartas, P.; Willson, G.; Romano, A.; Dammel, R. *Proc. SPIE* **2005**, *5753*, 64. (b) Conley, W.; Taylor, C.; Costner, E.; Willson, G.; Houlihan, F.; Romano, A.; Dammel, R. Understanding the photoresist surface–liquid interface: A progress report. 2nd International Symposium on Immersion Lithography, Bruges, Belgium, 12–15 September, 2005. (c) LeSuer, R. J.; Fan, F. F.; Bard, A. J.; Taylor, J. C.; Tsiartas, P.; Willson, C. G.; Conley, W.; Feit, G.; Kunz, R. *Proc. SPIE* **2004**, *5376*, 115.
- (121) Sato, M.; Yoshida, M.; Ishizuka, K.; Tsuji, H.; Endo, K. *Jpn. J. Appl. Phys.* **2005**, *44*, 5803.
- (122) Gaugiran, S.; Feilleux, R.; Sourd, C.; Warrick, S.; Farys, V.; Cruau, D.; Benndorf, M.; Mortini, B. *Microelectron. Eng.* **2007**, *84*, 1054.
- (123) Dammel, R. R. Ultrathin resists for immersion and EUV: Reflectivity control, integration, and fundamental issues. IEEE Lithography Workshop, Charlottetown, Prince Edward Island, Canada, 31 July–4 August, 2006.
- (124) (a) Tsuji, H.; Yoshida, M.; Ishizuka, K.; Hirano, T.; Endo, K.; Sato, M. *Proc. SPIE* **2005**, *5753*, 102. (b) Tsuji, H.; Yoshida, M.; Ishizuka, K.; Hirano, T.; Endo, K.; Ohmori, K. *J. Photopolym. Sci. Technol.* **2005**, *18*, 641.
- (125) Wada, K.; Kanna, S.; Kanda, H. *Proc. SPIE* **2007**, *6519*, 651908.
- (126) (a) Petrillo, K.; Patel, K.; Chen, R.; Li, W.; Kwong, R.; Lawson, P.; Varanasi, R.; Robinson, C.; Holmes, S.; Gil, D.; Kimmel, K.; Slezak, M.; Dabbagh, G.; Chiba, T.; Shimokawa, T. *Proc. SPIE* **2005**, *5753*, 52. (b) Smith, J.; Slezak, M.; Peterson, B.; Kusumoto, S.; Shimokawa,

- T.; Shima, M.; Petrillo, K.; Holmes, S.; Patel, K.; Lawson, P.; Varanasi, R. Immersion topcoat progress—The path to success. 2nd International Symposium on Immersion Lithography, Bruges, Belgium, 12–15 September, 2005.
- (127) Ishibashi, T.; Hanawa, T.; Suganaga, T.; Maejima, S.; Narimatsu, K.; Suko, K.; Terai, M.; Kumada, T.; Ando, T. *J. Photopolym. Sci. Technol.* **2006**, *19*, 547.
- (128) Enomoto, M.; Hatakeyama, S.; Niwa, T.; Tomita, T.; Kyoda, H.; Kitano, J.; Shimura, S.; Kawasaki, T. *Proc. SPIE* **2006**, *6153*, 61533L.
- (129) Tomita, T.; Shimoaoki, T.; Enomoto, M.; Kyoda, H.; Kitano, J.; Suganaga, T. *Proc. SPIE* **2006**, *6153*, 61533M.
- (130) (a) Ando, T.; Maemori, S.; Yokoi, S.; Takayama, T.; Ishizuka, K.; Hirano, T.; Yokoya, J.; Ohmori, K. Synthesis of topcoat process for 193 nm immersion lithography: A progress report. 3rd International Symposium on Immersion Lithography, Kyoto, Japan, 2–5 October, 2006. (b) Ito, S.; Matsunaga, K.; Kawamura, D.; Onishi, Y. Solvent effects for immersion properties of cover-coat materials. 2nd International Symposium on Immersion Lithography, Bruges, Belgium, September 12–15, 2005.
- (131) (a) Wei, A. C.; Nellis, G. F.; Abdo, A. Y.; Engelstad, R. L.; Chen, C.; Switkes, M.; Rothschild, M. *J. Microlith., Microfab., Microsyst.* **2004**, *3*, 28. (b) Wei, A.; Nellis, G.; Abdo, A.; Engelstad, R.; Chen, C.-F.; Switkes, M.; Rothschild, M. *Proc. SPIE* **2003**, *5040*, 713. (c) Abdo, A.; Nellis, G.; Wei, A.; El-Morsi, M.; Engelstad, R.; Brueck, S. R. J.; Neumann, A. *J. Vac. Sci. Technol. B* **2004**, *22*, 3454.
- (132) (a) Mulkens, J.; Streefkerk, B.; Jasper, J.; de Klerk, J.; de Jong, F.; Levasier, L.; Leenders, M. *Proc. SPIE* **2007**, *6520*, 652005. (b) Cromwijk, J. W.; Blanco Matecon, M.; Boudou, N.; Boom, H.; van Dommelen, Y.; Grouwstra, C.; Mulkens, J.; Pieters, M.; Uzunbajakau, S.; Wang, S. Defects performance and stability for immersion lithography at 45 nm and beyond. 4th International Symposium on Immersion Lithography, Keystone, CO, 8–11 October, 2007.
- (133) (a) Liang, F.-J.; Shiu, L.-H.; Chen, C.-K.; Chen, L.-J.; Gau, T.-S.; Lin, B. J. *J. Micro/Nanolith., MEMS, MOEMS* **2007**, *6*, 010501. (b) Shiu, L.-H.; Liang, F.-J.; Chang, H.; Chen, C.-K.; Chen, L.-J.; Gau, T.-S.; Lin, B. J. *Proc. SPIE* **2007**, *6520*, 652012. (c) Liang, F. J.; Chang, H.; Su, C. R.; Fu, T. C.; Chen, C. K.; Chen, L. J.; Gau, T. S.; Lin, B. J. *Proc. SPIE* **2007**, *6520*, 65204U.
- (134) Burnett, H.; Shedd, T.; Nellis, G.; Van Peski, C. *J. Vac. Sci. Technol. B* **2005**, *23*, 2721.
- (135) (a) Colburn, M.; Sundberg, L.; Levasseur, R.; Clancy, A.; Gronheid, R.; Van Roey, F.; Fyen, W.; Schuetter, S.; Harder, P.; Shedd, T.; Vervoort, M.; Grouwstra, C.; Moeram, R.; Rudack, A. Reproducible contact angle measurements for immersion materials evaluation. 3rd International Symposium on Immersion Lithography, Kyoto, Japan, 2–5 October, 2006. (b) Fyen, W.; O'Brien, S.; Wells, G.; Van Roey, F.; Rip, J.; Gronheid, R.; Maenhoudt, M. Static vs dynamic contact angles on photoresist layers: Comparison of measurement methods. 2nd International Symposium on Immersion Lithography, Bruges, Belgium, 12–15 September, 2005.
- (136) Sundberg, L. K.; Sanders, D. P.; Sooriyakumaran, R.; Brock, P. J.; Allen, R. D. *Proc. SPIE* **2007**, *6519*, 65191Q.
- (137) (a) Schuetter, S. D.; Shedd, T. A.; Nellis, G. F. *J. Micro/Nanolith., MEMS, MOEMS* **2007**, *6*, 023003. (b) Schuetter, S.; Shedd, T.; Nellis, G.; Romano, A.; Dammel, R.; Padmanaban, M.; Houlihan, F.; Krawicz, A.; Lin, G.; Rahman, D.; Chakrapani, S.; Neisser, M.; Van Peski, C. *J. Vac. Sci. Technol. B* **2006**, *24*, 2798.
- (138) (a) Bongiovanni, R.; Maluceili, G.; Priola, A. *J. Colloid Interface Sci.* **1995**, *171*, 283. (b) Morita, M.; Ogisu, H.; Kubo, M. *J. Appl. Polym. Sci.* **1999**, *73*, 1741.
- (139) Bassett, D. W.; Taylor, J. C.; Conley, W.; Willson, C. G.; Bonnecaze, R. T. *Proc. SPIE* **2006**, *6154*, 61544P.
- (140) (a) Schuetter, S.; Shedd, T.; Doxtator, K.; Nellis, G.; Van Peski, C.; Grenville, A.; Lin, S.-H.; Owe-yang, D. C. *J. Microlith., Microfab., Microsyst.* **2006**, *5*, 023002. (b) Schuetter, S. D.; Shedd, T. A.; Doxtator, K. A.; Nellis, G. F.; Van Peski, C. K. *Proc. SPIE* **2006**, *6281*, 62810Q. (c) Van Peski, C.; Grenville, A.; Engelstad, R.; Nellis, G.; Shedd, T.; Schuetter, S.; Doxtator, K.; Lin, S.-H.; Owe-Yang, D. C. Film pulling and meniscus instability as a cause of residual fluid droplets. 2nd International Symposium on Immersion Lithography, Bruges, Belgium, 12–15 September, 2005.
- (141) Shedd, T. A.; Schuetter, S. D.; Nellis, G. F.; Van Peski, C. K. *Proc. SPIE* **2006**, *6154*, 61540R.
- (142) Burnett, H.; Shedd, T.; Nellis, G.; El-Morsi, M.; Engelstad, R.; Garoff, S.; Varanasi, K. *J. Vac. Sci. Technol. B* **2005**, *23*, 2611.
- (143) (a) de Gennes, P. G.; Brochard-Wyart, F.; Quere, D. *Capillarity and Wetting Phenomena*; Springer: New York, 2004. (b) Petrov, J. G.; Sedev, R. V.; Petrov, P. G. *Adv. Colloid Interface Sci.* **1992**, *38*, 229.
- (144) (a) Schuetter, S. D.; Shedd, T. A.; Nellis, G. F. *J. Micro/Nanolith., MEMS, MOEMS* **2007**, *6*, 023003. (b) Shedd, T. A.; Schuetter, S. D.; Nellis, G. F.; Van Peski, C. K. *Proc. SPIE* **2006**, *6154*, 61540R.
- (145) Ando, T.; Ohmori, K.; Maemori, S.; Takayama, T.; Ishizuka, K.; Yoshida, M.; Hirano, T.; Yokoya, J.; Nakano, K.; Fujiwara, T.; Owa, S. *Proc. SPIE* **2006**, *6153*, 615309.
- (146) (a) Sanders, D. P.; Sundberg, L. K.; Brock, P. J.; Ito, H.; Truong, H. D.; Allen, R. D.; McIntyre, G. R.; Goldfarb, D. L. *Proc. SPIE* **2008**, *6923*, 692309. (b) Sanders, D.; Sundberg, L.; Ito, H.; Brock, P.; Sooriyakumaran, R.; Truong, H. New materials for surface energy control of 193 nm photoresists. 4th International Symposium on Immersion Lithography, Keystone, CO, 8–11 October, 2007. (c) Allen, R. D.; Brock, P.; Sanders, D. P.; Sundberg, L. K. U.S. 2008/0311506 A1. (d) Allen, R. D.; Brock, P.; Sanders, D. P.; Sundberg, L. K. U.S. 2008/0311530 A1.
- (147) Brandl, S.; Watso, R.; Holmes, S.; Wei, Y.; Petrillo, K.; Cummings, K.; Goodwin, F. *Proc. SPIE* **2006**, *6154*, 61540T.
- (148) (a) Kawamura, D.; Takeishi, T.; Matsunaga, K.; Shiobara, E.; Oonishi, Y.; Ito, S. *Proc. SPIE* **2006**, *6153*, 61531Q. (b) Matsunaga, K.; Kondoh, T.; Hayasaki, K.; Takeishi, T.; Kawamura, D.; Ito, S.; Kawasaki, T.; Kyoda, H. Novel defect control methodologies for high volume immersion lithography manufacturing. 3rd International Symposium on Immersion Lithography, Kyoto, Japan, 2–5 October, 2006.
- (149) Takahashi, N.; Shimura, S.; Kawasaki, T. *Proc. SPIE* **2007**, *6519*, 65191Z.
- (150) Nakano, K.; Nagaoka, S.; Yoshida, M.; Iriuchijima, Y.; Fujiwara, T.; Shiraishi, K.; Owa, S. *Proc. SPIE* **2008**, *6924*, 692418.
- (151) (a) Nakano, K.; Kato, H.; Fujiwara, T.; Shiraishi, K.; Iriuchijima, Y.; Owa, S.; Malik, I.; Woodman, S.; Terala, P.; Pellissier, C.; Zhang, H. *Proc. SPIE* **2007**, *6520*, 652016. (b) Nakano, K.; Nagaoka, S.; Owa, S.; Yamamoto, T.; Malik, I. Immersion defectivity analysis using volume production immersion exposure tool. 3rd International Symposium on Immersion Lithography, Kyoto, Japan, 2–5 October, 2006.
- (152) (a) Nakano, K.; Kato, H.; Owa, S. *Proc. SPIE* **2007**, *6519*, 65190D. (b) Nakano, K.; Kato, H.; Yoshida, M.; Nagaoka, S.; Fujiwara, T.; Iriuchijima, Y.; Owa, S. Analysis and improvement of immersion defectivity using volume production immersion lithography tool. 4th International Symposium on Immersion Lithography, Keystone, CO, 8–11 October, 2007. (c) Nakano, K.; Owa, S.; Malik, I.; Yamamoto, T.; Nag, S. *Proc. SPIE* **2006**, *6154*, 61544J. (d) Nakano, K.; Nagaoka, S.; Owa, S. Defectivity data taken with a full-field immersion exposure tool. 2nd International Symposium on Immersion Lithography, Bruges, Belgium, 12–15 September, 2005. (e) Kohno, H.; Nagasaka, H.; Akiyama, H.; Nakano, K.; Watanabe, S.; Owa, S. Resist properties for scanners: Leaching of chemicals and surface condition for scanning. 2nd International Symposium on Immersion Lithography, Bruges, Belgium, 12–15 September, 2005.
- (153) (a) Okoroanyanwu, U.; Kye, J.; Yamamoto, N.; Cummings, K. *Microlith. World* **2005**, *14* (4), 46, 18. (b) Okoroanyanwu, U.; Kye, J.; Levinson, H. J.; Yamamoto, N.; Cummings, K. Prospects & challenges of defectivity in water immersion lithography. 2nd International Symposium on Immersion Lithography, Bruges, Belgium, 14 September, 2005.
- (154) (a) Streefkerk, B.; Wagner, C.; Moerman, R.; Mulkens, J.; Bouchoms, I.; Van de Mast, F.; Vanoppen, P.; De Jong, F.; Modderman, T.; Kneer, B. Advancements in system technology for the immersion lithography era. 2nd International Symposium on Immersion Lithography, Bruges, Belgium, 12–15 September, 2005. (b) Nakano, K.; Nagaoka, S.; Owa, S. Defectivity data taken with a full-field immersion exposure tool. 2nd International Symposium on Immersion Lithography, Bruges, Belgium, 12–15 September, 2005.
- (155) Wei, Y.; Brandl, S.; Goodwin, F. *Proc. SPIE* **2008**, *6923*, 69231Y.
- (156) (a) Ban, K.; Park, S.; Bok, S.; Lim, H.; Heo, J.; Chun, H.; Kang, J.; Moon, S. *Proc. SPIE* **2007**, *6519*, 65191V. (b) Ban, K.; Bok, C.; Lee, S.; Lim, H.; Heo, J.; Jun, H.; Kim, T.; Moon, S. Reduction of immersion swelling defects. 3rd International Symposium on Immersion Lithography, Kyoto, Japan, 2–5 October, 2006.
- (157) (a) Wei, Y.; Petrillo, K.; Brandl, F.; Benson, P.; Housley, R.; Okoroanyanwu, U. *Proc. SPIE* **2006**, *6153*, 615306. (b) Wei, Y.; Petrillo, K.; Benson, P. *Solid State Technol.* **2006**, *7*, 73. (c) Petrillo, K.; Housley, R.; Benson, P.; Goodwin, F.; Wei, Y.; Brandl, S.; Martinick, B. Topcoat compatibility studies. 2nd International Symposium on Immersion Lithography, Bruges, Belgium, 12–15 September, 2005. (d) Brandl, S.; Housley, R.; Goodwin, F.; Benson, P.; Wei, Y.; Robinson, C.; Corliss, D.; Okoroanyanwu, U.; Watso, R.; Cummings, K. Immersion defect studies on the 1150i α -tool. 2nd International Symposium on Immersion Lithography, Bruges, Belgium, 12–15 September, 2005. (e) Schwarz, C.; Wei, Y.; Goodwin, F.; Benson, P.; Housley, R. Measuring resist top coat compatibility using ellipsometry. 2nd International Symposium on Immersion Lithography, Bruges, Belgium, 12–15 September, 2005. (f) Benson, P.; Housley, R.; Goodwin, F.; Wei, Y.; Katchur, N.; Tachikawa, T.; Ohmori, K. 193 nm immersion material top coat acid and resist photo acid generator interaction. 2nd International Sym-

- posium on Immersion Lithography, Bruges, Belgium, 12–15 September, 2005.
- (158) Shedd, T. A. *J. Microlith., Microfab., Microsyst.* **2005**, *4*, 033004.
- (159) Fan, Y.; Lafferty, N.; Bourov, A.; Zavyalova, L.; Smith, B. W. *Proc. SPIE* **2004**, *5377*, 477.
- (160) Lin, C. H.; Wang, L. A. *J. Vac. Sci. Technol. B* **2005**, *23*, 2684.
- (161) (a) De Bisschop, P.; Erdmann, A.; Rathsfeld, A. *Proc. SPIE* **2005**, *5754*, 243. (b) Erdmann, A.; Evanschitzky, P.; De Bisschop, P. *Proc. SPIE* **2005**, *5754*, 383.
- (162) Yao, T.; Yamamoto, H.; Yanagishita, Y.; Mutou, E.; Ishikawa, S.; Asai, S. Study on the effects of micro bubbles in immersion lithography. 2nd International Symposium on Immersion Lithography, Bruges, Belgium, 12–15 September, 2005.
- (163) Switkes, M.; Ruberti, J. W. *Appl. Phys. Lett.* **2004**, *84*, 4759.
- (164) Kawamura, D.; Takeishi, T.; Sho, K.; Matsunaga, K.; Shibata, N.; Ozawa, K.; Shimura, S.; Kyoda, H.; Kawasaki, T.; Ishida, S.; Toshima, T.; Oonishi, Y.; Ito, S. *Proc. SPIE* **2005**, *5754*, 818.
- (165) (a) Deegan, R. D.; Bakajin, O.; Dupont, T. F.; Huber, G.; Nagel, S. R.; Witten, T. A. *Nature* **1987**, *389*, 827. (b) Deegan, R. D.; Bakajin, O.; Dupont, T. F.; Huber, G.; Nagel, S. R.; Witten, T. A. *Phys. Rev. E* **2000**, *62*, 756.
- (166) Niyama, T.; Kawai, A.; Hori, S.; Narumoto, M.; Tamada, O.; Sanada, M. *Proc. SPIE* **2006**, *6153*, 61531U.
- (167) Niwa, T.; Scheer, S.; Carcasi, M.; Enomoto, M.; Tomita, T.; Hontake, K.; Kyoda, H.; Kitano, J. *Proc. SPIE* **2007**, *6519*, 651922.
- (168) Ishibashi, T.; Hanawa, T.; Suganaga, T.; Narimatsu, K.; Suko, K.; Terai, M.; Kumada, T.; Ando, T. *Proc. SPIE* **2006**, *6153*, 615331.
- (169) Niwa, T.; Enomoto, M.; Shimura, S.; Kyoda, H.; Kawasaki, T.; Kitano, J. *Proc. SPIE* **2005**, *5753*, 799.
- (170) Chang, C.-Y.; Yu, D.-C.; Lin, J. C. H.; Lin, B. J. *Proc. SPIE* **2006**, *6154*, 615417.
- (171) Nakagawa, H.; Nakamura, A.; Dougauchi, H.; Shima, M.; Kusumoto, S.; Shimokawa, T. *Proc. SPIE* **2006**, *6153*, 615431R.
- (172) (a) Yu, S.-S.; Lin, B. J.; Yen, A.; Ke, C.-M.; Huang, J.; Ho, B.-C.; Chen, C.-K.; Gau, T.-S.; Hsieh, H.-C.; Ku, Y.-C. *J. Microlith., Microfab., Microsyst.* **2005**, *4*, 043003. (b) Yu, S.-S.; Lin, B. J.; Yen, A. *J. Microlith., Microfab., Microsyst.* **2005**, *4*, 043004.
- (173) Huang, W.-S.; Heath, W. H.; Kwong, R.; Li, W.; Patel, K.; Varanasi, P. R. *Proc. SPIE* **2006**, *6153*, 61530S.
- (174) Hirayama, T.; Takasu, R.; Sato, M.; Wakiya, K.; Yoshida, M.; Tamura, K. U.S. Pat. 7371510, 2008.
- (175) Brock, P. J.; Cha, J. N.; Gil, D.; Larson, C. E.; Sundberg, L. K.; Wallraff, G. M. U.S. Pat. 2007/0117040 A1.
- (176) (a) Hinsberg, W. D., III. U.S. Pat. 7205093, 2007. (b) Hinsberg, W. D., III. U.S. Pat. 7348127, 2008.
- (177) (a) Grenville, A.; Liberman, V.; Rothschild, M.; Sedlacek, J. H. C.; French, R. H.; Wheland, R. C.; Zhang, X.; Gordon, J. *Proc. SPIE* **2002**, *4691*, 1644. (b) French, R. H.; Wheland, R. C.; Qiu, W.; Lemon, M. F.; Blackman, G. S.; Zhang, E.; Gordon, J.; Liberman, V.; Grenville, A.; Kunz, R.; Rothschild, M. *Proc. SPIE* **2002**, *4691*, 576. (c) French, R. H.; Gordon, J.; Jones, D. J.; Lemon, M. F.; Wheland, R. C.; Zhang, E.; Zumsteg, F. C.; Sharp, K. G.; Qiu, W. *Proc. SPIE* **2001**, *4346*, 89. (d) French, R. H.; Wheland, R. C.; Jones, D. J.; Hilfiker, J. N.; Synowicki, R. A.; Zumsteg, F. C.; Feldman, J.; Feiring, A. E. *Proc. SPIE* **2000**, *4000*, 1491. (e) Zimmerman, P. A.; van Peski, C.; Miller, D.; Proctor, A.; Callahan, R. P.; Cashion, M. The use of modified polytetrafluoroethylene for 157nm and 193 nm soft pellicles. International Symposium on Immersion and 157nm Lithography, Vancouver, Canada, 2–5 August, 2004. (f) Blakey, I.; George, G. A.; Hill, D. J. T.; Liu, H.; Rasoul, F.; Rintoul, L.; Whittaker, A. K.; Zimmerman, P. Analysis of the photodegradation at 157 nm of photolithographic-grade Teflon AF Pellicles. International Symposium on Immersion and 157nm Lithography, Vancouver, Canada, 2–5 August, 2004.
- (178) (a) Toriumi, M.; Ishikawa, T.; Kodani, T.; Koh, M.; Moriya, T.; Araki, T.; Aoyama, H.; Yamashita, T.; Yamazaki, T.; Furukawa, T.; Itani, T. *J. Photopolym. Sci. Technol.* **2003**, *16*, 607. (b) Toriumi, M.; Ishikawa, T.; Kodani, T.; Koh, M.; Moriya, T.; Yamashita, T.; Araki, T.; Aoyama, H.; Yamazaki, T.; Furukawa, T.; Itani, T. *J. Vac. Sci. Technol. B* **2004**, *22*, 27. (c) Feiring, A. E.; Crawford, M. K.; Farnham, W. B.; Feldman, J.; French, R. H.; Leffew, K. W.; Petrov, V. A.; Schadt, R. C., III; Wheland, R. C.; Zumsteg, F. C. *J. Fluor. Chem.* **2003**, *122*, 11. (d) Crawford, M. K.; Feiring, A. E.; Feldman, J.; French, R. H.; Periyasamy, M.; Schadt, R. C., III; Smalley, R. J.; Zumsteg, F. C.; Kunz, R. R.; Rao, V.; Lioa, L.; Holl, S. M. *Proc. SPIE* **2000**, *3999*, 357.
- (179) (a) Yamashita, T.; Ishikawa, T.; Yoshida, T.; Hayamai, T.; Araki, T.; Aoyama, H.; Hagiwara, T.; Itani, T.; Fujii, K. *Proc. SPIE* **2005**, *5753*, 564. (b) Yamashita, T.; Ishikawa, T.; Yoshida, T.; Hayami, T.; Aoyama, H. *Proc. SPIE* **2006**, *6153*, 615325. (c) Yamashita, T.; Ishikawa, T.; Hayami, T.; Aoyama, H. Novel fluorinated polymers for top coat in 193-nm lithography. 3rd International Symposium on Immersion Lithography, Kyoto, Japan, 2–5 October, 2006.
- (180) Kanda, H.; Kanna, S.; Inabe, H. U.S. Pat. 2006/0036005 A1.
- (181) (a) Toriumi, M.; Shida, N.; Watanabe, H.; Yamazaki, T.; Ishikawa, S.; Itani, T. *Proc. SPIE* **2002**, *4690*, 191. (b) Kodama, S.; Kaneko, I.; Takebe, Y.; Okada, S.; Kawaguchi, Y.; Shida, N.; Ishikawa, S.; Toriumi, M.; Itani, T. *Proc. SPIE* **2002**, *4690*, 76. (c) Takebe, Y.; Eda, M.; Okada, S.; Yokokoji, O.; Irie, S.; Otoguro, A.; Fujii, K.; Itani, T. *Proc. SPIE* **2004**, *5376*, 151.
- (182) (a) Shirota, N.; Takebe, Y.; Sasaki, T.; Yokokoji, O.; Toriumi, M.; Masuhara, H. *Proc. SPIE* **2006**, *6153*, 615324. (b) Shirota, N.; Takebe, Y.; Sasaki, T.; Wang, S.-Z.; Yokokoji, O. Development of new materials based on fluoropolymers for 193-nm immersion lithography. 3rd International Symposium on Immersion Lithography, Kyoto, Japan, 2–5 October, 2006. (c) Takebe, Y.; Shirota, N.; Sasaki, T.; Yokokoji, O. *Proc. SPIE* **2007**, *6519*, 65191Y.
- (183) Takebe, Y.; Shirota, N.; Sasaki, T.; Murata, K.; Yokokoji, O. *Proc. SPIE* **2008**, *6923*, 69231U.
- (184) (a) Hata, M.; Ryoo, M.-H.; Choi, S.-J.; Cho, H.-K. *J. Photopolym. Sci. Technol.* **2006**, *19*, 579. (b) Hata, M.; Kim, H.-W.; Yoon, J.-Y.; Ha, J.-H.; Ryoo, M.-H.; Woo, S.-G.; Cho, H.-K. *J. Photopolym. Sci. Technol.* **2005**, *18*, 621.
- (185) Huang, W.-S. S.; Burns, S. D.; Varanasi, P. R. U.S. Pat. 7320855, 2008.
- (186) (a) Allen, R. D.; Sooriyakumaran, R.; Sundberg, L. K. U.S. Pat. 7399581, 2008. (b) Allen, R. D.; Brock, P. J.; Larson, C. E.; Sooriyakumaran, R.; Sundberg, L. K.; Truong, H. U.S. Pat. 2007/0254236 A1.
- (187) Weigel, S. J.; Zhang, P.; Braymer, T. A.; Parris, G. E. U.S. Pat. 2007/0196773 A1.
- (188) Gallagher, M. K.; Wayton, G. B.; Prokopowicz, G. P.; Robertson, S. A. U.S. Pat. 2006/0105272 A1.
- (189) Allen, R. D.; Brock, P. J.; Larson, C. E.; Sooriyakumaran, R.; Sundberg, L. K.; Truong, H. U.S. Pat. 2007/0254236 A1.
- (190) Maeda, K.; Ootani, M.; Komoriya, H. U.S. Pat. 2007/0087125 A1.
- (191) Kimura, T.; Nishimura, Y.; Utaka, Y.; Nemoto, H.; Nakamura, A.; Chiba, T.; Nakagawa, H. U.S. Pat. 2007/0269734 A1.
- (192) Allen, R. D.; Brock, P. J.; Burns, S. D.; Goldfarb, D. L.; Medeiros, D.; Pfeiffer, D.; Pinnow, M.; Sooriyakumaran, R.; Sundberg, L. K. U.S. Pat. 2007/0254237 A1.
- (193) (a) Honda, K.; Morita, M.; Otsuka, H.; Takahara, A. *Macromolecules* **2005**, *38*, 5699. (b) Morita, M.; Ogisu, H.; Kubo, M. *J. Appl. Polym. Sci.* **1999**, *73*, 1741.
- (194) (a) Allen, R. D.; Brock, P. J.; Gil, D.; Hinsberg, W. D.; Larson, C. E.; Sundberg, L. K.; Wallraff, G. M. U.S. Pat. 7288362, 2007. (b) Allen, R. D.; Brock, P. J.; Gil, D.; Hinsberg, W. D.; Larson, C. E.; Sundberg, L. K.; Wallraff, G. M. U.S. Pat. 2008/0026330 A1. (c) Maeda, K.; Komoriya, H.; Sumida, S.; Miyazawa, S.; Ootani, M. U.S. Pat. 2005/0250898 A1.
- (195) (a) Ito, H.; Sundberg, L. K. U.S. Pat. 7358035, 2008. (b) Ito, H.; Sundberg, L. K. U.S. Pat. 2006/0292484 A1. (c) Ito, H.; Sundberg, L. K. U.S. Pat. 2006/0292485 A1. (d) Ito, H.; Sundberg, L. K. U.S. Pat. 2008/0145787 A1.
- (196) Hatakeyama, J.; Harada, Y.; Kawai, Y.; Endo, M.; Sasago, M.; Komoriya, H.; Ootani, M.; Miyazawa, K.; Maeda, K. U.S. Pat. 2007/0026341 A1.
- (197) Sanders, D. P.; Sundberg, L. K.; Sooriyakumaran, R.; Brock, P. J.; DiPietro, R. A.; Truong, H. D.; Miller, D. C.; Lawson, M. C.; Allen, R. D. *Proc. SPIE* **2007**, *6519*, 651904.
- (198) (a) Yamashita, T.; Ishikawa, T.; Morita, M.; Kanemura, T.; Aoyama, H. *Proc. SPIE* **2008**, *6923*, 69231Z. (b) Yamashita, T.; Kishikawa, Y.; Tanaka, Y.; Morita, M.; Kanemura, T.; Aoyama, H. Synthesis of novel α -fluoroacrylates and related polymers for immersion lithography. 5th International Symposium on Immersion Lithography Extensions, The Hague, Netherlands, 22–25 September, 2008.
- (199) Allen, R. D.; Breyta, G.; Brock, P.; DiPietro, R. A.; Sanders, D.; Sooriyakumaran, R.; Sundberg, L. *J. Photopolym. Sci. Technol.* **2006**, *19*, 569.
- (200) Harada, Y.; Hatakeyama, J. U.S. Pat. 2007/0298355 A1.
- (201) Harada, Y.; Hatakeyama, J.; Hasegawa, K. U.S. Pat. 2008/0085466 A1.
- (202) Kanda, H. U.S. Pat. 7316886, 2008.
- (203) Wang, D.; Xu, C.-B. U.S. Pat. 2007/0087286 A1.
- (204) (a) Rhodes, L. F.; Chang, C.; Kandanarachchi, P.; Seger, L. D.; Ishiduka, K.; Endo, K.; Ando, T. U.S. Pat. 2006/00234164 A1. (b) Rhodes, L. F.; Chang, C.; Kandanarachchi, P.; Seger, L. D.; Ishiduka, K.; Endo, K.; Ando, T. U.S. Pat. 2006/0235174 A1.
- (205) Hatakeyama, J.; Harada, Y.; Watanabe, T. U.S. Pat. 2007/0122736 A1.
- (206) (a) Li, W.; Lawson, M. C.; Varanasi, P. R. U.S. Pat. 7335456, 2008. (b) Li, W.; Lawson, M. C.; Varanasi, P. R. U.S. Pat. 2008/0038676 A1.
- (207) Hata, M.; Yoon, J.-Y.; Hah, J.-H.; Ryoo, M.-H.; Choi, S.-J.; Cho, H.-K. *Proc. SPIE* **2006**, *6153*, 61531Y.
- (208) Gallagher, M. K.; Wang, D. U.S. Pat. 2007/0212646 A1.
- (209) Jung, J. C.; Bok, C. K.; Lim, C. M.; Moon, S. C. U.S. Pat. 2006/0127803 A1.

- (210) (a) Chiba, T.; Kimura, T.; Utaka, T.; Nakagawa, H.; Sakakibara, H.; Dougauchi, H.; Waki, M. *WO 2006/035790 A1*. (b) Chiba, T.; Kimura, T.; Utaka, T.; Nakagawa, H.; Sakakibara, H.; Dougauchi, H. U.S. 2008/0038661 A1. (c) Nakamura, A.; Nakashima, H.; Tsuji, T.; Dougauchi, H.; Kouno, D.; Waki, M. *WO 2007/049637 A1*. (d) Khojasteh, M.; Popova, I.; Varanasi, P. R.; Sundberg, L.; Robinson, C.; Corliss, D.; Lawson, M.; Dabbagh, G.; Slezak, M.; Colburn, M.; Petrillo, K. *Proc. SPIE 2007, 6519, 651907*. (e) Khojasteh, M.; Huang, W.-S.; Lawson, M. C.; Patel, K. S.; Popova, I.; Varanasi, P. R. U.S. 2008/0032228 A1.
- (211) (a) Geoghegan, M.; Krausch, G. *Prog. Polym. Sci.* **2003**, *28*, 261. (b) Slep, D.; Asselta, J.; Rafailovich, M. H.; Sokolov, J.; Winsett, D. A.; Smith, A. P.; Ade, H.; Strzhemechny, Y.; Schwarz, S. A.; Sauer, B. B. *Langmuir* **1998**, *14*, 4860.
- (212) Wang, D.; Trefonas, P., III; Gallagher, M. K. U.S. 2007/0160930 A1.
- (213) Nishimura, Y.; Sugie, N.; Nakashima, H.; Natsume, N.; Kuono, D.; Watanabe, K. *WO 2008/047678 A1*.
- (214) Nafus, K.; Shimoaoki, T.; Enomoto, M.; Shite, H.; Otsuka, T.; Kosugi, H.; Shibata, T.; Mallmann, J.; Maas, R.; Verspaget, C.; van der Heijden, E.; van Setten, E.; Finders, J.; Wang, S.; Boudou, N.; Zoltesi, C. *Proc. SPIE 2009, 7273, 727338*.
- (215) Petrillo, K.; Johnson, R.; Conley, W.; Cantone, J.; Hetzer, D.; Dunn, S.; Winter, T.; van Dommelen, Y.; Jiang, A. *Proc. SPIE 2009, 7273, 72732C*.
- (216) (a) Lee, S. H.; Kim, J. W.; Kim, J. W.; Oh, S. K.; Park, C. S.; Lee, J. Y.; Kim, S. S.; Lee, J. W.; Kim, D. B.; Kim, J.; Ban, K. D.; Bok, C. R.; Moon, S. C. *Proc. SPIE 2007, 6519, 651925*. (b) Lee, J. W.; Oh, S. K.; Kim, J. W.; Lee, S. H.; Jeong, Y. H.; Kim, S. S.; Park, M. H.; Kim, D.; Kim, J.; Lee, G.; Moon, S.-C. *Proc. SPIE 2006, 6153, 615321*.
- (217) Wang, S.-Z.; Shirota, N.; Takebe, Y.; Sasaki, T.; Yokokoji, O. Highly water-repellent resin having fluorinated cyclic structures for immersion lithography photoresists. 3rd International Symposium on Immersion Lithography, Kyoto, Japan, 2–5 October, 2006.
- (218) Kim, S. S.; Kim, J. W.; Lee, J. Y.; Oh, S. K.; Lee, S. H.; Kim, J. W.; Lee, J. W.; Kim, D. B.; Kim, J.; Ban, K. D.; Bok, C. R.; Moon, S.-C. *Proc. SPIE 2007, 6519, 65191W*.
- (219) (a) Padmanaban, M.; Romano, A.; Lin, G.; Chiu, S.; Timko, A.; Houlihan, F.; Rahman, D.; Chakrapani, S.; Kudo, T.; Dammel, R. R.; Turnquest, K.; Rich, G.; Schuetter, S. D.; Shedd, T. A.; Nellis, G. F. *Proc. SPIE 2006, 6153, 615307*. (b) Padmanaban, M.; Romano, A.; Lin, G.; Chiu, S.; Timko, A.; Houlihan, F.; Rahman, D.; Dammel, R. R.; Turnquest, K.; Rich, G.; Schuetter, S. D.; Shedd, T. A.; Nellis, G. F. *J. Photopolym. Sci. Technol.* **2006**, *19*, 555.
- (220) Ando, N.; Lee, Y.; Miyagawa, T.; Edamatsu, K.; Takemoto, I.; Yamamoto, S.; Tsuchida, Y.; Yamamoto, K.; Honishi, S.; Nakano, K.; Tomoharu, F. *Proc. SPIE 2006, 6153, 615322*.
- (221) (a) Sanders, D. P.; Sundberg, L. K.; Sooriyakumaran, R.; Brock, P. J.; DiPietro, R. A.; Truong, H. D.; Miller, D. C.; Lawson, M. C.; Allen, R. D. *Proc. SPIE 2007, 6519, 651904*. (b) Sanders, D. P.; Sundberg, L. K.; Sooriyakumaran, R.; Allen, R. D. *Microlith. World* **2007**, *16* (3), 8. (c) Wallraff, G.; Sanders, D.; Larson, C.; Sundberg, L.; Sooriyakumaran, R.; Gil, D.; Tirapu, J.; Lawson, P.; Petrillo, K.; Allen, R.; Malik, I.; Radovanovic, S.; Steinbach, A. The role of evaporation and surface properties in defect formation in immersion lithography. 3rd International Symposium on Immersion Lithography, Kyoto, Japan, 2–5 October, 2006.
- (222) (a) Wang, D.; Caporale, S.; Andes, C.; Cheon, K.-S.; Xu, C. B.; Trefonas, P.; Barclay, G. *J. Photopolym. Sci. Technol.* **2007**, *20*, 687. (b) Wang, D.; Xu, C.; Caporale, S.; Trefonas, P. *Solid State Technol.* **2007**, *50*. (c) Barclay, G.; Trefonas, P.; Wang, D.; Robertson, S.; Xu, C. B.; Caporale, S.; Leonard, J. A new materials approach for 193 immersion lithography—Defect and leaching control. IEEE Lithography Workshop, Charlottetown, Prince Edward Island, Canada, 31 July–4 August, 2006.
- (223) Shimokawa, T.; Yamaguchi, Y.; Takahashi, J.; Kusumoto, S.; Shima, M. Recent progress in ArF lithography materials development. IEEE Lithography Workshop, Charlottetown, Prince Edward Island, Canada, 31 July–4 August, 2006.
- (224) (a) Kanna, S.; Inabe, H.; Yamamoto, K.; Fukuhara, T.; Tarutani, S.; Kanda, H.; Kenji, W.; Kodama, K.; Shitabatake, K. *Proc. SPIE 2006, 6153, 615308*. (b) Kanna, S.; Inabe, H.; Yamamoto, K.; Tarutani, S.; Kanda, H.; Saegusa, H.; Mizutani, K.; Kawabe, Y.; Iguchi, N.; Shitabatake, K. 193 nm immersion resist technology for non-topcoat application. 2nd International Symposium on Immersion Lithography, Bruges, Belgium, 12–15 September, 2005. (c) Kanna, S.; Kokubo, T.; Brzozowy, D. ArF immersion resist development status. International Symposium on Immersion and 157nm Lithography, Vancouver, Canada, 2–5 August, 2004.
- (225) Irie, M.; Endo, K.; Iwai, T. *J. Photopolym. Sci. Technol.* **2006**, *19*, 565.
- (226) Ohmori, K.; Ando, T.; Takayama, T.; Ishizuka, K.; Yoshida, M.; Utsumi, Y.; Endo, K.; Iwai, T. *Proc. SPIE 2006, 6153, 61531X*.
- (227) Padmanaban, M.; Lin, G.; Chakrapani, S.; Kudo, T.; Dammel, R. R. Recent advances in 193 nm resists for dry and wet applications. 4th International Symposium on Immersion Lithography, Keystone, CO, 8–11 October, 2007.
- (228) Naruoka, T.; Matsumura, N.; Syoano, A.; Kusumoto, S.; Yamaguchi, Y.; Arima, H.; Yoshida, Y.; Yoshihara, K.; Shibata, T. *Proc. SPIE 2009, 7273, 727328*.
- (229) Eon, D.; Carty, G.; Fernandez, V.; Cardiaud, C.; Tegou, E.; Bellas, V.; Argitis, P.; Gogolides, E. *J. Vac. Sci. Technol. B* **2004**, *22*, 2526.
- (230) Wang, D. U.S. 2006/0246373 A1.
- (231) (a) Kanda, H.; Kanna, S. U.S. 2007/0134588 A1. (b) Kanda, H.; Kanna, S.; Inabe, H. U.S. 2007/0059639 A1.
- (232) Allen, R. D.; Brock, P. J.; Larson, C. E.; Sanders, D. P.; Sooriyakumaran, R.; Sundberg, L. K.; Truong, H. D.; Wallraff, G. M. U.S. 2007/0254235 A1.
- (233) (a) Kanda, H.; Kanna, S. U.S. Pat. 7368220, 2008. (b) Fukuhara, T.; Kanna, S.; Kanda, H. U.S. 2007/0134590 A1.
- (234) Malik, S.; Brzozowy, D.; Sarubbi, T. *J. Photopolym. Sci. Technol.* **2007**, *20*, 457.
- (235) Kanda, H.; Inabe, H. U.S. 2006/0008736 A1.
- (236) (a) Jablonski, E. L.; Prabhu, V. M.; Sambasivan, S.; Lin, E. K.; Fischer, D. A.; Goldfarb, D. L.; Angelopoulos, M.; Ito, H. *J. Vac. Sci. Technol. B* **2003**, *21*, 3162. (b) Jablonski, E. L.; Prabhu, V. M.; Sambasivan, S.; Fischer, D. A.; Lin, E. K.; Goldfarb, D. L.; Angelopoulos, M.; Ito, H. *Proc. SPIE 2004, 5376, 302*.
- (237) (a) Ito, H.; Truong, H. D.; Allen, R. D.; Li, W.; Varanasi, P. R.; Chen, K. J.; Khojasteh, M.; Huang, W. S.; Burns, S. D.; Pfeiffer, D. *Polym. Adv. Technol.* **2006**, *12*, 104. (b) Breyta, G.; Ito, H.; Truong, H. D. U.S. 6794110, 2004. (c) Ito, H.; Truong, H.; Okazaki, M.; Miller, D. C.; Fender, N.; Brock, P. J.; Wallraff, G. M.; Larson, C. E.; Allen, R. D. *J. Photopolym. Sci. Technol.* **2002**, *15*, 591. (d) Ito, H.; Wallraff, G. M.; Fender, N.; Brock, P. J.; Hinsberg, W. D.; Mahorowala, A.; Larson, C. E.; Truong, H.; Breyta, G.; Allen, R. D. *J. Vac. Sci. Technol. B* **2001**, *19*, 2678.
- (238) Kanda, H.; Kanna, S.; Inabe, H. U.S. 2007/0178405 A1.
- (239) Sasaki, K.; Nakamura, T.; Hirayama, T.; Shimizu, K. H.; Utsumi, Y.; Hirono, T.; Irie, M.; Endo, K.; Yamada, T.; Motoike, N.; Oshita, K.; Omori, K. Defect reduction with topcoat less photo resist for 193 nm immersion lithography. 3rd International Symposium on Immersion Lithography, Kyoto, Japan, 2–5 October, 2006.
- (240) (a) Man, N.; Okumura, H.; Oizumi, H.; Nagai, N.; Seki, H.; Nishiyama, I. *Appl. Surf. Sci.* **2004**, *231*, 353. (b) Okumura, H.; Takeda, K.; Nagai, N. *J. Photopolym. Sci. Technol.* **2004**, *17*, 535. (c) Nagai, N.; Imai, T.; Terrada, K.; Seki, H.; Okumura, H.; Fujino, H.; Yamamoto, T.; Nishiyama, I.; Hatta, A. *Surf. Interface Anal.* **2002**, *34*, 545.
- (241) (a) Nakagawa, H.; Nakashima, H.; Wakamatsu, G.; Harada, K.; Nishimura, Y. *WO 2007/116664 A1*. (b) Nishimura, Y.; Harada, K.; Wakamatsu, G.; Nakashima, H.; Nakagawa, H.; Matsumura, N.; Kojima, S. *WO 2008/087840 A1*.
- (242) (a) Takemoto, I.; Ando, N.; Edamatsu, K.; Fuji, Y.; Kuwana, K.; Hashimoto, K.; Funase, J.; Yokoyama, H. *Proc. SPIE 2007, 6519, 65191X*. (b) Takemoto, I.; Ando, N.; Edamatsu, K.; Fuji, Y.; Hashimoto, K.; Funase, J.; Yokoyama, H. *J. Photopolym. Sci. Technol.* **2007**, *20*, 473.
- (243) Irie, M.; Yoshii, Y. U.S. 2008/0090171 A1.
- (244) Caporale, S. J.; Barclay, G. G.; Wang, D.; Jia, L. U.S. 2008/0193872 A1.
- (245) (a) Harada, Y.; Hatakeyama, J.; Kusaki, W. U.S. 2008/0090173 A1. (b) Harada, Y.; Hatakeyama, J.; Yoshihara, T.; Kusaki, W.; Kobayashi, T.; Hasegawa, K. U.S. 2008/0118860 A1.
- (246) Harada, Y.; Hatakeyama, J.; Yoshihara, T.; Kusaki, W.; Kobayashi, T.; Hasegawa, K. U.S. 2008/0118860 A1.
- (247) (a) Shirota, N.; Takebe, Y.; Wang, S.-Z.; Sasaki, T.; Yokokoji, O. *Proc. SPIE 2007, 6519, 651905*. (b) Shirota, N.; Murata, K.; Watanabe, K.; Takebe, Y.; Yokokoji, O. Advance of topcoat-less resist materials for immersion lithography. 4th International Symposium on Immersion Lithography, Keystone, CO, 8–11 October, 2007.
- (248) Hagiwara, T.; Ishibashi, T.; Terai, M.; Kumada, T.; Shirota, N.; Yokokoji, O.; Matsunobe, T.; Man, N.; Yoshikawa, K.; Tanahashi, Y.; Hanawa, T. *J. Photopolym. Sci. Technol.* **2008**, *21*, 679.
- (249) Shirota, N.; Murata, K.; Takebe, Y.; Yokokoji, O. Study of fluorinated materials for the extension of immersion lithography. 5th International Symposium on Immersion Lithography Extensions, The Hague, Netherlands, 22–25 September, 2008.
- (250) Sheehan, M. T.; Farnham, W. B.; Okazaki, H.; Sounik, J. R.; Clark, G. *Proc. SPIE 2008, 6923, 60232E*.
- (251) Otake, A.; Miura, M.; Tsuchiya, K.; Ogino, K. *J. Photopolym. Sci. Technol.* **2008**, *21*, 647.

- (252) Wu, S.; Tseng, A.; Lin, B.; Yu, C. C.; Lu, B.-J.; Liao, W.-S.; Wang, D.; Vohra, V.; Xu, C. B.; Caporale, S.; Barclay, G. *Proc. SPIE* **2008**, 6923, 602307.
- (253) (a) Kanna, S.; Inabe, H.; Yamamoto, K.; Fukuhara, T.; Tarutani, S.; Kanda, H.; Kenji, W.; Kodama, K.; Shitabatake, K. *Proc. SPIE* **2006**, 6153, 615308. (b) Kanna, S.; Inabe, H.; Yamamoto, K.; Fukuhara, T.; Tarutani, S.; Kanda, H.; Kenji, W.; Kodama, K.; Shitabatake, K. *J. Photopolym. Sci. Technol.* **2006**, 19, 593. (c) Kanna, S.; Inabe, H.; Yamamoto, K.; Tarutani, S.; Kanda, H.; Kenji, W.; Kodama, K.; Shitabatake, K. Non-topcoat resist design for immersion defectivity reduction. 3rd International Symposium on Immersion Lithography, Kyoto, Japan, 2–5 October, 2006.
- (254) Kato, H.; Oori, T.; Sho, K.; Matsunaga, K.; Shiobara, E.; Azuma, T.; Nichimura, Y.; Nakagawa, H.; Yamaguchi, Y.; Shiota, N.; Yokokoji, O.; Fujiwara, T.; Ishii, Y.; Ito, S. Critical issue of non-topcoat resist for ultra low k_1 lithography. 5th International Symposium on Immersion Lithography Extensions, The Hague, Netherlands, 22–25 September, 2008.
- (255) Sho, K.; Kato, H.; Kobayashi, K.; Iida, K.; Ori, T.; Muto, D.; Azuma, T.; Ito, S.; Fujiwara, T.; Ishii, Y.; Nishimura, Y.; Kawakami, T.; Shima, M. *Proc. SPIE* **2009**, 7273, 72733B.
- (256) (a) Mage, I.; Pinter, B.; Tuckermann, M.; Donsella, O. *Proc. SPIE* **2004**, 5375, 779. (b) Ono, Y.; Shimoaoki, T.; Naito, R.; Kitano, J. *Proc. SPIE* **2004**, 5376, 1206. (c) Shimoaoki, T.; Naito, R.; Kitano, J. *Proc. SPIE* **2004**, 5376, 1223.
- (257) (a) Arima, H.; Yoshida, Y.; Yoshihara, K.; Shibata, T.; Kushida, Y.; Nakagawa, H.; Nishimura, Y.; Yamaguchi, Y. *Proc. SPIE* **2009**, 7273, 727333. (b) Kushida, Y.; Makita, Y.; Kawakami, T.; Hoshiko, K.; Nakagawa, H.; Nishimura, Y.; Yamaguchi, Y. *J. Photopolym. Sci. Technol.* **2008**, 21, 641.
- (258) Shigemori, K.; Wang, S.; Tedeschi, L.; Tanriseve, G.; Maas, R.; Verspaget, C.; Marechal, R.; Lammers, A.; Mallmann, J.; Harumoto, M.; Hisai, A.; Asai, M. *Proc. SPIE* **2009**, 7273, 72732B.
- (259) Harumoto, M.; Negoro, S.; Hisai, A.; Tanaka, M.; Mori, G.; Slezak, M. *Proc. SPIE* **2009**, 7273, 72730P.
- (260) (a) Miyahara, O.; Shimoaoki, T.; Naito, R.; Yoshihara, K.; Kitano, J. *Proc. SPIE* **2006**, 6153, 61533K. (b) Carcasi, M.; Hatakeyama, S.; Nafus, K.; Moerman, R.; van Dommelen, Y.; Huisman, P.; Hooge, J.; Scheer, S.; Foubert, P. *Proc. SPIE* **2006**, 6153, 61533J.
- (261) Hagiwara, T.; Terai, M.; Ishibashi, T.; Miyauchi, T.; Hori, S.; Kumada, T.; Kumagai, T.; Sawano, A.; Doi, K.; Matsunobe, T.; Man, N.; Seki, H.; Tanahashi, Y.; Hanawa, T. *Proc. SPIE* **2009**, 7273, 727324.
- (262) Kim, M.-S.; Jung, H.-R.; Ryu, H.-W.; Lee, H.-G.; Hong, S.-M.; Kim, H. J.; Park, S.-N.; Gil, M.-G.; Kang, H.-S. *Proc. SPIE* **2008**, 6923, 60231T.
- (263) Crouse, M. M.; Uchida, R.; van Dommelen, Y.; Ando, T.; Shimitt-Weaver, E. P.; Takeshita, M.; Wu, S.; Routh, R. M. *J. Micro/Nanolith., MEMS, MOEMS* **2009**, 8, 011006.
- (264) Kim, R.; Wallow, T.; Kye, J.; Levinson, H. J.; White, D. *Proc. SPIE* **2007**, 6520, 65202M.
- (265) Ando, T.; Abe, S.; Takasu, R.; Iwashita, J.; Matsumaru, S.; Watababe, R.; Hirahara, K.; Suzuki, Y.; Tsukano, M.; Iwai, T. *Proc. SPIE* **2009**, 7273, 727308.
- (266) Ohmura, Y.; Matsuyama, T.; Nakashima, T.; Nagasaka, H.; Wakamoto, S.; Sukegawa, A.; Kohno, H.; Arai, Y.; Owa, S. Feasibility of high index immersion lithography. 3rd International Symposium on Immersion Lithography, Kyoto, Japan, 2–5 October, 2006.
- (267) (a) Sewell, H.; Mulkens, J.; McCafferty, D.; Markoya, L.; Hendricka, E.; Hermans, J.; Ronse, K. *Proc. SPIE* **2005**, 5753, 491. (b) Sewell, H.; McCafferty, D.; Wagner, C.; Markoya, L. *J. Photopolym. Sci. Technol.* **2005**, 18, 579. (c) Mulkens, J.; Graupner, P.; Sewell, H.; McCafferty, D. Immersion lithography beyond water. 2nd International Symposium on Immersion Lithography, Bruges, Belgium, 12–15 September, 2005. (d) Sewell, H.; McCafferty, D.; Markoya, L. ArF and F₂ immersion resist and fluid evaluation with interference lithography. International Symposium on Immersion and 157nm Lithography, Vancouver, Canada, 2–5 August, 2004.
- (268) (a) Zhou, J.; Lafferty, N. V.; Smith, B. W.; Burnett, J. H. *Proc. SPIE* **2007**, 6520, 65204T. (b) Smith, B. W.; Fan, Y.; Zhou, J.; Lafferty, N. V.; Estroff, A. *Proc. SPIE* **2006**, 6154, 61540A. (c) Smith, B.; Zhou, J.; Lafferty, N.; Fan, Y. Immersion lithography at 22nm high index and evanescent fields. 3rd International Symposium on Immersion Lithography, Kyoto, Japan, 2–5 October, 2006. (d) Zhou, J.; Fan, Y.; Bourov, A.; Lafferty, N.; Cropanese, F.; Zavyalova, L.; Estroff, A.; Smith, B. W. *Proc. SPIE* **2005**, 5754, 630. (e) Chen, T.; Milster, T.; Nam, D.; Yang, S. H. *Proc. SPIE* **2005**, 5754, 254. (f) Smith, B. W.; Fan, Y.; Slocum, M.; Zavyalova, L. *Proc. SPIE* **2005**, 5754, 141. (g) Smith, B.; Fan, Y.; Zhou, J.; Zavyalova, L.; Slocum, M.; Park, J.; Bourov, A.; Piscani, E.; Lafferty, N.; Estroff, A. Solid immersion and evanescent wave lithography at numerical apertures >1.60. 2nd International Symposium on Immersion Lithography, Bruges, Belgium, 12–15 September, 2005.
- (269) (a) Burnett, J. H.; Kaplan, S. G.; Shirley, E. L.; Horowitz, D.; Clauss, W.; Grenville, A.; Van Peski, C. *Proc. SPIE* **2006**, 6154, 615418. (b) Burnett, J. H.; Kaplan, S. G.; Shirley, E. L.; Horowitz, D.; Josell, D.; Clauss, W.; Grenville, A.; Van Peski, C. High-index materials for 193 nm immersion lithography. 3rd International Symposium on Immersion Lithography, Kyoto, Japan, 2–5 October, 2006. (c) Burnett, J. H. *J. Photopolym. Sci. Technol.* **2005**, 18, 655. (d) Burnett, J. H.; Kaplan, S. G.; Shirley, E. L.; Tompkins, P. J.; Webb, J. E. *Proc. SPIE* **2005**, 5754, 611. (e) Burnett, J. H.; Kaplan, S. G.; Shirley, E. L.; Horowitz, D.; Clauss, W.; Grenville, A.; Van Peski, C. High-index materials for 193 nm immersion lithography. 2nd International Symposium on Immersion Lithography, Bruges, Belgium, 12–15 September, 2005. (f) Burnett, J. H.; Kaplan, S. G.; Shirley, E. L.; Webb, J. High index materials for 193 nm and 157 nm immersion lithography. International Symposium on Immersion and 157nm Lithography, Vancouver, Canada, 2–5 August, 2004.
- (270) (a) Sewell, H.; Mulkens, J.; McCafferty, D.; Markoya, L.; Streefkerk, B.; Graupner, P. *Proc. SPIE* **2006**, 6154, 615406. (b) Sewell, H.; Mulkens, J.; McCafferty, D.; Markoya, L. *J. Photopolym. Sci. Technol.* **2006**, 19, 613. (c) Mulkens, J.; Leenders, M.; Donders, S.; McCafferty, D.; Sewell, H.; Markoya, L.; Graupner, P. High index immersion lithography for the 32-nm node and below. 3rd International Symposium on Immersion Lithography, Kyoto, Japan, 2–5 October, 2006.
- (271) (a) Nawata, T.; Inui, Y.; Mabuchi, T.; Mochizuki, N.; Masada, I.; Nishijima, E.; Sato, H.; Fukuda, T. *Proc. SPIE* **2008**, 6924, 69242L. (b) Nawata, T.; Inui, Y.; Masada, I.; Mabuchi, T.; Nishijima, E.; Sato, H.; Fukuda, T. Fluoride single crystals for the next generation lithography. 5th International Symposium on Immersion Lithography Extensions, The Hague, Netherlands, 22–25 September, 2008. (c) Nawata, T.; Inui, Y.; Masada, I.; Nishijima, E.; Mabuchi, T.; Mochizuki, N.; Satoh, H.; Fukuda, T. *Proc. SPIE* **2007**, 6520, 65201P. (d) Mabuchi, T.; Inui, Y.; Mochizuki, N.; Masada, I.; Nawata, T.; Sato, H.; Fukuda, T. High-index fluoride crystal for the next generation lithography. 4th International Symposium on Immersion Lithography, Keystone, CO, 8–11 October, 2007. (e) Nawata, T.; Inui, Y.; Masada, I.; Nishijima, E.; Satoh, H.; Fukuda, T. *Proc. SPIE* **2006**, 6154, 61541A. (f) Nawata, T.; Inui, Y.; Masada, I.; Mabuchi, T.; Nishijima, E.; Sato, H.; Fukuda, T. High-index fluoride materials for 193 nm immersion lithography. 3rd International Symposium on Immersion Lithography, Kyoto, Japan, 2–5 October, 2006. (g) Sato, H.; Inui, Y.; Nawata, T.; Nishijima, E.; Kuramoto, N.; Fukuda, T. New fluoride crystal as high-index material for hyper-NA immersion 193 nm lithography. 2nd International Symposium on Immersion Lithography, Bruges, Belgium, 12–15 September, 2005.
- (272) (a) Parthier, L.; Wehrhan, G.; Seifert, F.; Ansog, M.; Alchelle, T.; Seitz, S.; Letz, M. Development update of high index lens material LuAG for ArF hyper NA immersion systems. 5th International Symposium on Immersion Lithography Extensions, The Hague, Netherlands, 22–25 September, 2008. (b) Parthier, L.; Wehrhan, G.; Seifert, F.; Ansog, M.; Alchelle, T.; Seitz, S. High index lens material LuAG: Development status and progress. SEMATECH Litho Forum, Bolton Landing, NY, 12–14 May, 2008. (c) Parthier, L.; Wehrhan, G.; Keutel, D.; Knap, K. *Proc. SPIE* **2007**, 6520, 650. (d) Parthier, L.; Wehrhan, G.; Keutel, D.; Aichele, T.; Ansor, M. Development progress of high refractive LuAG for hyper NA immersion systems. 4th International Symposium on Immersion Lithography, Keystone, CO, 8–11 October, 2007. (e) Parthier, L.; Wehrhan, G.; Selle, M.; von der Gönna, G.; Keutel, D.; Knapp, K. 3rd International Symposium on Immersion Lithography, Kyoto, Japan, 2–5 October, 2006. (f) Parthier, et al. *Proc. SPIE* **2006**, 6154, 6154–46. (g) Parthier, L.; Wehrhan, G.; Knapp, K. Novel optical materials with extremely high refractive index and manufacturing potential analysis. 2nd International Symposium on Immersion Lithography, Bruges, Belgium, 12–15 September, 2005.
- (273) (a) Burnett, J. H.; Benck, E. C.; Kaplan, S. G.; Sirat, G. Y.; Mack, C. *Proc. SPIE* **2009**, 7274, 727421. (b) Sirat, G. Y.; Goldstein, M. *Proc. SPIE* **2008**, 6924, 69242T. (c) Mack, C.; Sirat, G. Y.; Goldstein, M. Uniaxial crystal last optical element for second- and third-generation immersion lithography. 5th International Symposium on Immersion Lithography Extensions, The Hague, Netherlands, 22–25 September, 2008. (d) Burnett, J.; Benck, E.; Kaplan, S.; Sirat, G. Spatial-dispersion-induced index anisotropy in sapphire. 5th International Symposium on Immersion Lithography Extensions, The Hague, Netherlands, 22–25 September, 2008.
- (274) Turro, N. J. *Modern Molecular Photochemistry*; Benjamin/Cummings Publishing: Menlo Park, CA, 1978; p 77.
- (275) Lopez-Gejo, J.; Kunjappu, J. T.; Conley, W.; Zimmerman, P.; Turro, N. J. *J. Micro/Nanolith., MEMS, MOEMS* **2007**, 6, 033003.
- (276) (a) French, R. H.; Peng, S.; Qiu, W.; Wheland, R. C. U.S. 2007/0215846 A1. (b) French, R. H.; Peng, S.; Wheland, R. C. WO 2005/

- 119371 A1. (c) French, R. H.; Peng, S.; Wheland, R. C. WO 2005/0286031 A1. (d) Peng, S.; Qiu, W.; French, R. H. U.S. 2006/0281028 A1.
- (277) (a) Lopez-Gejo, J.; Kunjappu, J. T.; Zhou, J.; Smith, B. W.; Zimmerman, P.; Conley, W.; Turro, N. *J. Chem. Mater.* **2007**, *19*, 3641. (b) Lopez-Gejo, J.; Kunjappu, J. T.; Zhou, J.; Smith, B. W.; Zimmerman, P.; Conley, W.; Turro, N. *J. Proc. SPIE* **2007**, *6519*, 651921.
- (278) (a) French, R. H.; Qiu, W.; Yang, M. K.; Wheland, R. C.; Lemon, M. F.; Shoe, A. L.; Adelman, D. J.; Crawford, M. K.; Tran, H. V.; Feldman, J.; McLain, S. J.; Peng, S. *Proc. SPIE* **2006**, *6154*, 615415. (b) Yang, M. K.; Kaplan, S. G.; French, R. H.; Burnett, J. H. *J. Micro/Nanolith., MEMS, MOEMS* **2009**, *8*, 023005.
- (279) (a) Costner, E. A.; Matsumoto, K.; Long, B. K.; Taylor, J. C.; Wojtczak, W.; Willson, C. G. *Proc. SPIE* **2008**, *6923*, 69230B. (b) Costner, E. A.; Long, B. K.; Navar, C.; Matsumoto, K.; Jockusch, Lei, X.; O'Connor, N.; Zimmerman, P.; Turro, N.; Willson, C. G. 5th International Symposium on Immersion Lithography Extensions, The Hague, Netherlands, 22–25 September, 2008. (c) Costner, E.; Matsumoto, K.; Willson, C. G. High index materials for immersion lithography. 4th International Symposium on Immersion Lithography, Keystone, CO, 8–11 October, 2007.
- (280) (a) Sanders, D. P.; Larson, C.; Sundberg, L.; Truong, L.; Allen, R.; Goldfarb, D.; Harder, P.; Schuetter, S.; Shedd, T. Oil or water: What's the difference for 193 nm immersion lithography. 3rd International Symposium on Immersion Lithography, Kyoto, Japan, 2–5 October, 2006. (b) Sanders, D. P.; Sundberg, L.; Larson, C.; Truong, L.; Allen, R.; Goldfarb, D.; Clancy, A. Oil or water: What's the difference for 193 nm immersion lithography. IEEE Lithography Workshop, Charlottetown, Prince Edward Island, Canada, 31 July–4 August, 2006.
- (281) <http://www.processfluid.com/en/products/MCS-2780.aspx> (accessed 2009).
- (282) Bruno, T. J.; Huber, M. L.; Laesecke, A.; Lemmon, E. W.; Perkins, R. A. Thermochemical and thermophysical properties of JP-10. NISTIR 6640; National Institute of Standards and Technology: Boulder, CO, 2006.
- (283) (a) Zhang, P.; Budhlall, B. M.; Parris, G. E.; Barber, L. C. U.S. 2005/0161644 A1. (b) Zhang, P.; Budhlall, B. M.; Parris, G. E.; Barber, L. C. U.S. 2005/0173682 A1. (c) Budhall, B.; Parris, G.; Zhang, P.; Gao, X.; Zarkov, Z.; Ross, B.; Kaplan, S.; Burnett, J. *Proc. SPIE* **2005**, *5754*, 622. (d) Budhlall, B. M.; Parris, G. E.; Zhang, P.; Gao, X.; Ross, B.; Hyder, I. Z. New immersion fluid for 193 nm immersion lithography. International Symposium on Immersion and 157nm Lithography, Vancouver, Canada, 2–5 August, 2004. (e) Kaplan, S. G.; Burnett, J. H.; Gao, X.; Zhang, P. Characterization of refractive properties of fluids for immersion photolithography. International Symposium on Immersion and 157nm Lithography, Vancouver, Canada, 2–5 August, 2004.
- (284) (a) French, R. H.; Sewell, R. H.; Yang, M. K.; Peng, S.; McCafferty, D.; Qiu, W.; Wheland, R. C.; Lemon, M. F.; Markoya, L.; Crawford, M. K. *J. Microolith., Microfab., Microsyst.* **2005**, *4*, 031103. (b) Peng, S.; French, R. H.; Qiu, W.; Wheland, R. C.; Yang, M.; Lemon, M. F.; Crawford, M. K. *Proc. SPIE* **2005**, *5754*, 427. (c) Peng, S.; French, R. H.; Qiu, W.; Wheland, R. C.; Crawford, M. K.; Lemon, M. F.; Yang, M. K. New developments in second generation 193 nm immersion fluids for lithography with 1.5 numerical aperture. 2nd International Symposium on Immersion Lithography, Bruges, Belgium, 12–15 September, 2005.
- (285) (a) Miyamatsu, T.; Nemoto, H.; Wang, Y. WO 2005/114711 A1. (b) Miyamatsu, T.; Nemoto, H.; Wang, Y. U.S. 2007/0164261 A1.
- (286) (a) Miyamatsu, T.; Wang, Y.; Shima, M.; Kusumoto, S.; Chiba, T.; Nakagawa, H.; Hieda, K.; Shimokawa, T. *Proc. SPIE* **2005**, *5753*, 10. (b) Wang, Y.; Miyamatsu, T.; Tominaga, T.; Makita, Y.; Nakagawa, H.; Nakamura, A.; Shima, M.; Kusumoto, S.; Shimokawa, T.; Hieda, K. Material design for highly transparent fluids of the next generation ArF immersion lithography. 2nd International Symposium on Immersion Lithography, Bruges, Belgium, 12–15 September, 2005.
- (287) (a) Wang, Y.; Miyamatsu, T.; Furukawa, T.; Yamada, K.; Tominaga, T.; Makita, Y.; Nakagawa, H.; Nakamura, A.; Shima, M.; Kusumoto, S.; Shimokawa, T.; Hieda, K. *Proc. SPIE* **2006**, *6153*, 61530A. (b) Furukawa, T.; Hieda, K.; Wang, Y.; Miyamatsu, T.; Yamada, K.; Tominaga, T.; Makita, Y.; Nakagawa, H.; Nakamura, A.; Shima, M.; Shimokawa, T. *J. Photopolym. Sci. Technol.* **2006**, *19*, 641. (c) Kusumoto, S.; Shima, M.; Wang, Y.; Shimokawa, T.; Sato, H.; Hieda, K. *Polym. Adv. Technol.* **2006**, *17*, 122.
- (288) (a) Furukawa, T.; Kishida, T.; Miyamatsu, T.; Kawaguchi, K.; Yamada, K.; Tominaga, T.; Slezak, M.; Hieda, K. *Proc. SPIE* **2007**, *6519*, 65190B. (b) Kawaguchi, K.; Kishida, T.; Furukawa, T.; Miyamatsu, T.; Tominaga, T.; Slezak, M.; Wang, Y.; Yamada, K.; Hieda, K. Third-generation fluid for ArF immersion lithography. 3rd International Symposium on Immersion Lithography, Kyoto, Japan, 2–5 October, 2006.
- (289) (a) Furukawa, T.; Kishida, T.; Yasuda, K.; Shimokawa, T.; Liu, Z.; Slezak, M.; Hieda, K. *Proc. SPIE* **2008**, *6924*, 692412. (b) Liu, Z.; Furukawa, T.; Kishida, T.; Yasuda, K.; Shimokawa, T.; Slezak, M.; Hieda, K.; Gonzales, W.; Torres, D. Characterization of high-refractive index materials for the next-generation ArF immersion lithography. 5th International Symposium on Immersion Lithography Extensions, The Hague, Netherlands, 22–25 September, 2008. (c) Furukawa, T.; Kishida, T.; Miyamatsu, T.; Kawaguchi, K.; Yamada, K.; Tominaga, T.; Liu, Z.; Slezak, M.; Hieda, K. High refractive index fluids and top coat design for the next generation ArF immersion lithography. 4th International Symposium on Immersion Lithography, Keystone, CO, 8–11 October, 2007.
- (290) (a) Santillan, J.; Otoguro, A.; Itani, T.; Fujii, K.; Kagayama, A.; Nakano, T.; Nakayama, N.; Tamatani, H.; Fukuda, S. *Proc. SPIE* **2006**, *6154*, 61544Q. (b) Santillan, J.; Otoguro, A.; Itani, T.; Fujii, K.; Kagayama, A.; Nakano, T.; Nakayama, N.; Tamatani, H.; Fukuda, S. *Microelectron. Eng.* **2006**, *83*, 651. (c) Kagayama, A.; Wachi, H.; Nakano, T.; Fukuda, S. High index fluids for second- and third-generation ArF immersion lithography. 4th International Symposium on Immersion Lithography, Keystone, CO, 8–11 October, 2007. (d) Otoguro, A.; Santillan, J.; Itani, T.; Fujii, K.; Kagayama, A.; Nakano, T.; Nakayama, N.; Tamatani, H.; Fukuda, S. Development of high refractive index fluids for 193-nm immersion lithography. 2nd International Symposium on Immersion Lithography, Bruges, Belgium, 12–15 September, 2005.
- (291) (a) Evans, D. F. *J. Chem. Soc.* **1953**, 345. (b) Tsuomura, H.; Mulliken, R. S. *J. Am. Chem. Soc.* **1960**, *82*, 5966. (c) Scurlock, R. D.; Ogilby, P. R. *J. Phys. Chem.* **1989**, *93*, 5493. (d) Parsons, B. F.; Chandler, D. W. *J. Phys. Chem. A* **2003**, *107*, 10544.
- (292) (a) Sakai, K.; Iwasaki, Y.; Mori, S.; Yamada, A.; Ogusu, M.; Yamashita, K.; Nishikawara, T.; Hara, S.; Watanabe, Y. *Jpn. J. Appl. Phys.* **2008**, *47*, 4853. (b) Sakai, K.; Iwasaki, Y.; Mori, S.; Yamada, A.; Ogusu, M.; Yamashita, K.; Nishikawara, T.; Tanaka, T.; Hasegawa, N.; Hara, S.; Watanabe, Y. *Proc. SPIE* **2008**, *6924*, 69242H. (c) Sakai, K.; Mori, S.; Sakamoto, E.; Iwasaki, Y.; Yamashita, K.; Hara, S.; Watanabe, Y.; Suzuki, A. Progress of high-index immersion exposure system. 5th International Symposium on Immersion Lithography Extensions, The Hague, Netherlands, 22–25 September, 2008. (d) Suzuki, A. Canon progress and plans for HIL. SEMATECH Litho Forum, Bolton Landing, NY, 12–14 May, 2008.
- (293) (a) Srinivasan, R.; White, L. S. *J. Am. Chem. Soc.* **1979**, *101*, 6389. (b) Scurlock, R. D.; Ogilby, P. R. *J. Phys. Chem.* **1989**, *93*, 5493, and references therein.
- (294) O'Connor, N. A.; Liberman, V.; Lei, X.; Lopez-Gejo, J.; Turro, N. J.; Zimmerman, P. A. *J. Photopolym. Sci. Technol.* **2008**, *21*, 607.
- (295) Liberman, V.; Rothschild, M.; Palmacci, S. T.; Zimmerman, P. A.; Grenville, A. *Proc. SPIE* **2007**, *6520*, 652035.
- (296) (a) Tran, H. V.; Hendrickx, E.; Van Roey, F.; Vandenberghe, G.; French, R. H. *J. Micro/Nanolith., MEMS, MOEMS* **2009**, *8*, 033006. (b) French, R. H.; Tran, H. V.; Adelman, D. J.; Rogado, N. S.; Kaku, M.; Mocella, M.; Chen, C. Y.; Hendrickx, E.; Van Roey, F.; Bernfeld, A. S.; Derryberry, R. A. *Proc. SPIE* **2008**, *6924*, 692417. (c) Tran, H. V.; Hendrickx, E.; French, R. H.; Adelman, D. J.; Rogado, N. S.; Kaku, M.; Mocella, M.; Schmieg, J. J.; Chen, C. Y.; Van Roey, F.; Bernfeld, A. S.; Derryberry, R. A. *J. Photopolym. Sci. Technol.* **2008**, *21*, 631. (d) French, R. H.; Bernfeld, A. S.; Tran, H. V.; Adelman, D. J.; Liberman, V.; Rothschild, M.; Hendrickx, E.; Van Roey, F. High refractive index fluid evaluations: Fluid radiation durability lifetimes and fluid/resist interactions. 5th International Symposium on Immersion Lithography Extensions, The Hague, Netherlands, 22–25 September, 2008. (e) French, R. H. Progress on high index immersion fluid: DuPont IF132. 2008 SEMATECH Litho Forum, Bolton Landing, NY, 12–14 May, 2008. (f) French, R. H.; Tran, H. V.; Adelman, D. J.; Rogado, N. S.; Qiu, W.; Feldman, J.; Nagao, O.; Kaku, M.; Mocella, M.; Wheland, R. C.; Yang, M. K.; Lemon, M. F.; Brubaker, L.; Fones, B.; Fischel, B. E.; Chen, C. Y. Cost effective single exposure immersion lithography with second generation immersion fluids for numerical apertures of 1.55 and 32 nm half pitches. 4th International Symposium on Immersion Lithography, Keystone, CO, 8–11 October, 2007.
- (297) (a) Sewell, H.; Mulken, J.; Graeupner, P.; McCafferty, D.; Markoya, L.; Donders, S.; Cortie, R.; Meijers, R.; Evangelista, F.; Samarakone, N. *Proc. SPIE* **2008**, *6924*, 692415. (b) Sewell, H.; Graeupner, P.; McCafferty, D.; Markoya, L.; Samarakone, N.; van Wijnen, P.; Mulken, J.; Benschop, J. *J. Photopolym. Sci. Technol.* **2008**, *21*, 613. (c) Donders, S.; Meijers, R.; Sewell, H.; Evangelista, F.; Cortie, R.; Badie, R.; Jurgens, D.; Graeupner, P. Critical immersion parameters in the development of high-n ArF immersion lithography. 5th International Symposium on Immersion Lithography Extensions, The Hague, Netherlands, 22–25 September, 2008. (d) Sewell, H.;

- Graepner, P.; Mulkens, J.; McCafferty, D.; Markoya, L.; Donders, S.; Evangelista, F.; Cortie, R.; Meijers, R.; Clauss, W.; Duesing, R.; Epple, A.; Samarakone, N. Update on high-n immersion lithography feasibility. SEMATECH Litho Forum, Bolton Landing, NY, 12–14 May, 2008.
- (298) Liberman, V.; Rothschild, M.; Palmacci, S. T.; Bristol, R.; Byers, J.; Turro, N. J.; Lei, X.; O'Connor, N.; Zimmerman, P. A. *Proc. SPIE* **2008**, *6924*, 692416.
- (299) (a) Tran, H. V.; French, R. H.; Adelman, D. J.; Feldman, J.; Qiu, W.; Wheland, R. C.; Brubaker, L. W.; Fischel, B. E.; Fones, B. B.; Lemon, M. F.; Yang, M. K.; Nagao, O.; Kaku, M.; Mocella, M.; Schmiege, J. J. *J. Photopolym. Sci. Technol.* **2007**, *20*, 729. (b) French, R. H.; Liberman, V.; Tran, H. V.; Feldman, J.; Adelman, D. J.; Wheland, R. C.; Qiu, W.; McLain, S. J.; Nagao, O.; Kaku, M.; Mocella, M.; Yang, M. K.; Lemon, M. F.; Brubaker, L.; Shoe, A. L.; Fones, B.; Fischel, B. E.; Krohn, K.; Hardy, D.; Chen, C. Y. *Proc. SPIE* **2007**, *6520*, 65201O. (c) French, R. H.; Shoe, A. L.; Wheland, R. C.; Tran, H. V.; Qiu, W.; Feldman, J.; McLain, S. J.; Yang, M. K.; Lemon, M. F.; Adelman, D. J.; Crawford, M. K. Second generation fluids for 193 nm immersion lithography: Optics, imaging, and fluid lifecycle. 3rd International Symposium on Immersion Lithography, Kyoto, Japan, 2–5 October, 2006.
- (300) (a) Furukawa, T.; Heida, K.; Miyamatsu, Y.; Wang, Y.; Yamada, K. U.S. 2008/0129970 A1. (b) Adelman, D. J.; French, R. H.; Lemon, M. F.; Peng, S.; Shoe, A. L.; Wheland, R. C. U.S. 2007/0182896 A1. (c) Schleisman, A.; Sandre, E.; Dulphy, H.; O'Brien, S. Anticipated requirements for 2nd generation fluid handling. 3rd International Symposium on Immersion Lithography, Kyoto, Japan, 2–5 October, 2006.
- (301) (a) Harder, P. M.; Shedd, T. A. *J. Micro/Nanolith., MEMS, MOEMS* **2008**, *7*, 033002. (b) Harder, P. M.; Shedd, T. A. *Proc. SPIE* **2007**, *6533*, 653305.
- (302) (a) Hendrickx, E.; Postnikov, S.; Foubert, P.; Gronheid, R.; Kim, B. *Proc. SPIE* **2007**, *6519*, 65190A. (b) Samarakonev, N.; Yick, P.; McCafferty, D.; Sewell, H.; Mulkens, J.; Robles, M. The impact of high-n immersion fluids on printed CDs and defectivity. 4th International Symposium on Immersion Lithography, Keystone, CO, 8–11 October, 2007. (c) Postnikov, S.; Hendrickx, E.; Kim, B.; Gronheid, R.; Ercken, M.; Foubert, P.; Jehoul, C.; Van Roey, F.; Versluijs, J.; Vandenbroeck, N.; Willems, P. Experimental procedure for high index liquid testing. 3rd International Symposium on Immersion Lithography, Kyoto, Japan, 2–5 October, 2006.
- (303) (a) Furukawa, T.; Kishida, T.; Yamada, K.; Miyamatsu, T.; Kawaguchi, K. JP 2008306072 A. (b) Furukawa, T.; Kishida, T.; Miyamatsu, T.; Kawaguchi, K.; Yamada, K.; Tominaga, T.; Liu, Z.; Slezak, M.; Hieda, K. High refractive index fluids and top coat design for the next generation ArF immersion lithography. 4th International Symposium on Immersion Lithography, Keystone, CO, 8–11 October, 2007.
- (304) Kaplan, S.; Burnett, J. H. *Appl. Opt.* **2006**, *45*, 1721.
- (305) (a) Zhou, J.; Fan, Y.; Bourov, A.; Smith, B. W. *Appl. Opt.* **2006**, *45*, 3077. (b) Zhou, J.; Fan, Y.; Bourov, A.; Lafferty, N.; Cropanese, F.; Zavyalova, L.; Estroff, A.; Smith, B. W. *Proc. SPIE* **2005**, *5754*, 630. (c) Smith, B.; Zavyalova, L.; Piscani, E.; Park, J.; Summers, D.; Zhou, J.; Cropanese, F.; Meute, J.; Conley, W. Immersion lithography for sub-45nm: Lab or fab? International Symposium on Immersion and 157nm Lithography, Vancouver, Canada, 2–5 August, 2004.
- (306) (a) Taylor, J. C.; Costner, E. A.; Goh, S.; Wojtczak, W.; Dewulf, D.; Willson, C. G. *J. Vac. Sci. Technol. B* **2008**, *26*, 506. (b) Costner, E.; Taylor, J. C.; Caporale, S.; Wojtczak, W.; Dewulf, D.; Conley, W.; Willson, C. G. *Proc. SPIE* **2006**, *6513*, 65130B. (c) Taylor, J. C.; Shayib, R.; Goh, S.; Chambers, C. R.; Conley, W.; Lin, S.-H.; Willson, C. G. *Proc. SPIE* **2005**, *5753*, 836.
- (307) (a) Zhang, P.; Budhlall, B. M.; Parris, G. E.; Barber, L. C. U.S. 2005/0161644 A1. (b) Zhang, P.; Budhlall, B. M.; Parris, G. E.; Barber, L. C. U.S. 2005/0173682 A1.
- (308) (a) Costner, E. A.; Matsumoto, K.; Long, B. K.; Taylor, J. C.; Wojtczak, W.; Willson, C. G. *Proc. SPIE* **2008**, *6923*, 69230B. (b) Costner, E. A.; Long, B. K.; Navar, C.; Matsumoto, K.; Jockusch, L.; X.; O'Connor, N.; Zimmerman, P.; Turro, N.; Willson, C. G. 5th International Symposium on Immersion Lithography Extensions, The Hague, Netherlands, 22–25 September, 2008. (c) Costner, E.; Matsumoto, K.; Willson, C. G. High index materials for immersion lithography. 4th International Symposium on Immersion Lithography, Keystone, CO, 8–11 October, 2007.
- (309) Kruger, S.; Revuru, S.; Zhang, S.-H.; Vaughn, D. D., II; Block, E.; Zimmerman, P.; Brainard, R. L. *Proc. SPIE* **2008**, *6923*, 69231O.
- (310) (a) Lee, K.; Kunjappu, J.; Jockusch, S.; Turro, N. J.; Widerschan, T.; Zhou, J.; Smith, B. W.; Zimmerman, P.; Conley, W. *Proc. SPIE* **2005**, *5753*, 537. (b) Zimmerman, P. A.; Conley, W.; Turro, N. J.; Lee, K.; Jockusch, S.; Kunjappu, J. Widenschpan, T. Amplification of the index of refraction of aqueous immersion fluids by ionic surfactants. International Symposium on Immersion and 157 nm Lithography, Vancouver, Canada, 2–5 August, 2004.
- (311) (a) Lopez-Gejo, J.; Kunjappu, J. T.; Turro, N. J.; Conley, W. *J. Micro/Nanolith., MEMS, MOEMS* **2007**, *6*, 013002. (b) Lopez-Gejo, J.; Kunjappu, J. T.; Turro, N. J.; Conley, W. *Proc. SPIE* **2006**, *6153*, 61530C.
- (312) (a) Brainard, R. L.; Kruger, S.; Block, E. *Proc. SPIE* **2007**, *6519*, 65192O. (b) Brainard, R. L.; Block, E. Models for predicting the index of refraction of compounds at 193 nm. 3rd International Symposium on Immersion Lithography, Kyoto, Japan, 2–5 October, 2006.
- (313) Irisawa, J.; Okazoe, T.; Eriguchi, T.; Yokokoji, O. *Proc. SPIE* **2005**, *5754*, 1040.
- (314) Schuetter, S.; Shedd, T.; Nellis, G.; Romano, A.; Dammel, R.; Padmanaban, M.; Houlihan, F.; Krawicz, A.; Lin, G.; Rahman, D.; Chakrapani, S.; Neisser, M.; Van Peski, C. *J. Vac. Sci. Technol. B* **2006**, *24*, 2798.
- (315) (a) Zimmerman, P. A.; Rice, B. J.; Piscani, E. C.; Liberman, V. *Proc. SPIE* **2009**, *7274*, 72742O. (b) Zimmerman, P. A.; Rice, B.; Rodriguez, R.; Zettel, M. F.; Trikeriotis, M.; Wang, D.; Yi, Y.; Bae, W. J.; Ober, C. K.; Giannelis, E. P. *J. Photopolym. Sci. Technol.* **2008**, *21*, 621. (c) Zimmerman, P. A.; Byers, J.; Rice, B.; Ober, C. K.; Giannelis, E. P.; Rodriguez, R.; Wang, D.; O'Connor, N.; Lei, X.; Turro, N. J.; Liberman, V.; Palmacci, S.; Rothschild, M.; Lafferty, N.; Smith, B. W. *Proc. SPIE* **2008**, *6923*, 69230A. (d) Lopez-Gejo, J.; Lee, K.; Kunjappu, J.; Turro, N. J.; Conley, W. Amplification of the index of refraction of aqueous immersion fluids: Nanoparticles dispersions. 2nd International Symposium on Immersion Lithography, Bruges, Belgium, 12–15 September, 2005.
- (316) Ionkin, A. S. U.S. 2008/0063990 A1.
- (317) Feldman, J. U.S. 2008/0061248 A1.
- (318) Deng, H.; Wang, Y.; Liou, H.-C.; Meagley, R. P.; Putna, E. U.S. 2005/0164502 A1.
- (319) Hirayama, T.; Wakiya, K.; Endo, K.; Yoshida, M.; Sakai, H. WO 2005/117074 A1.
- (320) (a) Chumanov, G.; Evanoff, D. D., Jr.; Luzinov, I.; Klep, V.; Zdyrko, B.; Conley, W.; Zimmerman, P. *Proc. SPIE* **2005**, *5753*, 847. (b) Chumanov, G.; Evanoff, D. D., Jr.; Luzinov, I.; Klep, V.; Zdyrko, B.; Conley, W.; Zimmerman, P. Nanocomposite liquids for 193 nm immersion lithography. International Symposium on Immersion and 157nm Lithography, Vancouver, Canada, 2–5 August, 2004.
- (321) (a) Jahromi, S.; Wienke, D.; Bremer, L. G. B. WO 2005/050324. (b) Jahromi, S.; Bruens, C.; Bremer, L.; Librechts, S.; Mostert, B.; Coussens, B. Development of high index fluids for immersion lithography. 2nd International Symposium on Immersion Lithography, Bruges, Belgium, 12–15 September, 2005.
- (322) (a) Trikeriotis, M.; Rodriguez, R.; Zettel, M. F.; Bakandritsos, A.; Bae, W. J.; Zimmerman, P.; Ober, C. K.; Giannelis, E. P. *Proc. SPIE* **2009**, *7273*, 72732A. (b) Zimmerman, P. A.; Rice, B.; Rodriguez, R.; Zettel, M. F.; Trikeriotis, M.; Bakandritsos, A.; Wang, D.; Yi, Y.; Bae, W.-J.; Ober, C. K.; Giannelis, E. P.; Li, S.; Brus, L.; Steigerwald, M.; Turro, N.; Lei, X.-G.; Jockusch, S.; Bloomstein, T.; Liberman, V.; Rothschild, M. High index fluids to enable 1.55 and higher NA 193 nm immersion imaging. 5th International Symposium on Immersion Lithography Extensions, The Hague, Netherlands, 22–25 September, 2008. (c) Zimmerman, P. A. High index fluids—Possible paths to NA > 1.55. 2008 SEMATECH Litho Forum, Bolton Landing, NY, 12–14 May, 2008. (d) Rodriguez, R.; Wang, D.; Yi, Y.; Andre, X.; Ober, C. K.; Giannelis, E. P.; Zimmerman, P. High refractive index nanoparticle fluids for 193 nm immersion lithography. 4th International Symposium on Immersion Lithography, Keystone, CO, 8–11 October, 2007.
- (323) (a) Bremer, L.; Tuinier, R.; Jahromi, S. *Langmuir* **2009**, *25*, 2390. (b) Jahromi, S.; Bremer, L.; Tuinier, R.; Liebrechts, S. Development of third generation immersion fluids based on dispersion of nanoparticles. 5th International Symposium on Immersion Lithography Extensions, The Hague, Netherlands, 22–25 September, 2008.
- (324) Hoffnagle, J.; Milliron, D.; Swanson, S.; Sanders, D.; Hinsberg, W. Fundamental analysis of nanoparticle-based high index immersion fluids. 4th International Symposium on Immersion Lithography, Keystone, CO, 8–11 October, 2007.
- (325) De Kruif, C. G.; van Iersel, E. M. F.; Vrij, A.; Russel, W. B. *J. Chem. Phys.* **1985**, *83*, 4717.
- (326) Studart, A. R.; Amstad, E.; Antoni, M.; Gauckler, L. J. *J. Am. Ceram. Soc.* **2006**, *89*, 2418.
- (327) (a) Bell, N. S.; Schendel, M. E.; Piech, M. *J. Colloid Interface Sci.* **2005**, *287*, 94. (b) Bell, N. S.; Rodriguez, M. A. *J. Nanosci. Nanotechnol.* **2004**, *4*, 283.
- (328) (a) Bergstrom, L.; Schilling, C. H.; Aksay, I. A. *J. Am. Ceram. Soc.* **1992**, *75*, 3305. (b) Bergstrom, L. *J. Chem. Soc., Faraday Trans. 1992*, *3201*. (c) Bergstrom, L.; Meur, A.; Arwin, H.; Rowcliffe, D. *J. Am. Ceram. Soc.* **1996**, *79*, 339.
- (329) Macosko, C. W., Ed. *Rheology: Principles, Measurements, and Applications*; VCH: New York, 1994; Chapter 10.

- (330) (a) Conley, W.; Warrick, S.; Garza, C.; Goirand, P.-J.; Gemmink, J.-W.; Van Steenwinckel, D. *Proc. SPIE* **2007**, *6520*, 65201L. (b) Conley, W. Life without water. 4th International Symposium on Immersion Lithography, Keystone, CO, 8–11 October, 2007. (c) Conley, W. *Proc. SPIE* **2007**, *6519*, 65190Q. (d) Conley, W.; Socha, R. *Proc. SPIE* **2006**, *6153*, 61531L. (e) Conley, W.; Warrick, S.; Garza, C.; Goirand, P.-J.; Gemmink, J.-W.; Van Steenwinckel, D. Application of beyond water immersion to device level imaging. 3rd International Symposium on Immersion Lithography, Kyoto, Japan, 2–5 October, 2006.
- (331) (a) Zimmerman, P. A.; Byers, J.; Piscani, E.; Rice, B.; Ober, C. K.; Giannelis, E. P.; Rodriguez, R.; Wang, D.; Whittaker, A.; Blakey, I.; Chen, L.; Dargaville, Liu, H. *Proc. SPIE* **2008**, *6923*, 692306. (b) Zimmerman, P. A.; Byers, J. Challenges for the development of high-index materials for generation-three 193 nm immersion lithography. 4th International Symposium on Immersion Lithography, Keystone, CO, 8–11 October, 2007.
- (332) McIntyre, G.; Sanders, D.; Sooriyakumaran, R.; Truong, H.; Allen, R. *Proc. SPIE* **2008**, *6923*, 692304.
- (333) Sooriyakumaran, R.; Sanders, D. P.; Truong, H.; Allen, R. D.; Colburn, M. E.; McIntyre, G. R. High refractive index polymer platforms for 193 nm immersion lithography. 4th International Symposium on Immersion Lithography, Keystone, CO, 8–11 October, 2007.
- (334) (a) Liu, H.; Blakey, I.; Conley, W. E.; George, G. A.; Hill, D. J. T.; Whittaker, A. K. *J. Micro/Nanolith., MEMS, MOEMS* **2008**, *7*, 023001. (b) Blakey, I.; Conley, W.; George, G. A.; Hill, D. J. T.; Liu, H.; Rasoul, F.; Whittaker, A. K.; Zimmerman, P. A. QSPR approach to the rational design of high refractive index polymers for 193 nm immersion lithography. 2nd International Symposium on Immersion Lithography, Bruges, Belgium, 12–15 September, 2005.
- (335) (a) Blakey, I.; Chen, L.; Dargaville, B.; Liu, H.; Whittaker, A. K.; Conley, W.; Piscani, E.; Rich, G.; Williams, A.; Zimmerman, P. *Proc. SPIE* **2007**, *6519*, 651909. (b) Whittaker, A. K.; Blakey, I.; Chen, L.; Dargaville, B.; Liu, H.; Conley, W.; Zimmerman, P. A. *J. Photopolym. Sci. Technol.* **2007**, *20*, 665. (c) Blakey, I.; Chen, L.; Dargaville, B.; Liu, H.; Whittaker, A. Update on High Index Resists. SEMATECH Immersion Technology Advisory Group Meeting — Open Session, Austin, TX, January 23, 2006.
- (336) Zimmerman, P. A.; van Peski, C.; Rice, B.; Byers, J.; Turro, N. J.; Lie, X.; Lopez-Gejo, J.; Liberman, V.; Palmacci, S.; Rothschild, M.; Whittaker, A.; Blakey, I.; Chen, L.; Dargaville, B.; Liu, H. *J. Photopolym. Sci. Technol.* **2007**, *20*, 643.
- (337) Blakey, I.; Conley, W.; George, G. A.; Hill, D. J. T.; Liu, H.; Rasoul, F.; Whittaker, A. K. *Proc. SPIE* **2006**, *6153*, 61530H.
- (338) Blakey, I.; Chen, L.; Dargaville, B.; Liu, H.; Hill, D.; George, G. A.; Rasoul, F.; Whittaker, A. K.; Conley, W. E.; Rice, B.; Zimmerman, P. Strategies for the generation of high refractive index polymers for 193 nm immersion photoresist formulations. 3rd International Symposium on Immersion Lithography, Kyoto, Japan, 2–5 October, 2006.
- (339) (a) Whittaker, A. K.; Blakey, I.; Liu, H.; Hill, D. J. T.; George, G. A.; Conley, W.; Zimmerman, P. *Proc. SPIE* **2005**, *5753*, 827. (b) Blakey, I.; Conley, W.; George, G.; Hill, D.; Liu, H.; Whittaker, A. K.; Zimmerman, P. High refractive index photoresists for 193 nm immersion lithography. International Symposium on Immersion and 157nm Lithography, Vancouver, Canada, 2–5 August, 2004.
- (340) (a) Matsumoto, K.; Costner, E.; Nishimura, I.; Ueda, M.; Willson, C. G. *Macromolecules* **2008**, *41*, 5674. (b) Matsumoto, K.; Costner, E.; Nishimura, I.; Ueda, M.; Willson, C. G. *Proc. SPIE* **2008**, *6923*, 692305. (c) Costner, E.; Matsumoto, K.; Willson, C. G. High index materials for immersion lithography. 4th International Symposium on Immersion Lithography, Keystone, CO, 8–11 October, 2007.
- (341) (a) Nishimura, Y.; Kawakami, T.; Hoshiko, K.; Tomimaga, T.; Shima, M.; Kusumoto, S.; Shimokawa, T.; Hieda, K. Novel photoresist materials development with high refractive index at 193 nm for next generation immersion lithography. 3rd International Symposium on Immersion Lithography, Kyoto, Japan, 2–5 October, 2006. (b) Nishimura, Y.; Kawakami, M.; Seiko, K. JP 2007320999A. (c) Kaori, S.; Nishimura, Y.; Matsumura, S.; Seiko, K. JP 2008224728A.
- (342) Gonsalves, K. E.; Wang, M.; Pujari, N. S. *Proc. SPIE* **2008**, *6923*, 69231P.
- (343) Bae, W. J.; Trikeriotis, M.; Rodriguez, R.; Zettel, M. F.; Piscani, E.; Ober, C. K.; Giannelis, E. P.; Zimmerman, P. *Proc. SPIE* **2009**, *7273*, 727326.
- (344) Sanders, D. P. Unpublished results.
- (345) (a) Sondi, I.; Fedynyshyn, T. H.; Sinta, R.; Matijevic, E. *Langmuir* **2000**, *16*, 9031. (b) Fedynyshyn, T. H.; Doran, S. P.; Lind, M. L.; Sondi, I.; Matijevic, E. *Proc. SPIE* **2000**, *3999*, 627. (c) Fedynyshyn, T. H.; Sinta, R. F.; Sworin, M.; Goodman, R. B.; Doran, S. P. *Proc. SPIE* **2001**, *4345*, 308.
- (346) (a) Owa, S.; Umatate, T. High index lithography (HIL) progress and plans. SEMATECH Litho Forum, Bolton Landing, NY, 12–14 May, 2008. (b) Ohmura, Y.; Nagasaka, H.; Matsuyama, T.; Nakashima, T.; Kobayashi, T.; Ueda, M.; Owa, S. *Proc. SPIE* **2008**, *6924*, 692413.

CR900244N